АКУСТИЧЕСКИЙ ЖУРНАЛ
АКАДЕМИЯ НАУК СССР

SOVIET PHYSICS

Acoustics

VOLUME 2 NUMBER 2

A Translation
of the
Journal of Acoustics
of the
Academy of Sciences of the USSR

Published by the
AMERICAN INSTITUTE OF PHYSICS
INCORPORATED

SOVIET PHYSICS

Acoustics

A translation of the "Journal of Acoustics" of the USSR.

A publication of the

AMERICAN INSTITUTE
OF PHYSICS

Governing Board

ALLEN V. ASTIN
ROBERT F. BACHER
W. S. BAIRD
H. A. BETHE
R. T. BIRGE
FRANK D. DEXTER
I. C. GARDNER
S. A. GOUDSMIT
CHARLES KITTEL
HUGH S. KNOWLES
R. B. LINDSAY
WILLIAM F. MEGGERS
HARRY F. OLSON
R. R. PALMER
R. F. PATON
ERIC RODGERS
RALPH A. SAWYER
FREDERICK SEITZ
H. D. SMYTH
MARK W. ZEMANSKY

Officers and Staff

FREDERICK SEITZ
Chairman, Governing Board
HENRY A. BARTON
Director
WALLACE WATERFALL
Executive Secretary
MARK W. ZEMANSKY
Treasurer
THEODORE VORBURGER
Advertising Manager
RUTH F. BRYANS
Publication Manager
KATHRYN SETZE
Assistant Treasurer
ALICE MASTROPIETRO
Circulation Manager
EUGENE H. KONE
Director of Public Relations

American Institute of Physics Advisory Board on Russian Translations

ELMER HUTCHISSON, *Chairman*

DWIGHT GRAY, MORTON HAMERMESH, VLADIMIR ROJANSKY,
VICTOR WEISSKOPF

"Soviet Physics—Acoustics" is published by the American Institute of Physics for the purpose of making available in English reports of current Soviet research in acoustics as contained in the "Journal of Acoustics" of the Academy of Sciences of the USSR, and will regularly consist of four issues per year.

Transliteration of the names of Russian authors follows the system employed by the Library of Congress.

This translating and publishing project was undertaken by the Institute in the conviction that dissemination of the results of research everywhere in the world is invaluable to the advancement of science. The National Science Foundation of the United States encouraged the project initially and is supporting it in large part by a grant. Translation and printing are being handled by Consultants Bureau, Inc.

The American Institute of Physics and its translators propose to translate faithfully all the scientific material in the "Journal of Acoustics" of the Academy of Sciences of the USSR appearing after January 1, 1955, the first year of its publication. The views expressed in the translated material, therefore, are intended to be those expressed by the original authors, and not those of the translators nor of the American Institute of Physics.

One volume is published annually. Volume 1 will contain all of the scientific material published in the original Russian journal during the calendar year 1955, and Volume 2 will contain all of the scientific material published in the original Russian journal during the calendar year 1956.

Subscription Prices:

Per year, beginning with Volume 2 (4 issues)	
United States and Canada	$20.00
Elsewhere	22.00
*Back Numbers (beginning with Volume 2)	
Single copies	$ 6.00

*Volume 1, consisting of two issues, is available only as a set at the yearly rates quoted above.

Subscriptions should be addressed to the American Institute of Physics, 57 East 55th Street, New York 22, New York.

Copyright by American Institute of Physics 1956

SOVIET PHYSICS

Acoustics

SOVIET PHYSICS – ACOUSTICS VOLUME 2, NUMBER 2

PROPAGATION OF WAVES IN A MEDIUM WITH RANDOM INHOMOGENEITIES OF THE INDEX OF REFRACTION

(SURVEY)

V. A. Krasil'nikov, A. M. Obukhov

1. The survey is devoted to the problem of "waves and fluctuations" which in recent years has been developed in connection with a number of problems of atmospheric acoustics, hydroacoustics, atmospheric optics and the propagation of radiowaves in the troposphere. Here we are discussing the study of phenomena which arise during the propagation of waves in the medium with weak random inhomogeneities which are caused by turbulence.

Thus, for example, when a sound wave is propagated in the atmosphere and is affected by inhomogeneities of the wind field and the temperature field, fluctuations in phase [1, 2] and signal level [3] take place; similar phenomena are observed when sound is propagated in the ocean [4] and when radiowaves are propagated in the troposphere [5].

The investigation of the fluctuations in the characteristics of the wave field requires the development of approximate methods for solving the wave equation for weakly inhomogeneous media and the utilization of statistical concepts. In this direction the authors have written a number of papers; certain results of these papers along with the results of a number of other authors are briefly discussed below.

2. To a sufficient degree of accuracy the phenomena of the propagation of sound waves in an inhomogeneous medium can be described by the wave equation

$$\frac{1}{c^2}\frac{\partial^2\varphi}{\partial t^2}=\nabla^2\varphi, \tag{1}$$

where the propagation velocity c of the wave depends upon the coordinate $\mathbf{r}\,(x, y, z)$.* The inhomogeneities of the index of refraction are presumed to be weak, i.e.,

$$c=c_0(1+\mu); \quad \mu\ll 1. \tag{2}$$

---

* The dependency of c upon time will not be explicitly considered, since we assume that the characteristics of the medium vary slowly with respect to time in comparison to the vibration frequency.

The classic method of solving Equation (1) when Condition (2) obtains is the perturbation method; when this method is used, the potential φ is expanded in a power series of the small parameter μ:

$$\varphi = \varphi_0 + \varphi_1 + \cdots \tag{3}$$

This method is widely utilized in solving problems concerning the scattering produced by small inhomogeneities, however its application encounters specific difficulties in calculating the characteristics of waves according to their passage through a sufficiently thick perturbed layer with a length L, which consists of "weak" ($\mu \ll 1$), but large inhomogeneities whose dimension $\underline{l}$ is appreciably greater than the wavelength λ ($\underline{l} \gg \lambda$). These difficulties are associated with the effect of "the buildup of the phase perturbation" to values which are comparable to π. In the limiting case of large and smooth inhomogeneities when $\underline{l} \gg \lambda$, it is possible to utilize the equations of ray theory:

$$\left.\begin{aligned}(\nabla\theta)^2 &= (1+\mu)^2,\\ 2\nabla \ln A\nabla\theta + \nabla^2\theta &= 0\end{aligned}\right\}, \tag{4}$$

where θ is the eikonal (a quantity which is proportional to the phase) and A is the amplitude. The approximate method of solving Equation (4), which is based upon the smallness of μ, and the corresponding linearization, was utilized in the papers cited in [5, 6]. Under these conditions the perturbations of the eikonal and of the signal level are represented by the Expressions

$$\begin{aligned}\theta' &= \int_0^L \mu\,dx,\\ \ln\frac{A}{A_0} &= -\frac{1}{2}\int_0^L \nabla^2\theta'\,dx,\end{aligned} \tag{5}$$

where A_0 is the amplitude of the unperturbed wave and the integral is taken along an unperturbed ray.

This method permits us to take into account the geometrical effects as long as the deviation angles of the ray are sufficiently small; however the region where this method can be applied is limited since it does not take diffraction effects into account.

It is possible to examine the problem of the fluctuations of phase and of wave-field level on the basis of more general equations which permit the approximate consideration of diffraction effects [7, 8].

Let us introduce the complex function

$$\psi(\mathbf{r}) = S + i\ln\frac{A}{A_0}, \tag{6}$$

where $S(\mathbf{r})$ is the phase. Assuming that

$$\varphi(\mathbf{r}, t) = A_0 \exp\{i(\omega t - \psi(\mathbf{r}))\} \tag{7}$$

and substituting (7) into Equation (1), we obtain:

$$\begin{aligned}(\nabla\psi)^2 + i\nabla^2\psi &= k_0^2(1+\mu)^2,\\ k_0 &= \frac{2\pi}{\lambda} = \frac{\omega}{c_0};\end{aligned} \tag{8}$$

for the unperturbed field corresponding to $\overline{\psi} = k_0 x$. Assuming in the general case that $\overline{\psi} = \psi_0 + \psi'$ and neglecting terms which contain $(\nabla\psi')^2$ from here on, we obtain the basic equation of the theory

$$2(\nabla\psi'\nabla\psi_0) + i\nabla^2\psi' = 2\mu k_0^2, \tag{9}$$

which is linear with respect to perturbations of the "complex phase" ψ'. Since in the derivation of this equation we neglected $(\nabla\psi')^2$ but not the magnitude of $(\psi')^2$ it is not necessary here to require a small perturbation of the phase and amplitude; what is required is that the relative variations of the wave field at distances of the order of λ should be small. From Equation (9) we can directly obtain Equations (5) if we neglect the diffraction term. It can be shown that in the region where the classical perturbation method is applicable the solution of Equation (9) (while retaining the diffraction term) leads to the same results as does the perturbation method.

When $\underline{1} \gg \lambda$, the region of applicability of the geometric approximation is limited by a specific critical distance $L_{cr} = \frac{2\pi 1^2}{\lambda}$ at which the diffraction effects begin to become substantial. In order to take these effects into account (in the spirit of the Fresnel Theory) it proves possible to utilize a simplified form of Equation (9):

$$2k_0\frac{\partial\psi'}{\partial x} + i\left(\frac{\partial^2\psi'}{\partial y^2} + \frac{\partial^2\psi'}{\partial z^2}\right) = 2\mu k_0^2. \tag{10}$$

The solution of this equation has the form

$$\psi'(x, y, z) = \frac{ik_0^2}{2\pi}\int_0^L\int_{-\infty}^{\infty}\int_{-\infty}^{\infty}\frac{\exp\left[-\frac{ik_0\rho^2}{2(x-\xi)}\right]}{x-\xi}\mu(\xi, \eta, \zeta)\,d\eta\,d\zeta\,d\xi, \tag{11}$$

where

$$\rho^2 = \sqrt{\eta^2 + \zeta^2}.$$

3. Since in a turbulent medium $\mu(x, y, z)$ can be treated as a random function of the coordinates, it is useful to pass over into a statistical examination of the problem.

The basic statistical characteristic of the pulsation field of $\mu(x, y, z) = \mu(M)$ is the correlation function $B\,\overline{(M_1, M_2)} = \overline{\mu(M_1)\,\mu(M_2)}$ which for a statistically isotropic field of the values of μ can be considered to be dependent solely upon the distance $\underline{r}$ between the points M_1 and M_2; for these conditions $\overline{\mu(x, y, z)} = 0$. The correlation functions at large values of $\underline{r}$ go to zero and, generally speaking, must be determined by experiment. In [8] the experimental data were approximated by B(r) functions of the form

$$B(r) = \overline{\mu}^2\exp\left(-\frac{r^2}{2l^2}\right); \tag{12}$$

Other forms of approximation also are possible [9].

For a statistical description of the field of $\mu(x, y, z)$ a so-called structural function

$$D(r) = \overline{[\mu(r + \vec{\rho}) - \mu(\vec{\rho})]^2}; \tag{13}$$

can also be utilized; its relationship to the function B(r) is as follows:

$$D(r) = 2B(0) - 2B(r). \tag{14}$$

The utilization where possible of the functions D(r) has specific advantages, since in the experimental determination of these functions the difficulty of isolating the average level is eliminated, and in addition these functions serve as the basic characteristics in the statistical theory of locally-isotropic turbulence [10, 11]. The experimental data which illustrates the application of this theory to the microstructure of a wind field is contained in the paper cited in [12].

Figure 1 shows the structural function of the temperature field; this function was obtained from the paper cited in [13] by means of a low-inertia resistance thermometer at a height of 1.5 meters above the earth's surface and at distances of up to 32 cm. The solid line shows the theoretical structural function of the temperature field (the "2/3 law") proposed in the papers cited in [14, 15]. The structural function of the index of refraction for sound differs from the structural function of the temperature field solely by a numerical coefficient which is not difficult to calculate.

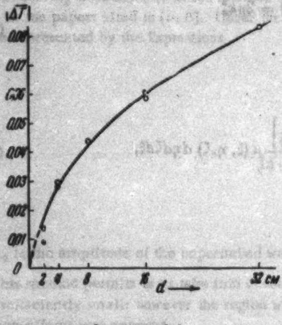

Fig. 1. Structural function of the temperature field (Fall, 1949, 8:10 pm).
$|\overline{\Delta T}| = Bd^{1/3}$; $B = 3\cdot 10^{-2}\,^\circ C\cdot cm^{-1/3}$

4. A general method for calculating the mean-square values of the fluctuations of the wave characteristics (phase, amplitude) can be indicated for a wave which is propagated in a medium with random inhomogeneities if the statistical properties (the correlation function) of the field of inhomogeneities are known. When applied to the simplest statement of the problem (geometric acoustics), this method consists of utilizing Formulas (5), squaring them and then averaging [5]. As a result we obtain the mean-square of the characteristic which is of interest to us (for example, the phase) in the form of a double integral which contains the correlation function:

$$\overline{S'^2} = \int_0^L\int_0^L \overline{\mu(x)\,\mu(x')}\,dx\,dx', \tag{15}$$

this double integral can easily be transformed into a single integral

$$\overline{S'^2} = 2L\overline{\mu^2}\int_0^L (L - r)\,B(r)\,dr \approx 2L\overline{\mu^2}\int_0^\infty B(r)\,dr \tag{16}$$

(for very large values of the distance L).

The utilization of a more accurate theory which is based upon Equation (10) permits us to express linearly the phase and amplitude perturbations in terms of fluctuations of μ (x, y, z) by means of the triple integral (11). The squaring and subsequent averaging lead to the representation of the mean-square of the corresponding fluctuations in terms of six-fold integrals which contain the correlation function; these six-fold integrals can be simplified in the subsequent analysis.

A specific calculation of the phase and amplitude fluctuations (when utilizing a correlation function of the Gaussian type (12) and taking diffraction effects into account) leads to the following Expressions [8]:

$$\overline{S'^2} \cong (2\pi)^2 \overline{\mu^2} \frac{lL}{\lambda^2}\left(1+\frac{1}{D}\operatorname{arc\,tan} D\right), \tag{17}$$

$$\overline{\left(\ln\frac{A}{A_0}\right)^2} \cong (2\pi)^2 \overline{\mu^2} \frac{lL}{\lambda^2}\left(1-\frac{1}{D}\operatorname{arc\,tan} D\right), \tag{18}$$

where $D = \frac{\lambda L}{2l}$.

In the limiting case $D \ll 1$ (comparatively small distances and $L \ll L_{cr}$)

$$\overline{S'^2} \cong (2\pi)^2 \frac{2\overline{\mu^2} Ll}{\lambda^2}, \tag{19}$$

$$\overline{\left(\ln\frac{A}{A_0}\right)^2} \cong \frac{\pi^2}{3} \overline{\mu^2} \frac{L^3}{l^3}. \tag{20}$$

These formulas coincide with the formulas obtained from the theory which is based on a geometric approximation.

In the other limiting case $D \gg 1$ (i.e., when $L \gg L_{cr}$) we obtained:

$$\overline{S'^2} \cong (2\pi)^2 \overline{\mu^2} \frac{Ll}{\lambda^2}, \tag{21}$$

$$\overline{\left(\ln\frac{A}{A_0}\right)^2} \cong (2\pi)^2 \overline{\mu^2} \frac{Ll}{\lambda^2}. \tag{22}$$

Thus for large values of L the expression for the phase fluctuations differs from the corresponding formula obtained from geometric concepts, but only by a numerical factor $\frac{1}{\sqrt{2}}$ (the proportionality of L is preserved). In addition, the dependency of the amplitude fluctuations of the wave upon L undergoes an abrupt change as it passes through the value L_{cr}, whereas at small values of L the quantity $\overline{\left(\ln\frac{A}{A_0}\right)^2}$ increases in proportion to L^3 and does not depend upon λ (this corresponds to the theory which utilizes the geometric approximation); for large values of L the fluctuations of the logarithm of the amplitude obey the same law of variation $\overline{\left(\ln\frac{A}{A_0}\right)^2} \sim L$, that the phase fluctuations obey (at the same time a dependency upon λ appears).

An analogous method of calculation can also be utilized for calculating the correlation of the fluctuations of the wave field characteristics at various points [16]. In solving problems of the theory of wave scattering by inhomogeneities, an expression for the potential of the perturbed field is utilized. The calculation of the mean-square of the potential of the perturbed field by means of the above-indicated method permits us to express the intensity of the scattered wave in terms of correlation functions of the pulsations [17, 9, 18].

In conclusion, let us provide some examples of specific calculations of the phase and amplitude fluctuations when sound is propagated in turbulent atmosphere.

In order to calculate the accuracy of determining a bearing according to observations which are made at two points that are at a distance d from one another (the base), it is of interest to calculate the mean-square of the fluctuations of the phase difference [19, 20]. This problem can be solved by the general method, and the result can be expressed in terms of the structural function of the wind field; the solution is of the form

$$\overline{(S_1 - S_2)^2} \cong \text{const} \left(\frac{\omega}{c^2}\right)^2 C^2 L d^{5/3}, \tag{23}$$

where the constant has a value of the order of unity, ω is the angular frequency and C is the so-called turbulence characteristic which appears in the expression for the structural function of the velocity field,

$$\overline{[\mathrm{v}(M_1) - \mathrm{v}(M_2)]^2} = C^2 d^{2/3}, \tag{24}$$

where v(M) is a pulsation of the wind velocity; for the conditions which obtain in the atmosphere (the earth layer) it has a value of several units in the CGS system [12, 21].

An analogous formula is also obtained when the field of a temperature pulsation is taken into account. Assuming that the structural function of the index of refraction is of the form

$$\overline{[n(M_1) - n(M_2)]^2} = H^2 d^{2/3}, \tag{25}$$

where H is the structural characteristic of the pulsation field of the index of refraction, it is possible to calculate [22] the mean-square value of the signal-level fluctuations on the basis of Equation (10):

$$\overline{\left(\ln \frac{A}{A_0}\right)^2} = 0{,}31 H^2 K^{7/6} L^{11/6}. \tag{26}$$

The character of the dependency of the signal-level fluctuations upon L (as well as the absolute values of these fluctuations) agree satisfactorily with the experimental results given in the paper cited in [23] and shown in Fig. 2. The theory developed above opens up the possibility of solving the converse problem – that of determining the structural turbulence characteristics from the results of acoustical measurements [19, 23].

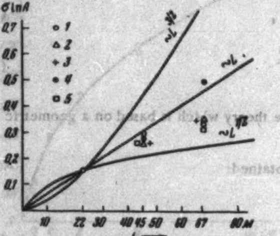

Fig. 2. The dependency of $\sqrt{\overline{(\ln A/A_0)^2}} = \sigma \ln A$ upon L (1948, height was 8 meters above the earth's surface). The measured data is given on one scale; the base values are the values of σ ln A which are obtained for a distance of 22 meters. Measurements: 1) August 1, frequency ν = 5000 cps; 2) July 31, frequency ν = 5000 cps; 3) July 31, frequency ν = 3000 cps; 4) August 9, frequency ν = 3000 cps; 5) August 10, frequency ν = 3000 cps.

LITERATURE CITED

[1] V. M. Bovsheverov, V. A. Krasil'nikov. "Preliminary experiments on the acoustical probing of the atmosphere with a monochromatic beam." Doklady Akad. Nauk SSSR 32, 7, 44-46 (1941).

[2] V. A. Krasil'nikov, "Some experiments on the propagation of sound in the atmosphere," Doklady Akad. Nauk SSSR 46, 3, 108-110 (1945).

[3] V. A. Krasil'nikov, K. M. Ivanov-Shits, "Some new experiments on the propagation of sound in the atmosphere," Doklady Akad. Nauk SSSR 67, 4, 639-642 (1949).

[4] M. J. Sheehy, "Transmission of 24-kc under-water sound from a deep source," J. Acoust. Soc. Am. 22, 22-24 (1950).

[5] V. A. Krasil'nikov, "The effect of pulsations in the atmospheric index of refraction upon the propagation of ultra-short radiowaves," Bull. Acad. Sci. USSR, Geog. and Geophys. Ser. 13, 1, 33-57 (1949).

[6] V. A. Krasil'nikov, "Fluctuations of the amplitude of sound when it is propagated in turbulent atmosphere," Doklady Akad. Nauk SSSR 58, 7, 1353-1356 (1947).

[7] S. M. Rytov, "Diffraction of light by means of ultrasonic waves," Bull. Acad. Sci. USSR, Phys. Ser. 1937, No. 2, 223-259.

[8] A. M. Obukhov, "The effect of weak atmospheric inhomogeneities upon the propagation of sound and light," Bull. Acad. Sci. USSR, Geophys. Ser. 1953, 2, 155-165.

[9] C. L. Pekeris, "Note on the scattering of radiation in inhomogeneous media," Phys. Rev. 71, 4, 268-269 (1947).

[10] A. N. Kolmagorov, "Local turbulence structure in an incompressible liquid for very large Reynolds numbers," Doklady Akad. Nauk SSSR 30, 4, 299-303 (1941).

[11] A. M. Obukhov, A. M. Iaglom "Microstructure of the turbulent stream," Applied Mathematics and Mechanics 15, 1, 3-96 (1951).

[12] A. M. Obukhov, "Characteristics of the microstructures of wind in the layer of atmosphere adjacent to the earth," Bull. Acad. Sci. USSR, Geophys. Ser. 1951, No. 3, 49-68.

[13] S. I. Krechmer, "Investigations of micropulsations of the temperature field in the atmosphere," Doklady Akad. Nauk SSSR 84, 1, 55-58 (1952).

[14] A. M. Obukhov, "Structure of the temperature field in a turbulent stream," Bull. Acad. Sci. USSR, Geog. and Geophys. Ser. 13, 1, 58-69 (1949).

[15] A. M. Iaglom, "The local structure of the temperature field in a turbulent stream," Doklady Akad. Nauk SSSR 69, 6, 743-746 (1949).

[16] L. A. Chernov, "The correlation of amplitude and phase fluctuations when waves are propagated in a statistically inhomogeneous medium," Doklady Akad. Nauk SSSR 98, 6, 953-956 (1954).

[17] A. M. Obukhov, "The scattering of sound in a turbulent stream," Doklady Akad. Nauk SSSR 30, 7, 616-620 (1941).

[18] V. A. Krasilnikov and V. I. Tatarskii, "Scattering of sound in a turbulent stream," Doklady Akad. Nauk SSSR 90, 2, 159-162 (1953).

[19] V. A. Krasil'nikov, "The propagation of sound in turbulent atmosphere," Doklady Akad. Nauk SSSR 47, 7, 486-489 (1945).

[20] V. I. Tatarskii, "Phase fluctuations of sound in a turbulent medium," Bull. Acad. Sci. USSR, Geophys. Ser. 1953, No. 3, 252-258.

[21] A. M. Obukhov, "Local structure of atmospheric turbulence," Doklady Akad. Nauk SSSR 67, 4, 643-646 (1949).

[22] V. I. Tatarskii. "Pulsations of the amplitude and phase of a wave which is propagated in weakly inhomogeneous atmosphere." Doklady Akad. Nauk SSSR 107, 2, 245-248 (1956).

[23] V. A. Krasil'nikov. "Phase fluctuations of ultrasonic waves when they are propagated in the layer of air adjacent to the earth." Doklady Akad. Nauk SSSR 88, 4, 657-660 (1953).

Moscow State University

Received February 21, 1956

THE MECHANISM OF CAVITATIONAL DAMAGE TO SURFACE FILMS IN AN ACOUSTIC FIELD

A. S. Bebchuk, L. O. Makarov, L. D. Rosenberg

A study of the process of the cavitational damage of a surface film which has been deposited upon a glass surface, conducted by means of high-speed cinematography, has shown that at least two different processes take place. The first of them is associated with the bursting of bubbles in the vicinity of the film surface, and it leads to intense local damage; the second is caused by the penetration of bubbles underneath the film, and this effect causes the film to peel off.

The damage to surface films which is caused by ultrasonic cavitation is widely utilized in such processes as, for example, ultrasonic cleaning and soldering. However, the physical picture of such processes as well as of other phenomena associated with cavitation is far from being clear. The majority of authors studied the results of cavitational damage and also investigated the cavitational endurance of various materials (see [1] and the literature cited there); however it is not possible to obtain a concept of the damage mechanism from these papers. In other papers which are devoted to ultrasonic cleaning, indications are encountered to the effect that along with cavitation the large accelerations which are developed in an intense acoustic field [2] also play a substantial part; certain authors [3] tend to explain the entire process of cleaning in terms of the effects of these accelerations.

This paper contains the results of our preliminary investigations of the physical processes of damage in coatings which are chemically passive with respect to liquid and which are deposited upon the surface of a solid body located in an intense acoustic field. The investigation was conducted by means of the high-speed cinematographic method.* In the capacity of a basic object we selected a thin layer of resin which was deposited upon the surface of a glass plate in the form of an alcohol solution and was then thoroughly dried. In order to be better able to distinguish pieces of the layer from cavitational bubbles, we introduced finely powdered graphite into the layer. Since the narrow-film camera SKS-1 which we utilized permitted us to take high-speed photographs (a speed which did not exceed 4,000 frames per second), we selected a comparatively low frequency – about 8 kc. The acoustic source consisted of a bar-shaped magnetostrictional dipole constructed in the form of a nickel cylinder 300 mm long, 25 mm in diameter and with walls 2 mm thick, which was cut along its axis. From the upper side the cylinder was covered by a soldered-on brass cap shaped in the form of a truncated cone whose upper surface had a diameter of 4–5 mm. This end of the dipole was inserted into a rectangular working vessel with dimensions of 40 × 10 × 50 mm through a rubber diaphragm; the lateral walls of this vessel were made from optically plane parallel glass plates. The lower end of the dipole was surrounded by the coil of the high-frequency generator which could supply up to 8 kw of oscillatory power. Since at this stage we were interested in a qualitative picture, measurements of the acoustic field were not conducted. We attempted many varied arrangements of the apparatus; the most fruitful of these variations was the one which is shown in Fig. 1. The glass plate upon which the investigated layer was deposited was stationed at an angle of about 45° with respect to the optical axis of the object-glass of the movie-camera. The object was illuminated by light beams from two light sources, and these light beams were concentrated at the investigated point in the acoustic

---

* Operator-engineer V. V. Lebedev (Laboratory of Scientific and Applied Photography and Cinematography of the Acad. Sci. USSR).

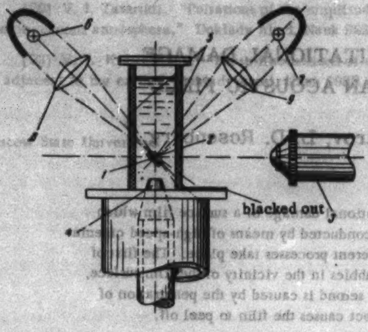

Fig. 1. Diagram showing the arrangement of the apparatus: 1) Glass plate; 2) film being damaged; 3) object-glass of the movie-camera; 4) end of the rod-shaped magnetostrictional dipole; 5) plane-parallel optical glasses; 6) source of light producing 0.5 kw with a mirror reflector; 7) light source producing 3.0 kw with a mirror reflector, 8) and 9) converging lenses.

field by means of a converging lens. As can be seen from the diagram of the experiment shown in Fig. 1, the powerful light beam from the three-kilowatt light source was normally incident upon the surface of the plate; at the same time the axis of this light beam was placed at an angle of 45° to the optical axis of the object-glass of the movie camera, and this practically eliminated the direct passage of light into the object-glass. The second, half-kilowatt, source of light was arranged in such a way that the axis of its light beam passed along the surface of the plate. Sectors of the surface which could create undesirable reflections that would pass into the object-glass were blacked out. A thin layer of resin was deposited upon the surface of the 3 mm wide glass plate in the form of a small spot in the central portion of the plate. The photographs which are shown were obtained with an object-glass with an aperature ratio of 1:4 for a focal length F = 85 mm. When the films were shown at a rate of 24 frames per second we slowed up the process by not less than a factor of 60.

Viewing the material obtained, we found that at least two different mechanisms of surface film damage could be observed. The first of them is

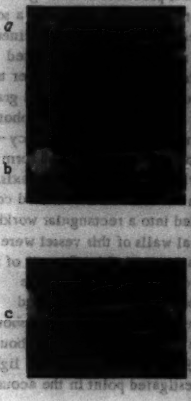

Fig. 2.

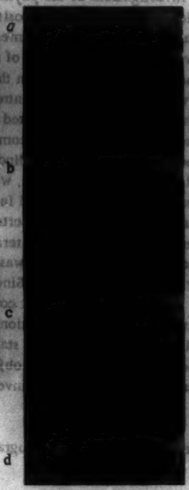

Fig. 3.

Fig. 4.

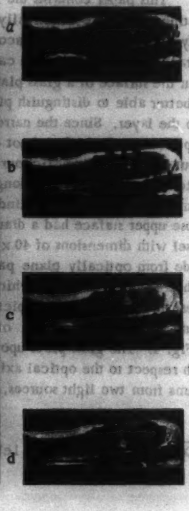

Fig. 5.

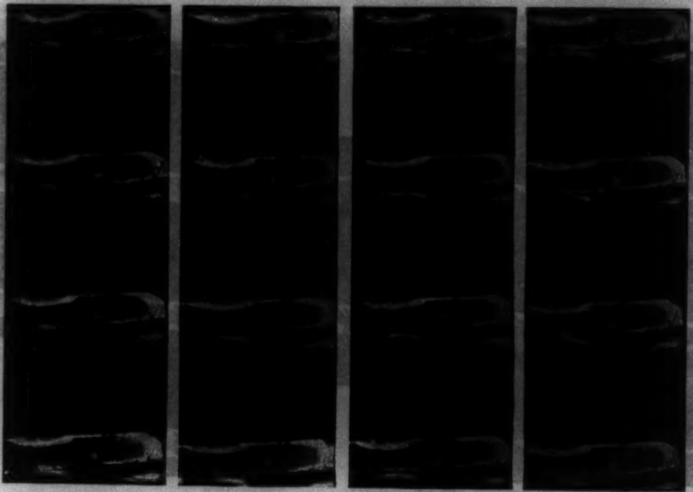

Fig. 6

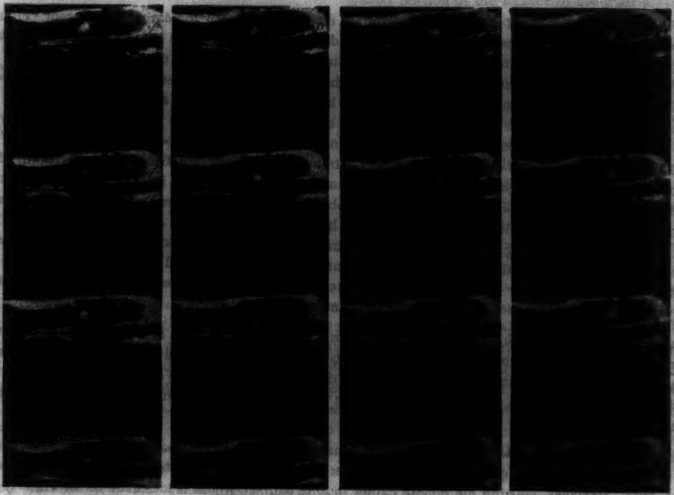

Fig. 7

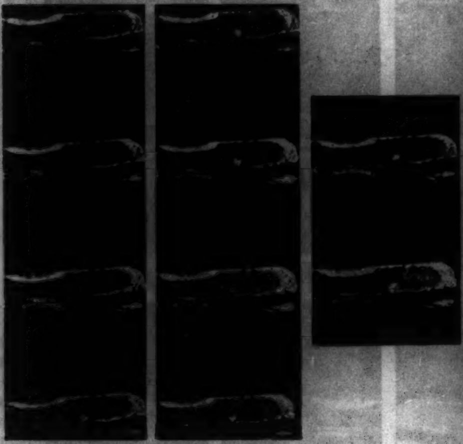

Fig. 8

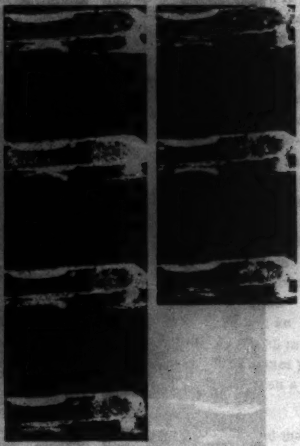

Fig. 9

shown in Fig. 2 where individual frames associated with the initial phase of the damage are shown. Figure 2,a shows the appearance of the plate with the surface film deposited upon it; at the left a bubble of air with the diameter ~ 1.7 mm is shown; small air bubbles are located on the remainder of the surface; no acoustic field is present. In Fig. 2,b (the next frame in time sequence) the acoustic field is turned on: the surface texture of both the large bubble and the small bubbles has changed – it has become pearl-like, and this is an indication that intensive vibrations have begun. Then the large bubble begins (evidently due to the effect of the ponderomotive forces of the acoustic field) to be displaced to the left and gradually passes out beyond the boundaries of the frame. The average rate of this displacement is approximately 0.5 m/sec. Parallel to the movement of the first bubble a second bubble is generated in the right-hand portion of the frame; Fig. 2,c shows the instant when the first bubble has been half hidden and the second bubble is in the stage of formation: two large bubbles which then combine into one are visible. The second bubble, having existed a certain amount of time (about 10 milliseconds), moves to the right (Fig. 3) at a rate of approximately 1 m/sec. and also disappears beyond the boundaries of the frame. Simultaneously, to the left of the center of the frame, several small bubbles combine and form a third bubble. This latter bubble grows to a diameter of 1.8-2.0 mm quite rapidly and oscillates in a stationary manner for 10 milliseconds (i.e., it remains in the same place).

The last two frames which show its stationary state are shown in Figs. 4, a and b. The following two frames (c and d) correspond to the process involved in its annihilation. It can be seen with complete clarity that this instant is associated with intense damage in the portion of the film which is adjacent to the bubble; Fig. 4,c clearly shows cracks, and Fig. 4,d shows a portion of the film which has been torn away and broken up into small parts which are carried away by the acoustic "wind".

From the photographs shown it follows that stationary oscillations, even those of large amplitude, do not produce any destructive effect upon the film itself, regardless of whether the bubble is an air bubble or a cavitational bubble. However, bursting the bubble causes intense damage which is localized in the vicinity of

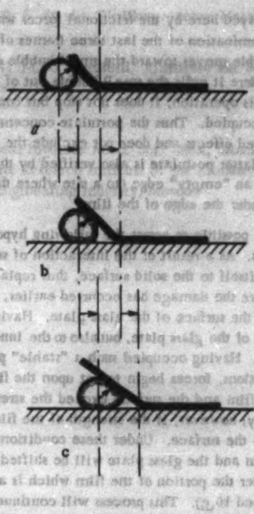

Fig. 10. Postulated mechanism by which the film is torn away from the surface (a, b, c).

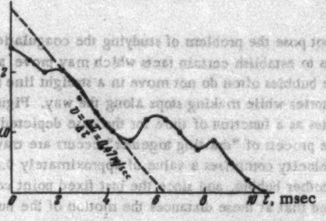

Fig. 11. Displacement of a coagulated bubble.

annihilation. It is interesting that at the instant of time which corresponds to Fig. 4,c, cracks can already be seen clearly while the bubble has not yet completely burst. It may be that (in accordance with the hypothesis asserted by Kornfeld [4]) a large bubble disintegrates into a number of parts, each of which bursts separately. It remains unclear what effect produces this bursting after the bubble has existed in a stationary state for approximately 10 milliseconds (such a period corresponds to 120 cycles of the fundamental frequency of the field). However, it is completely clear that this rapid, subdividing local damage is directly associated with some impact forces which are developed during the process of the annihilation of a bubble. In order to obtain more detailed information, it is necessary to utilize an appreciably higher cinematographic speed.

The second damage mechanism looks completely different: upon examining the subsequent portion of the moving-picture it is evident that at the edge of the film (the edge which bounds the location of the damage) bubbles of smaller dimensions are formed. Other bubbles which are formed further away are pulled to the boundary, coagulate with one another and penetrate between the film and the glass, peeling off and shifting large pieces of the film without damaging them. The individual stages of this process are shown in the frames of Fig. 5. From the frame 5,a it is evident that the greater portion of the surface of the glass plate has already been cleaned off, and that the film has remained only at the right-hand edge. At the boundary of the film a bubble is vibrating intensely; it peels off small pieces of the film and sometimes penetrates underneath the edge of the film, thus becoming partially invisible. Other bubbles (not shown on these frames) settle upon the edge of the film, penetrate between the film and the glass and cease being visible. After that a vertical crack (5,b) appears in the right-hand portion of the film. After some time still another crack is added, and this crack is directed almost at right angles to the first one (5,c). After that the entire remaining piece of the film slowly slides from its position in the direction of the forward edge of the glass plate and is carried away by the stream (5,d). The entire process which is described above is undoubtedly associated with the coagulation of cavitational bubbles – a phenomenon which plays an important part in the overall behavior of the bubbles. However, if under the conditions of ordinary coagulation a large bubble, while remaining in place, pulls a small bubble into itself, then the picture is altered when an edge of the surface film is present. A bubble which is located at an edge always remains stationary, and the second bubble approaches it regardless of the relationship between the bubble sizes. Thus, Fig. 6 shows a small bubble being pulled toward a large one which is located at the edge of the surface film, and in Fig. 7 we see the opposite phenomenon – a large bubble is being pulled toward a small one. In Fig. 8 we see the process of the coagulation of two small bubbles into a single bubble which is somewhat larger, and this phenomenon is followed by the subsequent incorporation of this bubble into a large bubble which is located at the edge of the film.

It is possible to assert a postulate to the effect that a role is played here by the frictional forces which keep a bubble which is located at an edge in a stationary position. An examination of the last three frames of Fig. 7 also supports this concept, since these frames show that the large bubble moves toward the small bubble only until the large bubble itself has moved up to the edge of the film. Here it pulls the small bubble out of the "nest" in which the latter has been sitting. But having carried out this operation, it does not stop but continues to move on and finally occupies the place which the small bubble occupied. Thus the postulate concerning the role played by the frictional forces does not explain all of the observed effects and does not exclude the postulate concerning the "attractive" properties of the edge of the film. The latter postulate is also verified by the case depicted in Fig. 9, where it is evident how the bubble is attracted to an "empty" edge (to a site where there are no other bubbles) and having reached this edge begins to "climb" under the edge of the film.

Basing ourselves on the experimentally obtained material, it is possible to assert the following hypotheses which explains the second mechanism of the damage to surface films. As a result of the interaction of surface forces the cavitational bubble, as any other bubble, strives to attach itself to the solid surface, thus replacing this surface by a portion of its own surface. At the edge of the film, where the damage has occurred earlier, there are undoubtedly sectors where the edge of the film has receded from the surface of the glass plate. Having arrived at such a site, a bubble attaches itself not only to the surface of the glass plate, but also to the inner surface of the free edge of the film; this is schematically shown in Fig. 10*a*. Having occupied such a "stable" position, the bubble does not cease to vibrate; as a result of its intensive vibrations, forces begin to act upon the film which tear it away from the surface. If the forces of adhesion between the film and the surface exceed the strength of the film itself, then the free portion of the film will simply tear away; however, if the strength of the film exceeds the adhesive forces, then a portion of the film will be separated from the surface. Under these conditions a bubble which is striving to retain its previous position with respect to the film and the glass plate will be shifted in the direction of the unseparated portion of the film and will "climb" under the portion of the film which is already separated from the surface (this is schematically shown in Fig. 10*b* and 10*c*). This process will continue until the entire film has been separated from the surface or until the separated portion of the film has been torn away.

Thus cavitational bubbles, as well as the destructive impact action which occurs at the instant of the annihilation of the bubbles, can tear the film away from the surface (comparatively more slowly) while effecting stationary vibrations.

In carrying out the work involved in this paper, we did not pose the problem of studying the coagulation process of the bubbles. However, the results obtained permit us to establish certain facts which may prove to be useful in further investigations. In the process of attraction the bubbles often do not move in a straight line (as, for example, is shown in Fig. 6); they describe complex trajectories while making stops along the way. Figure 11 shows the curve for the variation of the distance between bubbles as a function of time for the case depicted in Fig. 6. It is an important fact that all four sectors in which the process of "drawing together" occurs are traversed by the bubble with an approximately identical velocity; this velocity comprises a value of approximately 0.5 m/sec. Since the bubble begins its motion at 0.24 cm from another bubble, and since the last fixed point corresponds to a distance of 0.02 cm, it evidently should be postulated that at these distances the motion of the bubble is due to its entrainment by the stream of liquid.

The analysis of the data which was obtained for the motion of other bubbles showed that the velocity of their displacement in the sectors where bubbles come together lies within the limits of 0.4-0.7 m/sec. It is of interest to remind ourselves that (as has been indicated above) the velocity at which large bubbles recede (Figs. 2 and 3) is of the same order of magnitude: for bubble No. 1 this velocity is 0.5 m/sec., for bubble No. 2 it is 1.0 m/sec.

LITERATURE CITED

[1] A. T. Ellis, "Production of accelerated cavitation damage by an acoustic field in a cylindrical cavity," J. Acoust. Soc. Am. 7, 5, 913-921 (1955).

[2] Q. McKenna, "Ultrasonic cleaning of miniature devices." Trans. Inst. Radio Engrs., Ultrasonic Eng. 3, 16-22 (May 1955).

[3] S. Spizig, "Vollkommenere Metallreinigung mit Ultraschall," Werkstadt und Betrieb 88, 5, 239-242 (1955).

[4] M. O. Kornfeld, Elasticity and Strength of Liquids, (State Tech. and Theor. Lit. Press, Moscow-Leningrad, 1951).

Acoustical Institute Acad. Sci. USSR, Moscow
Scientific Research Institute of the Ministry of
Radio-Engineering Industry, Moscow

Received February 21, 1956

EXPERIMENTAL INVESTIGATION OF RELAXATION PROCESSES WHICH ARISE WHEN ULTRASONIC WAVES PASS THROUGH LIQUIDS

Iu. N. Bormosov, V. F. Nozdrev, V. D. Sobolev, A. M. Sultanov

The paper describes experimentally detected relaxation processes in acetates and formates. The investigation was conducted by means of the pulse and optical methods at frequencies of 1-30 megacycles. In the temperature range of −40 to +30° in methyl acetate, ethyl acetate, methyl formate, and ethyl formate several regions of complete relaxation were detected. In ethyl acetate an investigation was made of the absorption of ultrasonic waves, using a saturation line which included the critical region; the paper also establishes and investigates new relaxation phenomena. The authors have determined the time and frequency of relaxation which correspond to the center of relaxation in each relaxation region; they have also calculated the specific heats which are associated with the internal and external degrees of freedom, and the heats of activation. The paper discusses the possible mechanisms of the experimentally established relaxation processes.

The most complete picture of the particular features of liquid structure or of the processes which go on in liquids can be composed on the basis of ultrasonic measurements in the case when these measurements encompass the relaxation region for which dispersion and anomalous absorption of ultrasonic waves are characteristic. Several papers [1] are available on the investigation of the accoustic properties of liquids which are relaxational in experimentally attainable frequency ranges. However only one of these papers cites an investigation of one complete region of volume-viscosity relaxation.

In this paper we analyze the investigations which we conducted on the absorption of ultrasonic waves in ethers of acetic and formic acids over a wide range of frequencies and temperatures.

The absorption measurements were conducted by means of the pulse method [3] and the optical method, utilizing a dc amplifier designed with electrometer tubes [4]. During the measurements of absorption in ethyl acetate along the saturation line in the temperature range of 20-270°, we first utilized the pulse method involving two fixed distances and the method using one fixed distance [8].

The investigation of absorption in acetates and formates was performed in the interval of temperatures from −50 to +40° and in a frequency range of from 3 to 30 megacycles. In ethyl acetate the measurements were also conducted along the saturation line. An analysis of the curves shows an unusual variation of the dependency of ultrasonic absorption upon temperature and frequency in the indicated homologous series.

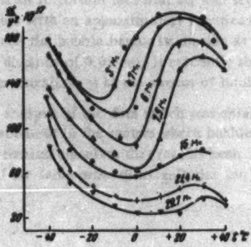

Fig. 1

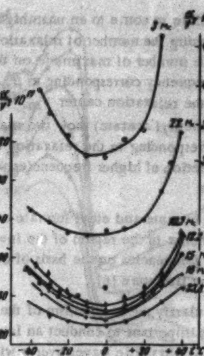

Fig. 2

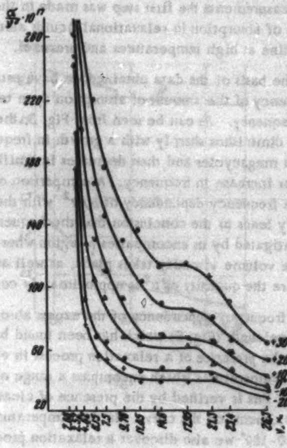

Fig. 3

In ethyl acetate in the range of temperatures from −40 to +40° the absorption coefficient α passes through a minimum. As can be seen from Fig. 1, the minimum is shifted in the direction of higher temperatures when the frequency is increased. With an increase of frequency the minimum becomes flatter and flatter, and at a frequency of 27.9 megacycles it has degenerated almost completely.

In ethyl formate (Fig. 2), in the range of temperatures from −40 to +40°, we also observe one absorption minimum. The other acetates and formates yield analogous results, and with an increase of the homolog number the minimum of the function $\alpha = f(T)$ is shifted toward higher temperatures.

It is of interest to note that if we examine the magnitude of the absorption α as a function of the given temperature θ [i.e., $\alpha = f(\theta)$], then for a given frequency applied to all substances of a single homologous series the minimum will correspond to approximately one and the same given temperature.

The manipulation of the resulting experimental data leads to new results. Figure 3 shows the curves for the dependency of the quantity α/ν^2 upon ν in methyl acetate (these curves are usually utilized in order to find the boundaries of the relaxation region). These curves show that in methyl acetate in the interval of temperatures and frequencies under study, there are two relaxation regions:* one region exists in the frequency interval 2-10 megacycles, and the other exists in the interval 15-30 megacycles. In ethyl acetate we also find that two regions of relaxation are established for the frequency interval 1-30 megacycles and the temperature interval of −40 to +40°. It is of interest to note that the interval of frequencies between the first and second relaxation regions in these substances is narrowed when the temperature increases.

In methyl formate and ethyl formate it is also possible to obtain two relaxation regions and to establish their boundaries; this can be achieved on the basis of the data provided by Sultanov [7] and from other data in the literature [6]. As in the case of acetates, the frequency interval between the first and second relaxation regions narrows with an increase in temperature. The frequency interval which corresponds to the first and second relaxation regions is in this case insignificantly displaced in the direction of lower frequencies in comparison with the cases of methyl acetate and ethyl acetate.

Our detection of two complete regions of relaxation in acetates and formates is verified if we plot graphs for the dependency of the absorption coefficient per wavelength $\mu = \alpha\lambda$ upon the frequency ν. It is known that in

---

* A more detailed analysis of our experimental data shows that in actual fact four relaxation regions with different phenomenological mechanisms exist in the indicated region of temperatures and frequencies. Concerning this see below.

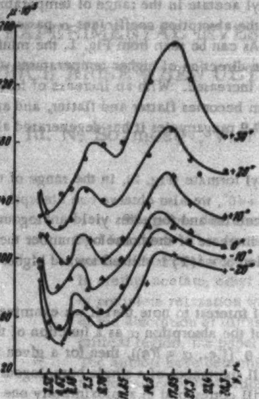

Fig. 4

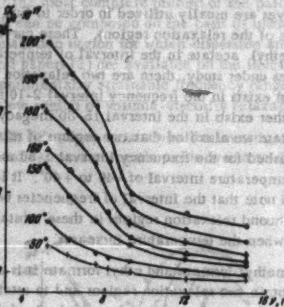

Fig. 5

this case it is possible to come to an unambiguous conclusion concerning the number of relaxation regions by determining the number of maximums on the curve $\mu = f(\nu)$. The frequency corresponding to μ_m will be the frequency of the relaxation center ν_m. In fact, the curves of Fig. 4 (methyl acetate) show two maximums, and the frequency corresponding to the relaxation center is displaced in the direction of higher frequencies when the temperature increases.

For methyl formate and ethyl formate one can also obtain two maximums in the region of the investigated temperatures and frequencies on the basis of our data [7] and the data in the literature [6].

In order to clarify the mechanism of the relaxation phenomena it was important to conduct an investigation of the absorption of ultrasonic waves over a wide range of temperatures. The measurements of ultrasonic absorption along the saturation line in ethyl acetate encompassed a frequency range of from 5 to 15 megacycles and a temperature range of from 20° to the critical point. By means of these measurements the first step was made in the investigation of absorption in relaxational liquids along the saturation line at high temperatures and pressures.

On the basis of the data obtained we have established the dependency of the amount of absorption upon temperature and frequency. As can be seen from Fig. 5, the quantity α/ν^2 diminishes sharply with a growth in frequency from 5 to 9 megacycles and then decreases insignificantly for a further increase in frequency. A comparison of our data on the frequency dependency of α/ν^2 with the relaxation theory leads to the conclusion that the frequency range investigated by us encompasses a region where relaxation of the volume viscosity takes place, as well as a region where the quantity α/ν^2 is approximately constant.

The frequency dependency of the excess absorption per one wavelength (Fig. 6) which has been found by us establishes the presence of a relaxation process in ethyl acetate at temperatures which encompass a range of from 160 to 210°; this is verified by the presence of clearly defined maximums on the curve. In the temperature region of 30-160° we also discover a relaxation process (See Fig. 5), however in the range of frequencies utilized (5-15 megacycles) an incomplete relaxation region is observed there.

The measurements which we have conducted afforded the possibility of calculating certain characteristics of the relaxation process. By using the maximums on the curves of the excess absorption per wavelength, we found the relaxation time; this time decreases with an increase in temperature for all of the relaxation processes which we discovered and is of the order of 10^{-8} sec. In accordance with the relaxation theory, the anomalous ultrasonic absorption and the relaxation of volume viscosity must be accompanied by dispersion.

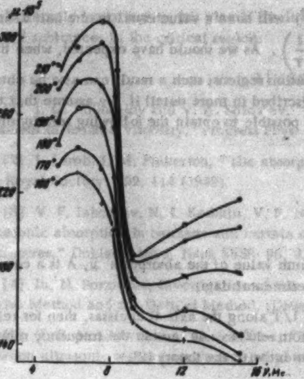

Fig. 6

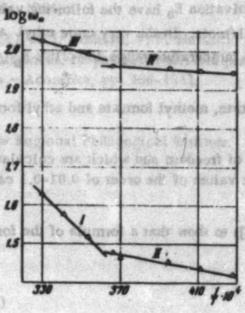

Fig. 7

This dispersion, in accordance with our data, is of the order of 0.01-0.1% in ethyl acetate and increases with an increase in temperature. The order of magnitudes of the relaxation times τ and of the dispersion for other substances which we investigated are the same as for ethyl acetate. The extensive experimental material which we obtained allowed us to determine the dependency of the maximum absorption per wave length μ_m upon temperature. For all of the relaxational regions which lie at temperatures below T_m [where T_m is the temperature corresponding to the minimum of the Function $\alpha/\nu^2 = \varphi(T)$], μ_m decreases with an increase in temperature.

For relaxation regions which lie above T_m the magnitude of μ_m increases with an increase in temperature. This is a convincing experimental proof of the fact that the relaxation processes discovered by us have different phenomenological mechanisms. It is known [1], for example, that in the case of interchangeable relaxation processes μ_m can only increase with an increase in temperature; however the structural relaxation permits a decrease in μ_m with an increase in temperature.

In order to describe the experimental facts which are examined above, it is possible to make use of certain relationships of phenomenological relaxation theory [1].

$$\alpha' = \frac{\omega^2}{2\rho c^3} \frac{\eta_0'}{1 + \omega^2 \tau^2}, \quad (1)$$

where η_0' is the coefficient of volume viscosity for $\omega \rightarrow 0$, c is the velocity of sound.

If we assume that in the substance examined the quantity $\omega\tau$ is of the order of unity, then α/ω^2 will decrease when the frequency increases. For the first and second relaxation regions, α/ω^2 decreases with an increase in frequency (see Fig. 3).

For a constant value of τ the coefficient of absorption will attain the following limiting values when the frequency is varied:

$$\alpha = \frac{\omega^2 \eta_0'}{2\rho c^3} \quad (2)$$

for $\omega\tau \ll 1$, and

$$\alpha_\infty = \frac{\eta_0'}{2\rho c^3 \tau^2} \quad (3)$$

for $\omega\tau \gg 1$.

In the intermediate region the frequency for which (α/ω^2) will have a value equal to one half of its initial value determines the relaxation time of volume viscosity $\left(\omega = \frac{1}{\tau}\right)$. As we should have expected, when the temperature increases, τ decreases for all the investigated relaxation regions; such a result can also be obtained from the theory. The discovered relaxation processes can be described in more detail if we assume that they take place at constant volume ($\Delta v = 0$). Thus in this case it is possible to obtain the following relationship for the dependency of τ_m upon temperature:

$$\tau_m = A \cdot e^{\frac{\Delta E_a}{RT}}. \tag{4}$$

Here τ_m is the relaxation time which corresponds to the maximum value of the absorption μ, A is a constant, E_a is the activation energy which qualitatively satisfies our experimental data.

In fact, if we plot log ω_m along the axis of ordinates and 1/T along the axis of abcissas, then for relaxation regions in ethyl acetate which lie in the temperature range of from –30° to +40° and in the frequency range 2-30 megacycles Formula (4) yields straight lines which are in agreement with the theory [2].

For all of the other investigated substances we obtain the same picture. The decomposition of the straight lines into four segments when the indicated method of checking Formula (4) is utilized is at the same time proof of the presence of not two, but of four relaxation processes in the investigated regions of temperatures and frequencies; these processes have various heats of activation (E_a).

For the four relaxation regions examined in Fig. 7 the heats of activation E_a have the following values: $E_a^{I} = 220$ cal/mole, $E_a^{II} = 42$ cal/mole, $E_a^{III} = 60$ cal/mole, $E_a^{IV} = 13$ cal/mole. In the very same ethyl acetate we have the following values for the relaxation region which lies in the temperature range 160-210°: $E_a^{V} = 199$ cal/mole.

The order of magnitude of the heats of activation for methyl acetate, methyl formate and ethyl formate is the same as that for ethyl acetate.

The specific heats which are associated with the internal degrees of freedom and which are calculated on the assumption that the relaxation processes take place for $\Delta v = 0$, have values of the order of 0.01-0.1 cal/mole · · degree.

It is not difficult (following the method of Lamb and Pinkerton [2]) to show that a formula of the form

$$\mu_m = \frac{1}{2} \pi (\gamma - 1) \frac{c_i}{c_{p_0}} \tag{5}$$

is applicable. Here $\gamma = \frac{c_{p_0}}{c_{v_0}}$; c_{p_0}, c_{v_0} are the equilibrium values of the specific heats, c_i is the specific heat which is associated with the internal degrees of freedom and which applies to all of the substances investigated by us when the relaxation process occurs under conditions where μ_m increases with an increase in temperature.

Thus, in accordance with our experimental data, it is possible to postulate that the relaxation processes which we have examined in methyl acetate, ethyl acetate, methyl formate and ethyl formate arise as a result of the excitation of the molecules of these substances under the condition v = const.

In the substances investigated the relaxation process is of a more complex character within the range of temperatures which are close to the solidifying temperatures of the substances. For a more detailed interpretation of the mechanism of relaxation phenomena in the substances which have been studied, it is necessary to extend the ranges of temperatures and frequencies which are investigated, and at the same time to utilize spectroscopic studies of the same substances.

Extremely important to this plan is the investigation of processes in liquid and vapor phases of the indicated substances in the critical region.

LITERATURE CITED

[1] I. G. Mikhailov and V. A. Solov'ev. "Absorption of ultrasonic waves in liquids and the molecular mechanism of volume viscosity," Progress Phys, Sci. (USSR) 1, 2-50 (1952).

[2] I. Lamb, I. M. Pinkerton, "The absorption dispersion of ultrasonic waves in acetic acid," Proceedings of the Royal Society 199, 114 (1949).

[3] V. F. Iakovlev, N. I. Koshkin, V. F. Nozdrev, "Application of the pulse method to the investigation of ultrasonic absorption in benzene and certain of its halogen derivatives in the vicinity of their solidifying temperatures," Doklady Akad. Nauk SSSR 96, 2, 273-276 (1954).

[4] Iu. N. Bormosov, Investigation of the Absorption of Ultrasonic Waves in Methyl Acetate by Means of the Pulse Method and the Optical Method, (Dissertation) (Moscow Regional Pedagogical Institute, 1956).

[5] V. F. Nozdrev and A. M. Sultanov, "The establishment and study of the two relaxation regions which arise when ultrasonic waves pass through ethyl acetate," Doklady Akad. Nauk SSSR 104, 6, 837-840 (1955).

[6] I. Karpovich, "Investigation of rotational isomers with ultrasound," J. Chem. Phys. 22, 10, 1767-73 (1954).

[7] A. M. Sultanov, Investigation of the Absorption of Ultrasonic Waves in Liquids Which are Relaxational In a Range of Experimentally Realizeable Ultrasonic Frequencies, (Dissertation) (Moscow Regional Pedagogical Institute, 1954).

[8] N. I. Koshkin, V. F. Nozdrev, V. D. Sobolev, M. G. Shirkevich, V. F. Iakovlev, "Pulse method of fixed distances, its physical basis and practical application," J. Acoustics (USSR) 2, 2, 161-166 (1956). [Soviet Physics – Acoustics, pp. 166-171].

Moscow Regional Pedagogical Institute

Received February 15, 1956

FOCUSING OF ACOUSTIC WAVES BY MEANS OF INHOMOGENEOUS MEDIA

L. M. Brekhovskikh

The field of a point-source emitter in a laminarly-inhomogeneous medium is represented in integral form, and the reflection coefficients of plane waves are introduced into this form. In the case of a frequency which is sufficiently high the reflection coefficients can be calculated by means of the Wenzel-Kramers-Brillouin method. The subsequent application of the inflection-point method to the integral yields the field in a ray approximation. The further development of this theory permits us to obtain the equation for caustic surfaces and to find the acoustic pressure both in the vicinity of the caustics and in the region of the point at which they are tangent. This process does not require (as is required in the paper by Haskell [8]) a preliminary determination of a solution in the form of a sum of normal waves. Examples are given.

The phenomena of wave focusing is frequently associated solely with special systems — lenses and mirrors. However, we immediately encounter this phenomenon when we investigate the propagation of acoustic waves in the atmosphere and in the ocean, as well as when we investigate the propagation of seismic waves in the core of the earth. Analogous phenomena are observed when radiowaves are propagated in the atmosphere. Below we shall develop a method for calculating the focusing of waves in laminarly-inhomogeneous media.

1. Let us initially examine focusing when a spherical wave is reflected from an inhomogeneous half-space. Let a non-directional point-source emitter be placed at the point 0 (Fig. 1). The half-space $z > 0$ shall be assumed to be homogeneous. The wave number and density for this half-space shall be defined by k_0 and ρ_0. Corresponding quantities in the inhomogeneous half-space $z < 0$ shall be defined as $k = k(z)$ and $\rho = \rho(z)$. We shall assume that these functions vary slowly enough so that it is possible to apply ray theory. In addition, let

$$k(0) = k_0, \ \rho(0) = \rho_0.$$

The sperical wave $\psi_0 = e^{ikR}$ R which emanates from 0 shall be represented in the form of a superposition of plane waves. Having reflected each of these plane waves from the boundary $z = 0$, we find the expression for the field of the reflected wave•

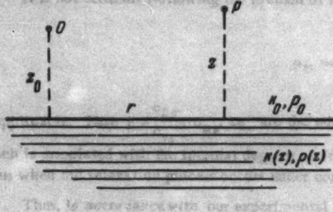

Fig. 1

$$\psi_{\text{refl}} = \frac{i}{2\pi} \int_{-\infty}^{+\infty}\int e^{i[k_x x + k_y y + k_z(z+z_0)]} \cdot V \frac{dk_x \cdot dk_y}{k_z}, \quad (1)$$

where V is the reflection coefficient for each of the plane waves; this coefficient depends upon $k_z = \sqrt{k_0^2 - k_x^2 - k_y^2}$

• The factor $e^{-i\omega t}$ is omitted everywhere.

We replace k_x and k_y by the new variables of integration ξ and α in accordance with the relationships $k_x = \xi \cos\alpha$, $k_y = \xi \sin\alpha$; in addition we place $x = r\cos\varphi$, $y = r\sin\varphi$. Since V depends solely upon ξ, integration with respect to α in (1) can be carried out. The integral yields a Bessel function for which we shall make use of an asymptotic representation by assuming that $k_0 r \gg 1$. Expressing the coefficient of reflection within the framework of geometric acoustics (the Wenzel-Kramers-Brillouin method) we have the expression:

$$V = e^{i\eta(\xi)},\ \eta(\xi) = 2\int\limits_0^{z_{\max}(\xi)} k_z\,dz - \frac{i\pi}{2}, \tag{2}$$

where $k_z = \sqrt{k^2(z) - \xi^2}$, and $z_{\max}(\xi)$ is found from the equation $k(z_{\max}) = \xi$. While proceeding in this manner, we assume that complete reflection takes place (i.e. $|V| = 1$). As a result we obtain from (1)

$$\psi_{\text{refl}} = \frac{e^{i\frac{\pi}{4}}}{\sqrt{2\pi r}}\int\limits_{-\infty}^{+\infty} e^{i(\xi r - w)}\frac{\sqrt{\xi}\,d\xi}{\beta}, \tag{3}$$

where

$$w \equiv -(z + z_0)\beta - \eta,\ \beta \equiv \sqrt{k_0^2 - \xi^2}. \tag{4}$$

We evaluate the integral (3) by means of the inflection-point method. For the inflection-point $\xi = \xi_0$ we have the equation $\left[\frac{\partial}{\partial\xi}(\xi r - w)\right]_{\xi_0} = 0$, or

$$r = w'(\xi_0). \tag{5}$$

Further, we make use of the expansion

$$\xi r - w = \xi_0 r - w(\xi_0) - \frac{1}{2}w''(\xi_0)(\xi - \xi_0)^2. \tag{6}$$

After that, we bring the slowly-varying factors out from under the integral sign in Expression (3), and by utilizing the known value of the Fresnel integral within infinite limits we find

$$\psi_{\text{refl}} = \frac{1}{\beta_0}\sqrt{\frac{\xi_0}{r w''(\xi_0)}}\cdot e^{i[\xi_0 r - w(\xi_0)]}. \tag{7}$$

As a result, we obtained the expression for the reflected wave in an approximation of ray acoustics. Both the phase $\xi_0 r - w(\xi_0)$ of the wave and its amplitude [which is given by the factor standing in front of the exponential in (7)] could also be obtained by means of elementary ray concepts – the former from the optical length of the ray and the latter from the law of expansion governing a tube of rays.

Let us note that ξ_0 and β_0 are associated with the angle of slip of the ray χ_0 (Fig. 2) by the relationship

$$\xi_0 = k_0 \cos \chi_0, \quad \beta_0 = \sqrt{k_0^2 - \xi_0^2} = k_0 \sin \chi_0.$$

The Equality (5) is an equation for a ray in the plane (rz); it should be assigned a simple geometric meaning. Substituting the value of w from (4) into Expression (5) we find

$$r = (z + z_0) \operatorname{ctg} \chi_0 + \Delta, \quad \Delta = -\left(\frac{\partial \eta}{\partial \xi}\right)_{\xi_0}. \tag{8}$$

Here $(z + z_0) \operatorname{ctg} \chi_0$ and Δ are horizontal distances which are correspondingly traversed by a ray in the upper (homogeneous) and lower (inhomogeneous) media (Fig. 2). We have expressed Δ by means of the derivative of the phase reflection coefficient in other papers of ours [1, 2] as well.

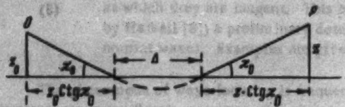
0
P
z_0
χ_0
Δ
χ_0
z
$z_0 \operatorname{Ctg} \chi_0$
$z \cdot \operatorname{Ctg} \chi_0$

Fig. 2

However, let us assume simultaneously with (5) that we have

$$w''(\xi_0) = 0. \tag{9}$$

Expression (7), which was found in a ray approximation, then yields an infinite value of acoustic potential. This case of focusing is the one which is of interest to us. Eliminating ξ_0 from (9) and (5), we find a relationship between r and z which represents the equation for the envelope of the family of rays (of the caustic). Each point on the caustic can be assigned its particular value of ξ_0. If we were interested in the value of the acoustic potential at any of the points which belong to the caustic, then for this purpose it would be sufficient to make use of an expansion of the form (6) where instead of retaining the quadratic term it would be necessary to retain the cubic term $-\frac{1}{6} w'''(\xi_0)(\xi - \xi_0)^3$.

However, we are interested not only in the field in the caustic, but also in the field in the vicinity of the caustic. For this purpose we select an arbitrary point r_0, and z_0 on the caustic, so that this point is determined by the following equations for a given value of ξ_0.

$$r_0 = w'(z_0, \xi_0), \quad w''(z_0, \xi_0) = 0. \tag{10}$$

Let us now take another point r, z_0 which lies on the same level $z = z_0$ and which is at a distance $u = r - r_0$ from the selected point. For this point the expansion of the phase under the integral sign in (3) in powers of $\xi - \xi_0$ with an accuracy of up to the cubic term will have the form:

$$\xi r - w = \xi_0 r - w_0 + u(\xi - \xi_0) - \frac{1}{6} w'''(\xi_0)(\xi - \xi_0)^3, \tag{11}$$

and in carrying out this process $w'(z_0, \xi_0)$ is replaced by r_0, in accordance with (10). Let us again bring $\sqrt{\xi}/B$ outside of the integral sign for the value $\xi = \xi_0$, and let us introduce the following definitions:

$$s = 2^{-1/3}|w'''(\xi_0)|^{1/3}(\xi-\xi_0) = 2^{-1/3}\left|\frac{d^2r}{d\xi_0^2}\right|^{1/3}(\xi-\xi_0);$$
$$t = \pm 2^{1/3}u\left|\frac{d^2r}{d\xi_0^2}\right|^{-1/3}. \qquad (12)$$

In the latter equality the sign is selected according to the following rule: plus (+) when $\frac{d^2r}{d\xi_0^2} < 0$, and minus (−) when $\frac{d^2r}{d\xi_0^2} > 0$; $d^2r/d\xi_0^2$ is found by differentiating Equation (5).

The resulting integral with respect to s from −∞ to +∞ can be separated into two integrals: from −∞ to 0 and from 0 to ∞. In the first of them let us replace s by −s. As a result, both integrals can be combined into one integral which can be taken from 0 to ∞ and which contains a cosine instead of exponents. We finally obtain

$$\psi_{\text{refl}} = 2^{1/3}\frac{1}{\beta_0}\sqrt{\frac{\xi_0}{r}}\left|\frac{d^2r}{d\xi_0^2}\right|^{-1/3}\cdot e^{i\left[\frac{\pi}{4}+\xi_0 r - w(\xi_0)\right]}\cdot v(t), \qquad (13)$$

where v(t) defines the well-known Airy integral [3]

$$v(t) = \frac{1}{\sqrt{\pi}}\int_0^\infty \cos\left(\frac{s^3}{3}+st\right)ds. \qquad (14)$$

In particular

$$v(0) = \frac{\sqrt{\pi}}{3^{2/3}\Gamma\left(\frac{2}{3}\right)} = 0.62927. \qquad (15)$$

The graph of the function v(t)/v(0) is shown in Fig. 3. When t < 0 the function v(t) is of an oscillating character, and for t > 0 it decreases monotonically. The maximum value of the function v(t) is obtained for t = −1.02, [i.e. the field on the caustic itself (t = 0) is not maximum].

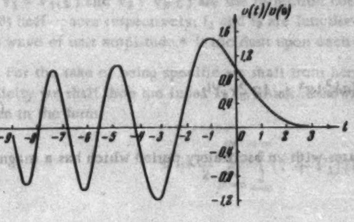

Fig. 3

The values t < 0 correspond to the convex side of the caustic. The oscillating character of the field in this region is due to the interference of the two rays which intersect at each point (Fig. 4). Conversely, there are no rays on the other side of the caustic. The field only penetrates into this region as a consequence of diffraction.

2. Let us examine an example. Let the velocity of sound vary according to law

$$z < 0,\ c^2(z) = \frac{c^2}{1+az},\ a > 0. \qquad (16)$$

when z < 0.

Elementary calculations according to Formulas (2) and (4) yield

$$\eta(\xi) = \frac{4}{3ak_0^2}\beta^3 - \frac{\pi}{2}, \quad w = \frac{\pi}{2} - (z+z_0)\beta - \frac{4}{3ak_0^2}\beta^3. \tag{17}$$

In accordance with (5), the equation for the rays in the reflected field will be

$$r = (z+z_0)\frac{\xi_0}{\beta_0} + \frac{4\xi_0\beta_0}{ak_0^2}, \tag{18}$$

where $\xi_0 = k_0 \cos\chi_0$, and χ_0 is the slip angle of the ray. The equation for the caustic is found by eliminating ξ_0 from (18) and from $\partial r/\partial\xi_0 = 0$. In parameter form this equation can be written:

$$ar = 4\sin 2\chi_0 \cos^2\chi_0, \quad a(z+z_0) = 4\sin^2\chi_0 \cos 2\chi_0. \tag{19}$$

Figure 4 depicts the caustic for the case under examination as well as the rays which form it. The course followed by the rays in the lower medium is now shown.

From (18) we find

$$\frac{d^2r}{d\xi_0^2} = \frac{16}{ak_0^2}\operatorname{ctg}^2\chi_0 \cdot \operatorname{ctg} 2\chi_0.$$

As a result the field on the caustic and in its vicinity will be

$$\psi_{\text{refl}} = \frac{\cos^{1/2}\chi_0}{(\cos 2\chi_0)^{1/2}} \frac{(2k_0^2a)^{1/3}}{(2k_0r)^{1/2}} e^{i\left[\frac{\pi}{4}+\xi_0 r - w(\xi_0)\right]} \cdot v(t). \tag{20}$$

in accordance with (13).

When the frequency is increased the acoustic intensity in the caustic increases as the cube root of the requency.

For the value of t we have

$$t = -\left|\frac{\partial^2 r}{\partial\xi_0^2}\right|^{-1/3} \cdot u = -u\,(ak_0^2 \operatorname{tg}^2\chi_0 \cdot \operatorname{tg} 2\chi_0)^{1/3}. \tag{21}$$

To the right of the caustic (for $t < 0$) the field oscillates with an oscillatory period which has a magnitude of the order of:

$$\Delta u \sim (ak_0^2 \operatorname{tg}^2\chi_0 \cdot \operatorname{tg} 2\chi_0)^{-1/3}. \tag{22}$$

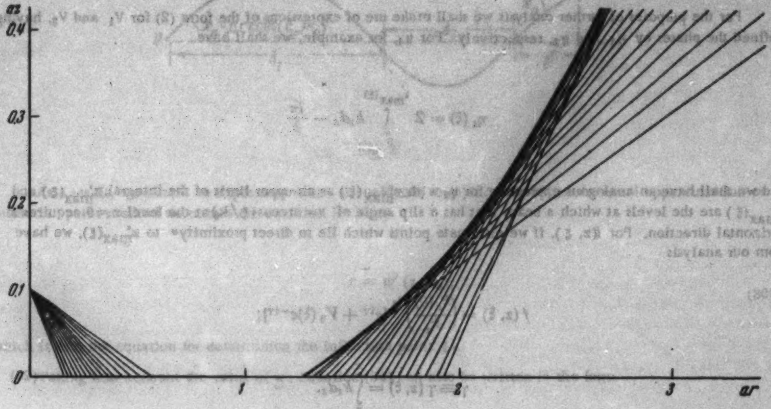

Fig. 4

3. Let us now examine a more complex case where waveguide sound propagation takes place in a laminarly inhomogeneous medium. Let us make the origin coincide with the emitter. In the completely general case the expression for the acoustic potential in each of the inhomogeneous half-spaces can be written [4]:

$$z>0,\ \psi=\frac{i}{2}\int_{-\infty}^{+\infty}\frac{1+V_1}{1-V_1V_2}f_2(z,\xi)\,H_0^{(1)}(\xi r)\,\frac{\xi d\xi}{\beta}; \tag{23}$$

$$z<0,\ \psi=\frac{i}{2}\int_{-\infty}^{+\infty}\frac{1+V_2}{1-V_1V_2}f_1(z,\xi)\,H_0^{(1)}(\xi r)\,\frac{\xi d\xi}{\beta}. \tag{24}$$

Here $V_1 = V_1(\xi)$ and $V_2 = V_2(\xi)$ are the reflection coefficients of plane waves from the lower ($z < 0$) and upper ($z > 0$) half-spaces respectively; f_1 and f_2 are functions which describe the field in these half-spaces when a plane wave of unit amplitude * is incident upon each of them.

For the sake of being specific we shall from here on examine only Expression (23), and for the sake of simplicity we shall drop the index in f_2. As was shown in the paper cited above, this expression can also be written in the form

$$\psi=\frac{i}{2}\sum_{N=0}^{\infty}\int_{-\infty}^{+\infty}(1+V_1)(V_1V_2)^N\cdot f(z,\xi)\,H_0^{(1)}(\xi r)\,\frac{\xi d\xi}{\beta}, \tag{25}$$

---

* For instance, if we are calculating V_1 and f_1, then the inhomogeneous half-space $z < 0$ is augmented by the half-space $z > 0$ from out of which the plane wave is considered to be incident. The parameters of the medium for $z = 0$ are presumed to be continuous.

which corresponds to the representation of the quantity $1/(1-V_1V_2)$ in the form of an infinite geometric progression in (23).

For the purposes of further analysis we shall make use of expressions of the form (2) for V_1 and V_2, having defined the phases by η_1 and η_2, respectively. For η_1, for example, we shall have

$$\eta_1(\xi) = 2\int_0^{z'_{\max}(\xi)} k_z d_z - \frac{i\pi}{2}$$

and we shall have an analogous expression for η_2 with $z''_{\max}(\xi)$ as an upper limit of the integral. $z'_{\max}(\xi)$ and $z''_{\max}(\xi)$ are the levels at which a beam that has a slip angle of $\chi = \arccos(\xi/k_0)$ at the level $z = 0$ acquires a horizontal direction. For $f(z, \xi)$, if we eliminate points which lie in direct proximity* to $z'_{\max}(\xi)$, we have from our analysis

$$f(z, \xi) = \left(\frac{k_z(0)}{k_z}\right)^{1/2}[e^{i\gamma} + V_2(\xi)e^{-i\gamma}];$$

$$\gamma \equiv \gamma(z, \xi) = \int_0^z k_z d_z. \tag{26}$$

Substituting (26) and the corresponding expressions for V_1 and V_2 into (25), we can represent ψ in the form of a sum of terms which have the form

$$\psi_{1N} = \frac{i}{2}\int_{-\infty}^{+\infty} e^{N(\eta_1+\eta_2)}e^{i\gamma}H_0^{(1)}(\xi r)\frac{\xi}{\beta}\left(\frac{k_z(0)}{k_z}\right)^{1/2}d\xi. \tag{27}$$

For a given N there will be three additional terms: ψ_{2N}, ψ_{3N} and ψ_{4N}, in which the quantities $V_1e^{i\gamma}$, $V_2e^{-i\gamma}$ and $V_1V_2e^{-i\gamma}$, will respectively appear under the integral sign in (27) in place of the factor $e^{i\gamma}$. The over-all field will be

$$\psi = \sum_{N=0}^{\infty}(\psi_{1N} + \psi_{2N} + \psi_{3N} + \psi_{4N}). \tag{28}$$

Making use of an asymptotic representation of the Hankel function, we write Expression (27) in the form

$$\psi_{1N} = \frac{e^{\frac{i\pi}{4}}}{\sqrt{2\pi r}}\int_{-\infty}^{+\infty} e^{i(\xi r - w)}\frac{\sqrt{\xi}}{\beta}\left(\frac{k_z(0)}{k_z}\right)^{1/2}d\xi;$$

$$w = -N(\eta_1 + \eta_2) - \gamma. \tag{29}$$

---

* The size of the region which is thus excluded is evaluated in [1].

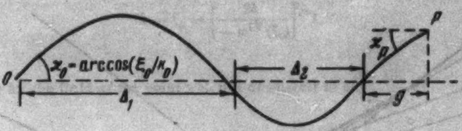

Fig. 5

As a result, we obtain an expression which is analogous to (3). As above, in the usual approximation of the inflection point method we obtain the equation for a ray

$$r = w'(z,\ \xi_0), \tag{30}$$

which is also the equation for determining the inflection point ξ_0.

Taking into account the value of $\underline{w}$, Equation (30) can also be written in the form

$$r = N(\Delta_1 + \Delta_2) + g(z),$$

where

$$\Delta_1 = -\frac{\partial\eta_1}{\partial\xi_0},\quad \Delta_2 = -\frac{\partial\eta_2}{\partial\xi_0},\quad g(z) = -\frac{\partial\gamma}{\partial\xi_0}. \tag{31}$$

The geometric meaning of the quantities which have been introduced here is evident from Fig. 5 where the case N = 1 has been depicted.

A large number of rays may arrive at the given point in the general case; these rays correspond both to identical and to different values of N. Further analysis is completely identical for any of the rays and is analogous to the analysis conducted in Part 1 of this paper.

In a ray approximation, taking into account the quadratic terms of the expansion of $\underline{w}$ in powers of $\xi - \xi_0$ we obtain from (29) a formula for ψ_{1N} which differs from (7) solely by the additional factor $(k_z(0)/k_z)^{1/2}$. Taking into account the relationships $w''(\xi_0) = \partial r/\partial\xi_0$, $k_z(0) = \beta_0 = k_0 \sin\chi_0$, $\xi_0 = k_0\cos\chi_0$, $k_z = k(z)\sin\chi_\rho$, where χ_0 and χ_ρ are the slip angles of the ray at the points where the emitter and receiver are located (these angles are related to each other by the relationship $k_0\cos\chi_0 = k(z)\cos\chi_\rho$), we obtain:

$$\psi_{1N} = \left[r\,\frac{\partial r}{\partial\xi_0}\,k(z)\,\mathrm{tg}\,\chi_0\sin\chi_\rho\right]^{-1/2}\cdot e^{i[\xi_0 r - w(\xi_0)]}. \tag{32}$$

The caustic is found by means of eliminating ξ_0 from Equation (30) and from the equation

$$\frac{\partial r}{\partial\xi_0} = w''(\xi_0) = 0. \tag{33}$$

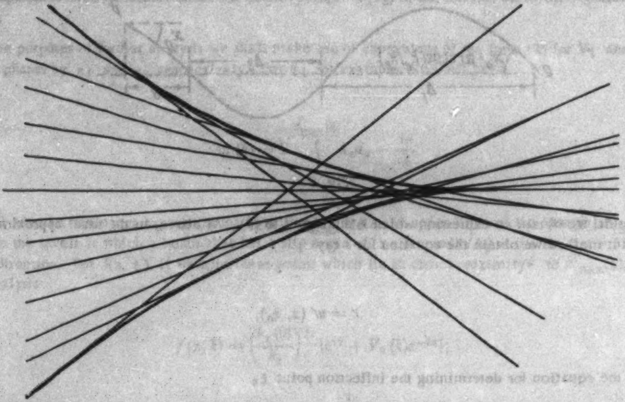

Fig. 6

The field on the caustic and in its vicinity is given by a formula which is analogous to (13), or by

$$\psi_{1N} = 2^{1/3}\left[rk(z)\,\mathrm{tg}\,\chi_0 \sin\chi_0\right]^{-1/2}\left|\frac{d^2r}{d\xi_0^2}\right|^{-1/3} e^{i\left[\frac{\pi}{4}+\xi_0 r - w(\xi_0)\right]}\,v(t). \tag{34}$$

The magnitude of t is determined as before by Relationship (13).

4. Expression (34), which we have obtained for the field in the vicinity of the caustic, ceases to be valid in the vicinity of the points where the caustics which satisfy the equations

$$r = w'(z,\ \xi_0),\quad w''(z,\ \xi_0) = 0,\quad w'''(z,\ \xi_0) = 0,$$

are tangent; the primes (as they do above) indicate differentiation with respect to ξ_0. At these points focusing takes place which is of a higher order than that which takes place in the caustic. In order to obtain the value of ϕ_{1N} near the point of tangency between caustics it is necessary to expand the expression for the phase (w) into a power series of $\xi-\xi_0$ which includes terms up to the fourth power. In doing this we obtain the following expression at the actual point of tangency of the caustics:

$$\psi_{1N} = \left[2\pi rk(z)\,\mathrm{tg}\,\chi_0 \sin\chi_0\right]^{-1/2} e^{i\left[\frac{\pi}{4}+\xi_0 r - w(\xi_0)\right]} \times \int\limits_{-\infty}^{+\infty} e^{-\frac{1}{24}w^{IV}(\xi_0)(\xi-\xi_0)^4}\,d\xi. \tag{35}$$

Here let us introduce a new variable of integration t in accordance with the relationship

$$\xi - \xi_0 = \left[\frac{24}{-w^{\mathrm{IV}}(\xi_0)}\right]^{1/4} t,$$

and then we will obtain for the field at the point which is of interest to us:

$$\psi_{1N} = [\pi rk(z)\,\mathrm{tg}\,\chi_0 \sin\chi_0]^{-1/2}\left[\frac{6}{-w^{\mathrm{IV}}(\xi_0)}\right]^{1/4} I_0, \tag{36}$$

$$\text{where } I_0 = \int_{-\infty}^{+\infty} e^{it^4}\,dt = 1.813\,e^{i\frac{\pi}{8}}.$$

The field in the vicinity of the point of tangency of the caustics is investigated in the paper cited in [5]. Figure 6 shows the region of tangency of the caustics and the paths of the corresponding rays. Let us note that the theory developed above is completely analogous to the theory of focusing in optical systems which have aberration [6]. The author has already indicated comparatively long ago [7] one important case of the focusing of acoustic waves in inhomogeneous media. The theory which has been developed here can be applied without difficulty to the case examined in [7]. The problem of focusing in the waveguide propagation of sound is also touched upon in [8]. However, the method developed there seems to us to be more unwieldy, and it requires, for example, the preliminary computation of a solution which has the form of a sum of normal waves.

LITERATURE CITED

[1] L. M. Brekhovskikh and I. D. Ivanov, "Extending the boundaries for the applicability of ray theory in the investigation of wave propagation in laminated media," Doklady Akad. Nauk SSSR 83, 4, 545-548.

[2] L. M. Brekhovskikh, "Reflection of pulse wave beams," Prog. Phys. Sci. 50, 4, 539-576 (1953).

[3] V. A. Fok, Tables of Airy Functions (Moscow, 1946).

[4] L. M. Brekhovskikh, "The field of a point source in a laminarly-inhomogeneous medium," Bull. Acad. Sci. USSR Phys. Ser. 13, 5, 505-514 (1949).

[5] T. Pearcey, "The structure of an electromagnetic field in the neighborhood of a cusp of a caustic," Phil. Mag. 37, 311-317 (1946).

[6] L. Brillouin, "Sur. une methode de calcul approchee de certaines integrales, dite methode de col," Ann. ecole norm. super. 33, 17 (1916).

[7] L. M. Brekhovskikh, "The propagation of sound in an underwater acoustic channel," Doklady Akad. Nauk SSSR 69, 157-160 (1949).

[8] N. A. Haskell, "Asymptotic approximation for the normal modes in sound channel wave propagation," J. Appl. Phys. 22, 157-168 (1951).

Acoustics Institute Acad. Sci. USSR, Moscow Received February 28, 1956

THE PROBLEM OF WAVEGUIDE PROPAGATION OF SOUND IN INHOMOGENEOUS MEDIA

Iu. L. Gazarian

The paper derives and investigates the field of a point-source spherical emitter which is located in a laminarly-inhomogeneous medium in which the velocity of sound varies according to the law indicated by Epstein.

At the present time there is a standard mathematical procedure for calculating the field of a point-source spherical harmonic emitter which is located in a laminarly-inhomogeneous medium; this method leads to an integral representation of the field. From the physical point of view the process of solution can be represented as the decomposition of the field of a point source in free space into plane waves (homogeneous and inhomogeneous), the obtaining of some analog for these plane waves in the medium under investigation, and the subsequent integration over the resulting functions.

Thus, for each specific case represented by a sound velocity which varies according to a particular function (the density of the medium is presumed to be constant) the finding of the integral representation of the field reduces to finding solutions which are analogous to plane waves in a homogeneous space. These analogs of plane waves are obtained by solving a wave equation which is written in the rectangular system of coordinates in such a way that one of its axes is directed perpendicular to the layers of the medium; the method used in this solution is the separation-of-variables method. The character of such solutions is determined by the selected function according to which the velocity of sound varies. In the oft-examined case of a medium which consists of several homogeneous layers the solutions reduce to a combination of incident and reflected plane waves. However, in the case where the properties of the medium vary continuously the solutions become more complex. However, it should be noted that this increase in complexity is only a seeming one. The point is that from a mathematical point of view the solution will be the simpler, the smoother the function which is given for the variation of sound velocity. From this point of view the solution in the case of several homogeneous layers (i.e., when the function which represents the sound velocity is given in such a manner that it is not only not smooth, but is also a discontinuous function) is considerably more complex than when a sound-velocity function is given in terms of some analytical function. Such a point of view can be illustrated by utilizing the problem of the waveguide propagation of sound in a laminarly-inhomogeneous medium. The problem in this case reduces to finding the poles of the expression under the integral sign in the intergral representation and to the investigation of their dependency upon frequency. In order to verify what has been said above, it is sufficient to indicate that in the simplest case of a homogeneous layer which lies upon a homogeneous half-space the calculation of the poles leads to a transcendental equation which in the case of frequencies which are not too great can only be solved empirically. At the same time, as we shall show below, in the case when the velocity of sound is given by an analytical function which approximates a homogeneous layer that lies between two homogeneous half-spaces the poles are expressed very simply in terms of frequency.

The law utilized below for the dependency of the propagation velocity of the wave was proposed by Epstein [1] for the electromagnetic case; this law showed that solutions which are analogous to plane waves can be expressed in terms of elementary and hypergeometric functions. Assuming that in the acoustic case the density of the medium is constant and the z axis is directed vertically upwards, the dependency of the sound velocity $c(z)$ upon height can be conveniently represented in the following form:

$$\frac{1}{c^2(z)} = \frac{A}{\mathrm{ch}^2 \frac{z}{H}} + B \,\mathrm{th}\, \frac{z}{H} + C.$$

Here

$$A = \frac{1}{c_0^2} - \frac{1}{2}\left(\frac{1}{c_\infty^2} + \frac{1}{c_{-\infty}^2}\right), \quad B = \frac{1}{2}\left(\frac{1}{c_\infty^2} - \frac{1}{c_{-\infty}^2}\right), \quad C = \frac{1}{2}\left(\frac{1}{c_\infty^2} + \frac{1}{c_{-\infty}^2}\right),$$

where $c_\infty = c(+\infty)$, $c_{-\infty} = c(-\infty)$, $c_0 = c(0)$. The parameter H characterizes the thickness of the intermediate layer. If $A > \left|\frac{B}{2}\right|$ (which we shall assume is fulfilled), then a sound channel exists whose axis is located at a height

$$z = H \,\mathrm{arth}\, \frac{B}{2A}.$$

Let us note that the whole problem will be considerably simplified when the velocities in the upper and lower half-spaces are equal to each other at infinity. When this condition obtains $B = 0$, and $c(z)$ is an even function of z (the symmetrical Epstein layer). If the dependency upon time is given by the factor $(-i\omega t)$ (which we shall discard from here on), then the velocity potential φ of the point-source spherical emitter which is located at the point $(0, z_0)$ of a cylindrical coordinate system (r, z) is given by the formula

$$\varphi(r, z) = \frac{H}{2} \int_{-\infty}^{+\infty} \Phi_1(\zeta)\,\Phi_2(\zeta_0)\,\Gamma\left(\nu + \frac{\lambda+\mu}{2}\right)\Gamma\left(1 - \nu + \frac{\lambda+\mu}{2}\right) H_0^{(1)}(\xi r)\,\xi d\xi.$$

when $z \geq z_0$. Here $\nu = \frac{1}{2} + \sqrt{\frac{1}{4} + A\omega^2 H^2}$ (the arithmetic root is taken), $\zeta = z/H$,

$\zeta_0 = z_0/H$, $\mu^2 = H^2(\xi^2 - k_\infty^2)$, $\lambda^2 = H^2(\xi^2 - k_{-\infty}^2)$, where $k_\infty = \omega/c_\infty$, $k_{-\infty} = \omega/c_{-\infty}$,

$$\Phi_1(\zeta) = e^{-\mu\zeta}\frac{(1+e^{-2\zeta})^\nu}{\Gamma(1+\mu)} F\left(\nu + \frac{\mu+\lambda}{2},\ \nu + \frac{\mu-\lambda}{2};\ 1+\mu;\ -e^{-2\zeta}\right)$$

(for $\zeta < 0$ the analytical continuation of the hypergeometric series should be used). $\Phi_2(\zeta_0)$ is obtained from $\Phi_1(\zeta)$ by the replacement of (λ, μ, ζ) by $(\mu, \lambda, -\zeta_0)$. In the integral it is assumed that special points which lie upon the real axis are circumvented and that over the integration path $\mathrm{Re}\,\mu, \lambda \geq 0$, $\mathrm{Im}\,\mu, \lambda \leq 0$. The field for $z < z_0$ is obtained by replacing ζ by ζ_0 and vice versa. In the case of a symmetrical layer $\lambda = \mu$ and Φ_1 reduces to a spherical function:

$$\Phi_1(\zeta) = P_{\nu-1}^{-\mu}(\mathrm{th}\,\zeta).$$

In investigating the field in the vicinity of the channel axis at distances from the emitter which are sufficiently great, the path of integration can be deformed upwards in the complex plane of ξ. When this occurs the function $\varphi(r, z)$ reduces to two lateral waves and a sum of normal waves; the former are determined by line integrals whose paths follow two vertical loops which encompass the branching points; the latter are determined by subtraction at those poles of the function under the integral sign which are affected when the contour is deformed. The amplitude of the lateral waves decreases as $1/r^2$, and the normal waves decreases as $1/\sqrt{r}$; thus the problem reduces to investigating only the normal waves. It proves to be true that the only poles which can be affected during the deformation of the contour are the zeros of $\dfrac{1}{\Gamma\left(1-\nu+\frac{\lambda+\mu}{2}\right)}$.

Thus the s-th pole is determined by the relationship

$$\lambda+\mu=2(\nu-1-s),$$

where s = 0, 1, 2, ... The path of integration can be assumed to pass along the upper sheet of a four-sheet Riemann surface. At low frequencies all of the poles lie on the lower sheets on the real axis. When the frequency increases they are shifted along the real axis and approach the branching points which are furthest away from the origin. At a certain critical frequency ω_0 a zero pole arrives at a branching point and passes through into an upper sheet, going farther away from the origin along the real axis with an increase of the frequency. Since after it arrives on an upper sheet which lies in the right half-plane the pole is affected by a deformation of the integration path, a transition through the critical frequency denotes the appearance of a normal wave. The remaining poles also behave in exactly the same way when the frequency increases.

For the s-th normal wave the critical frequency is determined from the equation

$$H\omega_s\sqrt{2B}+1+2s-\sqrt{1+4AH^2\omega_s^2}=0$$

(here it is assumed that $B \geq 0$ for the sake of being specific), and for the zero normal wave it is necessary to choose a root which is different from zero in the case where $B \neq 0$. When $B = 0$, $\omega_0 = 0$ (i.e., the zero normal wave exists at all frequencies).

The value of the s-th pole is given by the expression

$$\xi_s=\sqrt{k_{-\infty}^2+\left[\frac{\Delta}{2H}+\frac{H}{2\Delta}\left(k_{\infty}^2-k_{-\infty}^2\right)\right]^2}, \text{ where } \Delta=2(\nu-1-s).$$

The velocity potential of the s-th normal wave is given by the expression

$$(H\varphi)_s=i(-1)^s\frac{\pi}{\Gamma(1+s)}\frac{\Gamma(2\nu-1-s)}{\Gamma(\lambda)\Gamma(\mu)}\exp\left\{\frac{\mu-\lambda}{2}(\zeta+\zeta_0)\right\}\times$$
$$\times\frac{G_s\left(2\nu-1-2s,\ 1+\mu,\ \frac{1-\operatorname{th}\zeta}{2}\right)}{(2\operatorname{ch}\zeta)^{\nu-1-s}}\frac{G_s\left(2\nu-1-2s,\ 1+\lambda,\ \frac{1+\operatorname{th}\zeta_0}{2}\right)}{(2\operatorname{ch}\zeta_0)^{\nu-1-s}}H_0^{(1)}(r\xi_s). \tag{1}$$

Here G_s is a Jacobian polynomial of the s-th order. It can be proven that (1) is symmetrical with respect to ζ, ζ_0.

The solution is considerably simplified in the case of a symmetrical layer. When this condition obtains, the even-order normal waves are even functions of z, and the odd-order normal waves are odd functions of z.

For the even normal waves (1) can be written in the form

$$(H\varphi)_{2\sigma} = i(\nu - 1 - 2\sigma)\frac{\Gamma\left(\sigma + \frac{1}{2}\right)}{\Gamma(\sigma + 1)}\,\frac{\Gamma\left(\nu - \sigma - \frac{1}{2}\right)}{\Gamma(\nu - \sigma)} \times$$
$$\times \frac{G_\sigma\left(\nu - 2\sigma - \frac{1}{2},\ \frac{1}{2},\ \mathrm{th}^2\zeta\right)}{\mathrm{ch}^{\nu - 1 - 2\sigma}\zeta}\,\frac{G_\sigma\left(\nu - 2\sigma - \frac{1}{2},\ \frac{1}{2},\ \mathrm{th}^2\zeta_0\right)}{\mathrm{ch}^{\nu - 1 - 2\sigma}\zeta_0} \times$$
$$\times H_0^{(1)}\left\{\frac{r}{H}\sqrt{H^2 k_\infty^2 + (\nu - 1 - 2\sigma)^2}\right\}$$
$$(\sigma = 0,\ 1,\ 2,\ \ldots).$$

For odd waves:

$$(H\varphi)_{2\sigma+1} = i4(\nu - 2 - 2\sigma)\frac{\Gamma\left(\sigma + \frac{3}{2}\right)}{\Gamma(\sigma + 1)}\,\frac{\Gamma\left(\nu - \sigma - \frac{1}{2}\right)}{\Gamma(\nu - \sigma - 1)}\,\mathrm{th}\,\zeta\,\mathrm{th}\,\zeta_0 \times$$
$$\times \frac{G_\sigma\left(\nu - 2\sigma - \frac{1}{2},\ \frac{3}{2},\ \mathrm{th}^2\zeta\right)}{\mathrm{ch}^{\nu - 2 - 2\sigma}\zeta}\,\frac{G_\sigma\left(\nu - 2\sigma - \frac{1}{2},\ \frac{3}{2},\ \mathrm{th}^2\zeta_0\right)}{\mathrm{ch}^{\nu - 2 - 2\sigma}\zeta_0} \times$$
$$\times H_0^{(1)}\left\{\frac{r}{H}\sqrt{H^2 k_\infty^2 + (\nu - 2 - 2\sigma)^2}\right\}.$$
$$(\sigma = 0,\ 1,\ 2,\ \ldots).$$

Let us note that in the case of a symmetrical layer we can easily obtain a solution when there is an absolutely reflecting boundary on the axis of the channel: it is sufficient to introduce an imaginary emitter which is either in phase or in phase-opposition with the actual emitter. When this is done the field reduces either to doubled even normal waves or to doubled odd normal waves.

In conclusion let us provide a graph of the factors which produce the amplitude distribution of the normal waves with respect to the height dimension for the case of a symmetrical layer (see Figure). The dimensionless

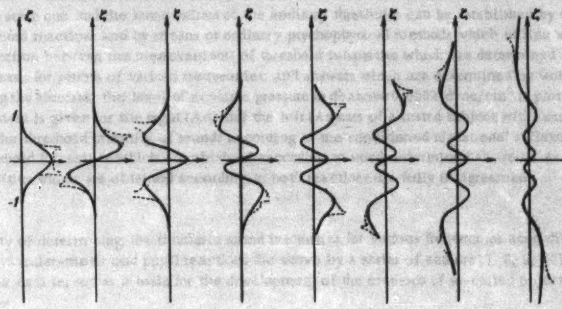

height ζ is plotted along the axis of ordinates. The dimensionless quantity ν which characterizes the remaining parameters is assumed to be equal to 8.5 (the case when there are 8 normal waves and the frequency lies approximately half-way between the eigth and ninth critical frequencies). The graph also shows the values obtained by the Wenzel-Kramers-Brillouin method by means of a dotted line.

LITERATURE CITED

[1] P. S. Epstein, "Reflection of waves in an inhomogeneous absorbing medium," Proc. Nat. Acad. Sci. US 16, 10, 627-637 (1930).

Acoustics Institute of the Acad. Sci. USSR, Moscow Received February 21, 1956

SOME NEW METHODS OF MEASURING HUMAN HEARING AND THE RESULTS OBTAINED BY THESE METHODS

G. V. Gershuni

The article provides the essential data for new methods of auditory measurement which are based upon the utilization of the conditioned reactions of human beings to sound. The data provided shows: 1) that the absolute auditory thresholds and differential limits for the frequency and intensity of pure tones can be measured in human beings with the same reliability by means of these reactions as they can by means of word response; 2) that in certain cases conditioned reflexes are detected which are sub-threshold within the limits of from 1 to 6 db with respect to word response.

On the basis of the facts obtained, attention is focused upon the meaning of the central mechanisms which sharpen and deepen the degree of discrimination between the frequencies and intensities of tonal signals.

As we know, the fundamental quantitative characteristics of hearing in a human being are observed by means of utilizing so-called psychophysical methods. In these methods the answer reactions of a human being to sound signals which are applied to him are based upon the utilization of word instructions which emanate from the experimentor. In relation to the considerable development of the investigative methods of conditioned reactions in human beings during the past few years, it is natural that the question should arise as to whether it is possible to measure hearing on the basis of utilizing other, more elementary reactions than those which are dependent upon words. For this purpose the author and his co-workers developed methods for measuring hearing according to various response reactions to sound: by means of the conditioned cutaneo-galvanic method [1, 3], by means of the nictational method [2], by means of the electro-cortical method [3, 4], by means of the eye-movement method [5], by means of the pupil method [6]. Measurement of the absolute auditory thresholds was possible by means of all of the indicated reactions.* These measurements showed that in adults with normal hearing who are in an awakened state one and the same values of the auditory thresholds can be established by means of the various conditioned reactions and by means of ordinary psychophysical methods which utilize word answers. Figure 1 gives a comparison between the measurements of threshold intensities which are determined by conditioned nictational reflexes for sounds of various frequencies, and answers which are determined by words; the frequencies are plotted along the abscissa, the level of acoustic pressure in db above 0.0002 dyne/cm^2 is plotted along the ordinate. The data is given for the right (Ad) and the left (As) ears of a tested subject with normal hearing. The crosses denote the threshold intensity of sounds according to the conditioned nictational reflexes. The circles denote the threshold intensities which are obtained according to word-determined answers. As can be seen, the threshold intensities which are obtained according to both reactions are fully in agreement.

---

* The possibility of determining the threshold sound intensities for various frequencies according to conditioned skin-galvanic, vascular-motor and pupil reactions are shown by a series of authors [7, 8, 9, 10], and this fact coupled with our data served as a basis for the development of the methods of so-called objective audiometry in various countries.

However, a measuring process which leads to the attainment of one and the same threshold values may require the application of a various number of stimuli when utilizing word answers and various procedures for generating the conditioned reactions. Figure 2 shows the results of measuring threshold sound intensities by means of the method of constant stimuli (for a 1,000 cps tone), using word-response reactions and conditioned nictational reflexes during various periods of their generation. The sound intensity in db above a level of 0.0002 dyne/cm^2 is plotted along the axis of abscissas; the percentage of positive answers at a given sound intensity level is plotted along the axis of ordinates. The threshold intensity is calculated by using points which correspond to 50% positive answers. Curve 1 corresponds to data obtained during the earlier periods of the generation of conditioned nictational reflexes. The threshold intensity is 13.5 db. Curve 2 corresponds to data obtained in the later stages of stable conditioned nictational reflexes. This curve coincides with the dotted curve that connects the black circles which express the data for the word-response answers; it can be seen that the threshold intensities for both reactions coincide at a level of 9 db. Curve 3 corresponds to data obtained in the very late stage of the extended generation of conditioned nictational reflexes. The threshold intensity has a level of 6 db (i.e., is 3 db below the threshold of word-response answers).

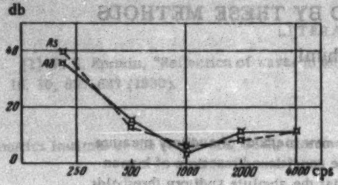

Fig. 1

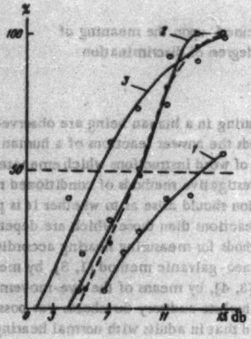

Fig. 2

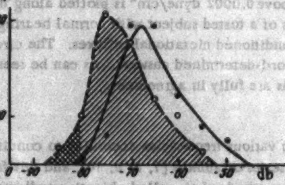

Fig. 3

Thus it can be detected that under the specific conditions of an extended generation of conditioned reactions in people with normal hearing the absolute thresholds determined by certain reactions may prove to be 1-6 db below the thresholds established by word-response answers [6, 11]. Thus Figure 3 shows distribution curves for the threshold intensities of tonal signals (1,000 cps) which evoke word-response answers (the solid circles) and conditioned cutaneo-galvanic reactions (open circles). The intensity in db from a level of 1 dyne/cm^2 is plotted along the abscissa; the frequency of occurrences in percentages of the over-all number of answers is plotted along the ordinate. The cross-hatched area at the left indicates the region where overlapping of the reactions is absent at the smallest intensity; the lined area indicates the region where the reactions overlap. The threshold intensity, calculated from the maximum answer frequency, is 68 db for answers which are dependent upon words; the threshold intensity for conditioned cutaneo-galvanic reactions is 75 db.

The measurement of the limiting variations in the frequency (Δf) and the intensity (ΔJ) of pure tones, which was accomplished by utilizing conditioned nictational reflexes, made it possible to detect the same magnitudes of differential thresholds in experimental subjects as those threshold magnitudes which were established in these subjects by the ordinary psychophysical method. Thus Figure 4 shows the agreement between the results of measuring threshold variations in the frequency (Δf) (Figure 4,a) and intensity (ΔJ) (Figure 4,b) from the word-response answers and from the conditioned nictational reactions.

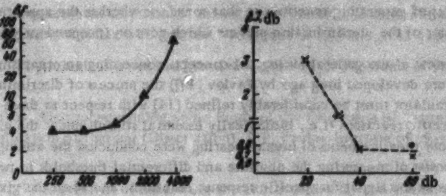

Fig. 4

TABLE

	Variant I	Variant II	Difference
Threshold intensity (I_0) of a 500 cps tone with a duration of 0.2 sec. (in db from a level of 0.0002 dynes/cm^2).	20	45	25 db
Minimum limit of frequency variation (Δf) of a 1000 cps tone with a duration of 1 sec. The level is 30 db.	5	70-100	65-95 cps
Minimum limit of intensity variation (ΔI) of a 1000 cps tone. The level is 30 db.	1	15-18	14-17 db

Figure 4,a shows the data obtained from the measurement of the differential frequency thresholds. The frequency is plotted along the abcissa, and the threshold variation of frequency in cps is plotted along the ordinate. The dots indicate the data obtained from measurements involving word-response answers, and the triangles indicate the data obtained from conditioned nictational reflexes. Figure 4,b shows the data obtained from the measurement of the differential intensity thresholds. The sound intensity (a 1,000 cps tone) in db above a level of 0.0002 dynes/cm^2 is plotted along the abscissa ; the threshold intensity variations in db are plotted along the ordinate. Crosses indicate the data obtained from the conditioned nictational reflexes; the hollow circles indicate the data obtained from word-response answers.

When we examine the facts which are presented above it becomes evident that the quantitative characteristics of human hearing can be established on the basis of utilizing various systems of organism response reactions. From this point of view, reactions which are utilized in the usual psychophysical methods of measurement can be characterized (as we have already said) as a group of word-response reactions. Reactions which are utilized in the methods of auditory measurement which have been worked out by us and by other researchers can be characterized as a group of experimentally-created conditioned reactions which are formed on the basis of various biologically existing systems of reactions – defensive, thermo-regulatory, alimentary, play (in children) etc. The utilization of various systems of reaction appreciably broadens the possibilities of auditory measurement, since if under specific conditions of a given type reactions are either absent, or are misrepresented, or are non-authentic, then it is within the powers of the experimentor to develop a new system of conditioned reactions to sound by means of which it is possible to accomplish the measurement. The development of such a situation has particularly important practical significance for the investigation of hearing in children (especially in children of an early age), for the investigation of various central auditory disorders and for the examination of hearing in adults [2, 12].

In examining the above discussed procedure for measuring hearing by means of various reactions, the question arises as to whether the actual process of discriminating between the specific properties of sound is associated with the process of generating reactions to that sound, or whether the appearance of the reaction only serves as a simple indicator of the discrimination process which goes on independently in the nervous system.

From the point of view of the general biological concepts concerning an organism as a self-regulatory system (these concepts were developed long ago by Pavlov [13]) the process of discriminating between the properties of an external stimulator must be considerably refined [14] with respect to those stimuli which become conditioned signals of specific reactions (i.e., biologically essential stimuli under the given conditions). Under the conditions for which our measurements of human hearing were conducted the attempt at obtaining an answer to this question had to consist of measuring the absolute and differential thresholds in two typical cases: when the given pure tone serves as the signal for specific response reactions, and when the given tone does not represent such a signal (i.e., when the pure tone is, in accordance with the terminology utilized in the physiology of higher nervous activity, an indifferent stimulator). If the first variant is the general case of measuring hearing by means of conditioned reactions, then the second variant (which consists of measuring hearing without the presence of response reactions that serve as an indicator of the discrimination process) is at first glance impossible of achievement.

However, it is possible to attempt an approach to such an investigation by means of indirect measurements. Among a number of attempts that were made in our laboratory at studying this problem, the following one is considered. In this attempt [15] the indicator of the discrimination process consisted of the effect produced by the measured sound upon the characteristics (concealed periods) of the conditioned reactions which were generated not in response to the measured acoustic stimulator, but in response to some other stimulator which differed from it in its properties. In utilizing such a method of measurement it was possible to investigate threshold intensities of a pure tone and the minimum limits of the variation in frequency and intensity which occurred in the two above indicated experimental variants — in one case the tonal stimulator served as a signal for specific response reactions, and in the other case it served as an indifferent stimulator (the state of the subject in the latter case could psychologically be defined as a state which consisted of a complete lack of attention to the stimulator). The results of the measurements obtained are shown in the table (it should be indicated here that so far sufficient data has been amassed for the measurement of threshold intensities); they show with sufficient clarity that when one and the same tonal stimulator serves as the signal for the response reactions (Variant I) or is an indifferent (Variant II) stimulator, the degree of discrimination of that tone evidences tremendous discrepancies.

The facts which have been presented indicate that the process of discriminating between the properties of sounds is associated with the conditions under which the reactions to these sounds are generated. Therefore the generated conditioned reaction is not only an indicator of the discrimination process, but is also a factor which affects the quantitative characteristics of the discrimination process by means of the central mechanisms (for which analogs may be constructed with feedback mechanisms to a definite degree).

It is well known that in the literature devoted to the theories of hearing the problem concerning the mechanism which guarantees a high degree of discrimination with respect to the frequency of sound is being actively debated [16]. Various central mechanisms are being discussed, in particular those central mechanisms which must guarantee the subsequent "refining" of the frequency analysis of the sound, which is accomplished in the cochlea. In discussing these "refining" mechanisms attention is turned to the additional significance of a number of processes, in particular the pulsation frequency in the nerve ducts, the time dispersion in the synapses of the auditory channels etc. However, in discussing the possible mechanisms of the "refining" effect, it must be said that at the present time insufficient attention is being given to the significance of those higher central mechanisms which, as the data provided in this paper shows, can cause either a corresponding "refinement" or "dulling" of the degree of discrimination with respect to the acoustic stimulator, depending upon the conditions under which the reactions to that stimulator are generated. It can be assumed that a special feature of these mechanisms is the fact that a variability of the auditory characteristics is guaranteed which corresponds to the conditions which are created for the activity of the organism.

LITERATURE CITED

[1] G. V. Gershuni and I. I. Korotkin, "Subsensory conditioned reflexes produced by acoustic stimuli," Doklady Akad. Nauk SSSR 57, 417-420 (1947).

[2] R. V. Avakian, "Measurement of threshold intensities of sounds and differential frequency thresholds by means of conditioned nictational reflexes in humans," Problems of Physiological Acoustics 3, 53-59 (1955).

[3] G. V. Gershuni, "Physiological bases of objective audiometry," Problems of Physiological Acoustics. 1950, No. 2, 3-7.

[4] V. A. Kozhevnikov, Electroencephalographic Study of the Formation of Temporary Communications by Means of Auditory Stimulation of Humans (Dissertation), I. P. Pavlov Institute of Physiology of the Acad. Sci. USSR, 1951.

[5] A. M. Maruseva, "The problem of measuring the limits of the discrimination between acoustic signals in a human," Problems of Physiological Acoustics 1955, No. 3, 60-66.

[6] G. V. Gershuni, "Reflex reactions in terms of their relationship to sensations when external stimuli act upon the sensory organs," Physiological Journal USSR 35, 541-56 (1949).

[7] J. E. Bordley and W. G. Hardy, "A study in objective audiometry with a use of a psychogalvanic response," Ann. Otol. Rhinol. and Laryngol.58, 751-759 (1949).

[8] R. Maspetiol, L. Gougerot and E. Korine,"L'audiometrie objective par etude du reflexe psychogalvanique," La semaine des Hopitaux 27, 2867-78 (1954).

[9] Ia. Z. Brailovskii, "The cochleo-pupilar reflex and its significance in the examination of the auditory function," Bulletin of Otorhinolaryngology 16, 4, 25-30 (1954).

[10] O. S. Vinogradova and E. N. Sokolov, "Study of the sensitivity of the auditory analyzer in deaf children by the method of registering vascular reactions," Problems of Physiological Acoustics 3, 67-74 (1955).

[11] G. V. Gershuni, "The special features of cutaneo-galvanic reactions and the reactions of alpha-rhythm suppression which arise in humans due to the effects of sub-threshold and super-threshold acoustic stimuli," Journal of Higher Nervous Activity 5, 665-676 (1955).

[12] G. V. Gershuni, "Study of the activity of the human auditory analyzer on the basis of using various reactions," Problems of Physiological Acoustics 3, 45-52 (1955).

[13] I. P. Pavlov, Natural Science and the Brain (1909); Complete Works (1949). Vol. 3, pp. 95-104.

[14] I. P. Pavlov, Lectures on the Functioning of the Great Hemispheres of the Brain (1926); Complete Works (1947). Vol. 4, pp. 100-101.

[15] L. A. Chistovich, "The variation of the discrimination threshold of acoustic stimulation when the signal-value of the stimulus varies," Physiological Journal USSR 41, 485-492 (1955).

[16] E. G. Weaver and M. Lawrence, Physiological Acoustics (Princeton University Press, New Jersey, 1954).

I. P. Pavlov Institute of Physiology of the
Acad. Sci. USSR, Leningrad

Received February 8, 1956

A MODULATION METHOD OF MEASURING ULTRASONIC DISPERSION

V. A. Zverev

The paper describes a method for the direct measurement of wave dispersion; this method is based upon the variation in the nature of the modulation of a wave when it is propagated in a dispersing medium. Results are given for experiments which were made for the purpose of verifying this method and for determining its possibilities in measuring ultrasonic dispersion.

The study of the dispersion of elastic and electromagnetic waves in various media is of great significance with regard to clarifying structures of these media and the mechanisms of the processes which go on in the media. Very many papers have been devoted to the investigation of the dispersion of elastic and electromagnetic waves of various frequency ranges. However, because of the low sensitivity of the existing methods of measuring dispersion, it has not been possible up to now to verify the existence of a number of subtle dispersion phenomena in acoustics which have been theoretically predicted; a number of assertions concerning experimentally observed dispersion phenomena give rise to serious doubts [1].

Usually the magnitude of the dispersion is determined by comparing the results of measuring the phase velocity c at various frequencies ω. It is evident that in doing this the scattered nature of the values for c, which is caused by the inaccuracy of the measurements, will maximize a small dispersion; in addition, the observed difference in the values of c can be caused not by dispersion but by small variations in the investigated medium during the process of measurement.

This fact clarifies the necessity for developing a special method for the measurement of dispersion — a method which is free from the limitations of the existing methods of measurement. A number of papers of such a nature have been written during recent years by American authors [2, 3]. Here a method of direct dispersion measurement [4, 5] is described, and this method is applicable both in the case of elastic and in the case of electromagnetic waves; in principle it has unlimited sensitivity.

We shall characterize the dispersion by the quantity $D = \frac{d^2k}{d\omega^2}$, where $k = \omega/c$ is the wave number. We shall call the quantity D the dispersion parameter. It is easy to see that in the absence of dispersion $D = 0$. We have developed a method of directly measuring the quantity D (and therefore the dispersion as well); this method is based upon the variation of the nature of the modulation in the wave which is propagated in the dispersing medium.

Before passing on to a description of the method let us briefly dwell upon several properties of the modulated oscillation.

Let us examine an oscillation of the form:

$$u = B(t)\sin[\omega_0 t + \Phi(t)] = A_0 \sin(\omega_0 t - \varphi_0) + A_1 \sin(\omega_1 t - \varphi_1) + A_2 \sin(\omega_2 t - \varphi_2), \tag{1}$$

where $\omega_{1,2} = \omega_0 \pm \Omega$; $\Omega \ll \omega_0$.

The form of the modulating functions $B(t)$ and $\Phi(t)$ in (1) depends upon the relationship between the amplitudes A_0, A_1, A_2 and the phases φ_0, φ_1, φ_2; the latter enter solely into the following combination:

$$\Theta = \varphi_0 - \frac{\varphi_1 + \varphi_2}{2}. \tag{2}$$

This combination of phases proves to be the sole combination which is invariant with respect to the variation of the time origin. Let us call it the phase invariant of the oscillation described by (1). In accordance with (1) the quantity $B^2(t)$ can be represented in the form

$$B^2(t) = M_0 + M_1 \cos(\Omega t + \alpha) + M_2 \cos(2\Omega t + \beta). \tag{3}$$

We shall assume that by means of a quadratic detector and filter we can isolate the harmonic wave with a modulation frequency Ω from the oscillation in Equation (1). The amplitude of this harmonic will be

$$M_1 = 2A_0 \sqrt{A_1^2 + A_2^2 + 2A_1A_2 \cos 2\Theta}. \tag{4}$$

When Θ varies, M_1 changes from a maximum $2A_0(A_1 + A_2)$ to a minimum $2A_0(A_1 - A_2)$. In the case when $A_1 = A_2$, the magnitude of M_1 passes through zero each time that $\cos 2\Theta = -1$. Let us note that when $A_1 = A_2 \ll A_0$ this condition corresponds to phase modulation and the condition $\cos 2\Theta = 1$ corresponds to amplitude modulation of the oscillation described by Equation (1) (i.e., a variation in Θ leads to a change of phase modulation into amplitude modulation and vice versa).

Let us now assume that an emitter which oscillates according to the Law (1) radiates a plane wave in the positive direction of the x axis. Then at some point which is at a distance x from the emitter the phases of the harmonic components in (1) will be:

$$\varphi_1 = \varphi_{10} - k_1 x;\ \varphi_2 = \varphi_{20} - k_2 x;\ \varphi_0 = \varphi_{00} - k_0 x, \tag{5}$$

where φ_{i0} are the phases at the point where the emitter is located, and $k_i = \frac{w_i}{c(w_i)}$ $(i = 0, 1, 2)$.

From Equations (2) and (5) we obtain the phase invariant at point x:

$$\Theta_x = \Theta_0 - \left(k_0 - \frac{k_1 + k_2}{2}\right) x. \tag{6}$$

Expanding the quantities k_i into a power series of Ω in the vicinity of ω_0 and limiting ourselves to terms with Ω^3, we have

$$\Theta_x = \Theta_0 - \frac{1}{2} D x \Omega^2. \tag{7}$$

It follows from the equation we have obtained that when dispersion is present in the medium the phase invariant of the oscillation will vary to the degree that the wave is propagated. From Equations (4) and (7) it follows that the distance between the planes where the nature of the modulation is identical is $L = 2\pi/D\Omega^2$. In principle it is possible to find D by measuring L, but for a small dispersion such a measurement is difficult. In such a case the measurement of the dispersion can be accomplished in the following manner. We shall measure the magnitude of θ_0 at the emitter and shall observe the magnitude of M_1 at two points in the medium which are a distance d apart along the x axis. The difference between the input values of θ_0 which result in a minimum M_1 at the first and second observation points yields a variation of the phase invariant in the medium when the wave is propagated to a distance d; according to this variation the value of D is determined on the basis of Equation (7). The accuracy of measuring the value of D is determined by the accuracy with which it is possible to ascertain the presence of a minimum in M_1. This in turn is determined solely the the level of the intrinsic noise of the amplifying apparatus utilized. By utilizing amplifiers with a sufficiently narrow band pass for measuring M_1 it is possible to attain (in principle) a sensitivity which is as high as desired.

For the purpose of experimentally verifying the above discussed concepts an investigation was conducted of the dispersion of longitudinal acoustic waves in a thin wire ($r \ll \lambda$, where r is the radius of the wire, λ is the wavelength). In this case the theory leads to the formula

$$D = \frac{3}{4}\frac{\sigma^2 r^2 \omega}{c^3}, \tag{8}$$

where σ is the Poisson coefficient.

We conducted our experiments on a nickel wire with a radius of 0.4 mm at $\omega_0 = 2\pi \cdot 10^6$ radians/sec; $\Omega = 2\pi \cdot 10^3$ radians/sec. The velocity of sound c was $5.3 \cdot 10^5$ cm/sec according to our measurements. The selection of the material of the wire was based upon the fact that it had a strong magnetostrictional effect; this effect was utilized for the excitation and reception of acoustic waves.

The block diagram of the experiment is depicted in Fig. 1. The modulated waves in the form of pulses are fed from the generator 1 to the coil 2. Here they are simultaneously radiated in the directions of the ends P and Q. Each time that a pulse which has been subjected to reflection passes through the coil 3 the pulse excites an emf in this coil, and this emf is received by the amplifier 4. The location of the coils along the wire was such that each successive pulse traversed a path which was 1.6 meters longer than the previous one. The picture of the pulses which are obtained on the screen of oscilloscope 9 is shown in Fig. 2,a. An oscilloscope 8 is inserted after detector II and the filter which passes the frequency Ω. If the magnitude of the deflection on oscilloscope 9 is caused by the value of the quantity M_0 (3), then the magnitude of the deflection on oscilloscope 8 is caused by the value of the quantity M_1. The corresponding picture is given in Fig. 2,b. The ratio of the amplitudes of pulses having the same number is proportional to the depth of amplitude modulation at the frequency Ω. If in the first pulse the amplitude modulation is close to zero, then in each of the succeeding pulses the depth of modulation increases. This can be explained by the variation of the magnitude of Θ due to dispersion when x increases. The results of the quantitative measurements are in complete agreement with the theoretical Formula (8).

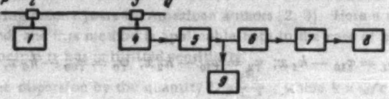

Fig. 1. 1) Generator of the modulated waves; 2) transmitting coil; 3) receiving coil; 4) amplifier; 5) detector I; 6) modulation frequency filter; 7) detector II; 8, 9) oscilloscopes.

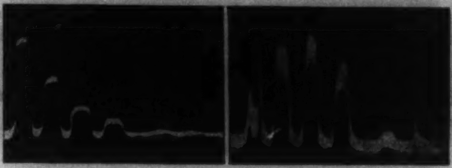

Fig. 2. Pictures on the oscilloscope screens: a) after detector I; b) after detector II.

The detection of dispersion under the very same conditions by means of measuring the phase velocity separately at various frequencies would have required measurement of the phase velocity of sound with a relative accuracy of 10^{-4}.

The above method of measuring dispersion is applicable only in the case of traveling waves. When standing waves are present the change in the nature of modulation occurs every quarter wavelength. This fact complicates the method of conducting the experiment, and therefore it is preferable to conduct the measurements with a traveling wave. In the experiments which have just been described, a pulse operating regime was utilized in order to obtain a traveling wave. In experiments in which the described method was utilized in a liquid a continuous operating regime was utilized in order to obtain the maximum sensitivity; this required the utilization of a sound receiver which would not violate the traveling-wave regime. We utilized an optical indicator which consisted of a unit for observing the diffraction of light by ultrasonic waves. The first diffraction maximum fell upon a photoelement at whose output a modulation-frequency filter was connected. When the acoustic field is weak and when the light beam is normally incident upon the acoustic beam, the intensity of the first diffraction maximum is proportional to B^2. By shifting the light beam it is possible to investigate the dependency of the spectrum of B^2 upon $\underline{x}$ and to determine the magnitude of D. Experiments were conducted in water at a frequency of 1 megacycle and at a modulation frequency of 100 kc; the purpose of these experiments was to determine the sensitivity of the method we have described. In conducting these experiments it was ascertained that dispersion was absent. The sensitivity of the unit to a variation of the phase invariant when the filter had a bandwidth of the order of 1 kc was of the order of 10^{-3}. This corresponds to a magnitude of D which is of the order of 10^{-15} $\mathrm{sec}^2/\mathrm{cm}$ at a path length of 10 cm (i.e., to a variation of the sound velocity by an amount of the order of 1 cm/sec. for a frequency variation of 100 kc.

I express my deep appreciation to G. S. Gorelik for his valuable advice.

LITERATURE CITED

[1] I. G. Mikhailov, Ultrasonic Wave Propagation in Liquids, State Tech. and Theor. Lit. Press, Moscow, 1949.

[2] F. E. Fox and T. M. Marion, "Ultrasonic dispersion in water solution of magnesium sulfate," J. Acoust. Soc. Am. 25, 4, 661-668 (1953).

[3] T. King, McCubbin, "Dispersion of the velocity of sound in water between 500 and 1500 kilocycles," J. Acoust. Soc. Am. 26, 2, 247-249 (1954).

[4] V. A. Zverev, A Certain New Method of Investigating Ultrasonic Dispersion, Collected Works Dedicated to the Memory of Academician A. A. Andronov (Acad. Sc. USSR Press, Moscow-Leningrad, 1955). pp. 657-680.

[5] V. A. Zverev, "Modulation method of measuring ultrasonic dispersion," Doklady Akad. Nauk SSSR 91, 4, 791-794 (1953).

Gorky Physics-Engineering Research Institute
of the Gorky State University

Received January 17, 1956

THE SCATTERING AND RADIATION OF WAVES BY STATISTICALLY INHOMOGENEOUS AND STATISTICALLY OSCILLATING SURFACES

M. A. Isakovich

The paper examines the application of the Kirchoff principle to the problem of wave scattering at a plane surface with statistical distribution of the reflection coefficient, and the problem of radiation by statistically oscillating surfaces.

The paper cited in [1] discussed the problem of the scattering of acoustic (as well as electromagnetic) waves at a statistically roughened surface which had roughnesses with dimensions much larger than the wavelength of the incident radiation. The problem was solved by means of utilizing the Kirchoff principle – the field at the scattering surface was given according to the laws of geometric optics. Further analogous results were obtained in the paper cited in [2] as well.

In this present paper the Kirchoff principle is applied to two more diffraction problems: to the problem of the scattering of waves from a plane surface with a statistical distribution of the local reflection coefficient, and to the problem of the radiation of sound by statistically oscillating surfaces.

Scattering from a Plane Surface with a Statistical Distribution of the Reflection Coefficient

The introduction of the concept of a local reflection coefficient already presupposes the application of the Kirchoff principle. It is assumed that the field at a given point in the plane is the same as if the entire plane had the same properties as it does in the vicinity of the given point. Thus it is necessary to require a sufficiently slow change in the properties of the surface from point to point.

Let the plane $z = 0$ of a Descartesian coordinate system coincide with the scattering plane. Denoting the angle of slip for the incident plane wave by ψ and assuming that the axis $\underline{x}$ lies in the incident plane, let us write the potential of the wave in the form $\Phi = e^{ik(x\cos\psi - z\sin\psi)}$. Applying the Kirchoff principle to the Green formula and following the operations indicated in [1], we obtain the potential of the scattered field in the Frauenhofer region at a distance which is much greater than the dimensions of the scattering surface; this expression is of the form

$$\Phi = \frac{k(\sin\psi + \sin\chi)}{4\pi r}\iint\limits_S V\exp\{ik[x(\cos\psi - \cos\chi\cos\varphi) - y\cos\chi\sin\varphi]\}\,dS. \qquad (1)$$

Here $\underline{r}$ is the distance to the observation point, V is the reflection coefficient (a statistical function of the point); the definitions of the angles are clear from the figure;* the integration is conducted over the entire scattering surface whose area we shall define as S. Let $V = V_0 + \zeta$, where $V_0 = \overline{V}$[*] is the average value of the coefficient of reflection. Then

---

* In the figure the angle χ is erroneously denoted by the letter $\underline{h}$.

$$\Phi = V_0 \frac{k(\sin\psi + \sin\chi)}{4\pi r} \iint \exp\{ik[x(\cos\psi - \cos\chi\cos\varphi) - y\cos\chi\sin\varphi]\}\, dS +$$
$$+ \frac{k(\sin\psi + \sin\chi)}{4\pi r} \iint \zeta \exp\{ik[x(\cos\psi - \cos\chi\cos\varphi) - y\cos\chi\sin\varphi]\}\, dS. \quad (2) \tag{2}$$

The first term yields the reflection from a homogeneous plate of area S with a reflection coefficient V_0. The second term, with which we shall be dealing exclusively from here on, yields the unknown scattering. Here ζ is the fluctuation of the reflection coefficient (a statistical function); the average value of ζ is equal to zero. In carrying out the Kirchoff principle, ζ varies little at distances which are of the order of a wavelength. Let us note that (as always when the Kirchoff principle is utilized) Formula (2) can be utilized only for those directions for which calculation yields a large value of the scattered field.

The average intensity of the scattered field is found according to the formula

$$I = \overline{\Phi\Phi^*} = \frac{k^2(\sin\psi + \sin\chi)^2}{16\pi^2 r^2} \iiiint \overline{\zeta(x, y)\zeta^*(x', y')} \times$$
$$\times \exp\{ik[(x - x')(\cos\psi - \cos\chi\cos\varphi) - (y - y')\cos\chi\sin\varphi]\}\, dx\,dx'\,dy\,dy' \tag{3}$$

Here the asterisk denotes a complex-conjugate quantity. For the unidimensional problem (ζ depends only upon $\underline{x}$; the observation is conducted in the plane of incidence) we have, assuming that the length of the surface in the direction of the $\underline{y}$ axis is equal to unity,

$$I = \frac{k^2(\sin\psi + \sin\chi)^2}{16\pi^2 r^2} \int_0^L \int_0^L \overline{\zeta(x)\zeta^*(x')} \exp[ik(x - x')(\cos\psi - \cos\chi)]\, dx\,dx'. \tag{4}$$

Here L is the length of the scattering area along the $\underline{x}$ axis.

Let us now assume that the amplitude and phase of the quantity ζ are statistically independent and that all the values of the phase from 0 to 2π have an equal probability. Then the statistical properties of the real and imaginary portions of ζ will be identical. If we denote the mean-square value of ζ by σ^2, and the correlation coefficient of the real or imaginary portion of ζ by $r(x-x') = r(\tau)$, then $\overline{\zeta(x)\zeta^*(x')} = \sigma^2 r(\tau)$. If in addition, we assume that the radius of correlation τ_0 of the quantity ζ is small in comparison to L, then Equation (4) can be written in the form

$$I = L \frac{k^2\sigma^2(\sin\psi + \sin\chi)^2}{16\pi^2 r^2} \int_{-\infty}^{+\infty} r(\tau)\, e^{-ik(\cos\psi - \cos\chi)\tau}\, d\tau. \tag{5}$$

If, for example, the correlation coefficient is of the form $r(\tau) = e^{-|\tau|/\tau_0}$, then

$$I = L \frac{k^2\sigma^2(\sin\psi + \sin\chi)^2}{8\pi^2 r^2} \frac{\tau_0}{1 + (k\tau_0)^2(\cos\psi - \cos\chi)^2}. \tag{6}$$

---

[*] The line above the letter V here and further on indicates an aggregate average.

For a two-dimensional inhomogeneity (under the condition that it is isotropic) we find analogously

$$I = S\frac{k^2\sigma^2(\sin\psi+\sin\chi)^2}{8\pi r^2}\int_0^\infty r(\tau)\,J_0\left(k\tau\sqrt{\cos^2\psi+\cos^2\chi-2\cos\psi\cos\chi\cos\varphi}\right)\tau\,d\tau. \tag{7}$$

For the correlation coefficient $r(\tau) = e^{-|\tau|/\tau_0}$ we obtain

$$I = S\frac{k^2\sigma^2(\sin\psi+\sin\chi)^2}{8\pi r^2}\,\frac{\tau_0^2}{1+(k\tau_0)^2(\cos^2\psi+\cos^2\chi-2\cos\psi\cos\chi\cos\varphi)}. \tag{8}$$

From Equations (6) and (8) it is evident that when the radius of correlation is increased the directional characteristic of the scattering becomes sharper and its maximum approaches the direction of mirror reflection from the plane.

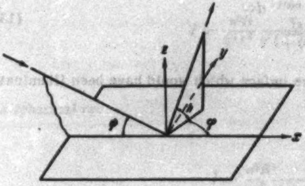

Radiation From a Statistically Oscillating Surface

As in the preceding problem, we shall begin by examining the unidimensional case. If the emitting surface is flat, then the field can be found by utilizing a single-term Green formula and expressing the potential in terms of the normal velocity u at the surface. If the normal velocity depends solely upon x, then it is possible to write

$$\Phi = \frac{1}{2\pi r}\int_0^L u(x)\,e^{-ik\cos\chi x}\,dx, \tag{9}$$

in the Frauenhofer region for a given frequency of radiation, where χ is the angle of slip for the direction of observation and the width of the surface in the direction of the y axis is assumed to be equal to unity. The average intensity will be equal to

$$I = \overline{\Phi\Phi^*} = \frac{1}{4\pi^2 r^2}\iint \overline{u(x)\,u^*(x')}\,e^{-ik\cos\chi(x-x')}\,dx\,dx'. \tag{10}$$

Introducing the same postulates that we introduced in the previous section and retaining the same notation, we obtain

$$I = L\frac{\sigma^2}{4\pi^2 r^2}\int_{-\infty}^{+\infty} r(\tau)\,e^{ik\cos\chi\tau}\,d\tau. \tag{11}$$

For the correlation coefficient of $r(\tau) = e^{-|\tau|/\tau_0}$ we obtain

$$I = \frac{\sigma^2}{2\pi^2 r^2}\,\frac{L\tau_0}{1+(k\tau_0)^2\cos^2\chi}. \tag{12}$$

Formulas (11) and (12) are precise ones. We shall now obtain, utilizing the Kirchoff principle, approximate formulas for the radiation from curved surfaces.

Let the radiating surface be a cylinder which has a generant parallel to the y axis and a velocity distribution which is dependent solely upon the arc length of the directional. If the radius of curvature of the directional is much greater than the radiating wavelength, then according to the Kirchoff principle the field at the surface can be considered equal to the field which would be created by a tangent plane having the same distribution of normal velocities. Further, if sectors which are large in comparison to the displacement correlation radius of points on the surface are also much smaller than the radius of curvature, then it is again possible to use the single-term Green Formula (9) for them; the fields which are created in a given direction by various sectors will be combined on the basis of energy calculations. Thus in this case it can be assumed that each surface element of length dL (large in comparison to the correlation radius) will create an intensity

$$dI = dL\frac{\sigma^2}{4\pi^2 r^2}\int r(\tau)\, e^{ik\cos\chi\tau} d\tau,$$

where χ will now vary from point to point on the surface. The resultant intensity will therefore be equal to

$$I = \frac{\sigma^2}{4\pi^2 r^2}\int dL \int r(\tau)\, e^{ik\cos\chi\tau}\, d\tau. \tag{13}$$

The external integration is conducted only over that portion of the surface which would have been illuminated by a source located at the observation point.

For $r(\tau) = e^{-|\tau|/\tau_0}$, we obtain

$$I = \frac{\sigma^2\tau_0}{2\pi^2 r^2}\int \frac{dL}{1+(k\tau_0)^2\cos^2\chi} = \frac{\sigma^2\tau_0}{2\pi^2 r^2}\int \frac{R(\chi)\, d\chi}{1+(k\tau_0)^2\cos^2\chi}, \tag{14}$$

where $R(\chi)$ is the radius of curvature. For example, for a circular cylinder the limits of integration are equal to 0 and π, and from Equation (14) we find

$$I = \frac{\sigma^2 R}{2\pi r^2}\frac{\tau_0}{\sqrt{1+(k\tau_0)^2}}, \tag{15}$$

where R is the radius of the cylinder.

It is interesting that for $k\tau_0 \gg 1$ the field intensity does not depend upon the correlation radius; it proves to be equal to the intensity created by an in-phase oscillating cylinder with a velocity-amplitude of σ for the points on its surface. The physical reason for this fact becomes clear if we take into account that the radiation has cylindrical symmetry and that the radiation resistance of a unit area under the assumed conditions is equal to ρc both for a statistically oscillating as well as for an in-phase oscillating cylinder.

Analogously we can solve the problem for any curved surface. It is not difficult to see (see, for example, [1]) that in this case an element of the surface creates an intensity

$$dI = dS\frac{\sigma^2}{2\pi r^2}\int_0^\infty r(\tau)\, J_0(k\tau\cos\chi)\tau d\tau). \tag{16}$$

For $r(\tau) = e^{-|\tau|/\tau_0}$ we have a resultant intensity

$$I = \frac{\sigma^2 \tau_0^2}{2\pi r^2} \iint \frac{\frac{1}{K}\, d\Omega}{[1+(k\tau_0)^2 \cos^2 \chi]^{3/2}}, \tag{17}$$

where K is the Gaussian curvature of the surface, and $d\Omega$ is the element of the solid angle which is utilized in a spherical depiction of the surface. Thus for a sphere with a radius R we find

$$I = \frac{\sigma^2 R^2}{r^2} \frac{\tau_0^2}{1+(k\tau_0)^2}. \tag{18}$$

Here as well, the intensity of the field does not depend upon the correlation when the correlation is large.

In conclusion we shall find the intensity which is created at the axis of symmetry by the oscillations of a cylindrical arc with a central angle of 2α and by a spherical arc with a central angle of 2α. For a cylindrical arc,

$$I = \frac{\sigma^2 R}{\pi^2 r^2} \frac{\tau_0}{\sqrt{1+(k\tau_0)^2}} \operatorname{arc\,tan}[\tan\alpha \sqrt{1+(k\tau_0)^2}].$$

For a spherical arc,

$$I = \frac{\sigma^2 R^2}{r^2} \frac{\tau_0^2}{1+(k\tau_0)^2} \left[1 - \frac{\cos\alpha}{\sqrt{1+(k\tau_0)^2 \sin^2\alpha}}\right].$$

Thus when the surface has a small sag ($\tan\alpha \sqrt{1+(k\tau_0)^2} \ll 1$ and $(k\tau_0)^2 \sin^2\alpha \ll 1$ respectively) the formulas yield values for the field which would be radiated by a flat sheet having the same area. For large central angles the field of the arc is equal to the field of a complete cylinder or sphere.

LITERATURE CITED

[1] M. A. Isakovich, "Scattering of waves from a statistically uneven surface," J. Exptl.-Theoret. Phys. 23, 3, 305-314 (1952).

[2] C. Eckart, "The scattering of sound from the sea surface," J. Acoust. Soc. Am. 25, 566-570 (1953).

Acoustics Institute of the Acad. Sci. USSR, Moscow

Received February 21, 1956

THE UTILIZATION OF LAYERS THAT ELIMINATE THE FORMATION OF TRANSVERSE WAVES WHEN A LONGITUDINAL WAVE IS REFLECTED FROM THE BOUNDARY OF A SOLID BODY

M. A. Isakovich

The paper poses and solves the problem of the suppression of the transverse waves which arise when sound is reflected in solid bodies; the solution is accomplished by means of a solid layer which is deposited upon the surface of the solid body.

1. As is known, when a longitudinal sound wave is reflected from the boundary of a solid body, a reflected transverse wave also arises; the amplitude of this transverse wave is determined by the mechanical parameters of the material and by the angle of incidence of the wave. The appearance of two reflected waves (instead of one wave as is the case in a liquid) is associated with the nature of the conditions at the free boundary of the solid body where it is required that both the normal and the tangent stress components become zero.

In a number of cases (for example, in sound optics) the appearance of an additional reflected wave may be undesirable. In relation to this, the present paper indicates a method for eliminating transverse waves which arise when a longitudinal wave is reflected from the boundary of a solid body. The method consists of depositing a solid layer of definite thickness upon the boundary of the solid body; this layer is made of a different material and is rigidly coupled (for example, by soldering) with the original body. When a certain condition is fulfilled (this condition is imposed upon the parameters of the materials and upon the angle of incidence; it will be formulated below) it is possible to select a layer of such thickness that the transverse wave will not appear and the longitudinal wave will be reflected entirely in the form of a longitudinal wave; during this process both longitudinal and transverse standing waves will be excited.

A certain analogy to translucent layers in acoustics and optics can be indicated here; however, in contrast to the known cases, the wave which here interferes with reflection and which can be eliminated is a wave of a different type than the incident wave.

2. Utilizing the usual method of calculating long acoustic lines, we introduce the condition that the reflected transverse wave must be absent for some given frequency ω. This condition will correlate the parameters of the materials of the body and the layer, as well as angle of incidence of the longitudinal wave, to the unknown thicknesses of the layer.*

Let the plane longitudinal wave be incident at an angle of slip χ upon the boundary $z = 0$ of a solid body beyond which a solid layer of thickness $\underline{h}$ consisting of another substance is located; let this layer be rigidly coupled with the body over the entire contact surface. We shall denote the densities of the materials and the propagation velocities of the longitudinal and transverse waves in the body and in the layer respectively by ρ, c_l, c_t and ρ', c_l', c_t'. From here on we shall utilize the prime to distinguish quantities which relate to the layer from quantities which relate to the body or which relate equally to the body and to the layer.

Let us introduce the scalar and vector displacement potentials φ and $\vec{\psi}$. If the incident plane of the wave is assumed to be the plane $\underline{xz}$, then in view of the symmetry of the conditions only the component along the $\underline{y}$ axis will be different from zero in the vector potential. The equations of motion can thus be written in the following form:

---

* During the entire calculation we shall neglect the absorption of acoustic waves.

$$\Delta\varphi + k_l^2\varphi = 0; \quad \Delta\psi + k_t^2\psi = 0. \tag{1}$$

Here $k_l = \omega / c_l$ and $k_t = \omega / c_t$ are the wave numbers of the longitudinal and transverse waves respectively. The particle displacements (which take place parallel to the xz plane) are expressed by the formulas:

$$\begin{aligned} u_x &= \frac{\partial\varphi}{\partial x} - \frac{\partial\psi}{\partial z}, \\ u_z &= \frac{\partial\varphi}{\partial z} + \frac{\partial\psi}{\partial x}. \end{aligned} \tag{2}$$

The stresses in the medium are written in the form

$$\begin{aligned} \sigma_{xz} &= \rho c_t^2\left[-k_t^2\psi + 2\left(\frac{\partial^2\varphi}{\partial x\,\partial z} - \frac{\partial^2\psi}{\partial z^2}\right)\right], \\ \sigma_{zz} &= \rho c_t^2\left[-k_t^2\varphi + 2\left(-\frac{\partial^2\varphi}{\partial x^2} + \frac{\partial^2\psi}{\partial x\,\partial z}\right)\right]. \end{aligned} \tag{3}$$

In the general case six reflected and refracted waves (three longitudinal and three transverse) appear at the boundary between the solid body and the layer; the trace of these waves will travel along the boundary with the same velocity as the trace of the incident wave. Figure 1 shows the wave vectors for all of these waves; these vectors are laid off from one point on the boundary of the solid body. Their projections upon the x axis are equal to one another and are equal to the projection $k_l \cos \chi$ of the wave vector of the incident wave φ_0. Let us introduce the notation for the potentials of the individual plane waves in accordance with the diagram. Here ψ_r is that reflected transverse wave which it is desired to suppress.

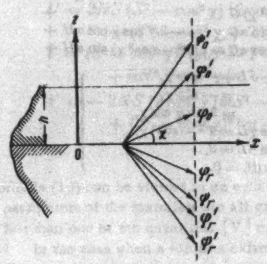

Fig. 1

The potentials in the solid body and in the layer will respectively be equal to

$$\left.\begin{aligned} \varphi &= \varphi_0 + \varphi_r, & \psi &= \psi_r, \\ \varphi' &= \varphi_0' + \varphi_r', & \psi' &= \psi_0' + \psi_r'. \end{aligned}\right\} \tag{4}$$

If we assume that the amplitude of the incident wave is unity, then the potentials of the individual waves can be written in the following form:

$$\begin{aligned} \varphi_0 &= \exp\left[ik_l(x\cos\chi + z\sin\chi)\right], & \varphi_r' &= D\exp\left[ik_l(x\cos\chi - zN)\right], \\ \varphi_r &= A\exp\left[ik_l(x\cos\chi - z\sin\chi)\right], & \psi_0' &= E\exp\left[ik_l(x\cos\chi + zS)\right], \\ \psi_r &= B\exp\left[ik_l(x\cos\chi - zT)\right], & \psi_r' &= F\exp\left[ik_l(x\cos\chi - zS)\right]. \\ \varphi_0' &= C\exp\left[ik_l(x\cos\chi + zN)\right], & & \end{aligned} \tag{5}$$

Here the following notation has been introduced:

$$T=\sqrt{\frac{c_l^2}{c_t^2}-\cos^2\chi},\quad N=\sqrt{\frac{c_l^2}{c_l'^2}-\cos^2\chi},\quad S=\sqrt{\frac{c_l^2}{c_t'^2}-\cos^2\chi}.$$

At the contact surface between the body and the layer, the boundary positions must be fulfilled which guarantee that the normal and tangent velocities, as well as the normal and tangent stresses in the body and in the layer, are equal:

$$u_x=u'_x,\quad u_z=u'_z;\quad \sigma_{xz}=\sigma'_{xz},\quad \sigma_{zz}=\sigma'_{zz}\ \text{for}\ z=0. \tag{6}$$

At the free boundary of the layer, the boundary conditions must be fulfilled which guarantee that the normal and tangent stresses are equal to zero:

$$\sigma'_{xz}=0,\quad \sigma_{zz}=0\ \text{for}\ z=h. \tag{7}$$

In accordance with (2), (3), (5), it is possible to write (6) and (7) in the following form:

$$\left\{\begin{array}{l}
\cos\chi A + TB - \cos\chi G + \\
-\sin\chi A + \cos\chi B - NH + \\
2\sin\chi\cos\chi A + (T^2-\cos^2\chi)B + 2mN\cos\chi H + \\
-(T^2-\cos^2\chi)A + 2T\cos\chi B + m(S^2-\cos^2\chi)G + \\
-i2N\cos\chi\sin\alpha G - 2N\cos\chi\cos\alpha H + \\
-(S^2-\cos^2\chi)\cos\alpha G - i(S^2-\cos^2\chi)\sin\alpha H +
\end{array}\right.$$

$$\left.\begin{array}{r}
+SL = -\cos\chi, \\
-\cos\chi K = -\sin\chi, \\
-m(S^2-\cos^2\chi)K = 2\sin\chi\cos\chi, \\
+2mS\cos\chi L = T^2-\cos^2\chi, \\
+(S^2-\cos^2\chi)\cos\beta K + i(S^2-\cos^2\chi)\sin\beta L = 0, \\
-i2S\cos\chi\sin\beta K - 2S\cos\chi\cos\beta L = 0.
\end{array}\right\} \tag{8}$$

Here the following notation has been introduced:

$$C+D=G,\quad C-D=H,\quad E+F=K,\quad E-F=L,$$

$$\frac{\rho' c_t'^2}{\rho c_t^2}=m,\quad k_l N h=\alpha,\quad k_l S h=\beta.$$

In order for the reflected transverse wave to be absent, the amplitude B must become zero. In order for that to take place, the determinant

$$\begin{vmatrix} \cos\chi & -\cos\chi & -\cos\chi & 0 & 0 & S \\ -\sin\chi & -\sin\chi & 0 & N & -\cos\chi & 0 \\ 2\sin\chi\cos\chi & 2\sin\chi\cos\chi & 0 & 2mN\cos\chi & -m(S^2-\cos^2\chi) & 0 \\ -(T^2-\cos^2\chi) & T^2-\cos^2\chi & m(S^2-\cos^2\chi) & 0 & 0 & 2mS\cos\chi \\ 0 & 0 & -i2N\cos\chi\sin\alpha & -2N\cos\chi\cos\alpha & (S^2-\cos^2\chi)\cos\beta & i(S^2-\cos^2\chi)\sin\beta \\ 0 & 0 & -(S^2-\cos^2\chi)\cos\alpha & -i(S^2-\cos^2\chi)\sin\alpha & -i2S\cos\chi\sin\beta & -2S\cos\chi\cos\beta \end{vmatrix} \tag{9}$$

must be equal to zero.

Expanding the determinant and carrying out simplifications, we come finally to the following condition for the absence of the reflected transverse wave:

$$U + V\sin\alpha\sin\beta + W\cos\alpha\cos\beta = 0. \tag{10}$$

Here

$$\begin{aligned} U &= 2NS(S^2-\cos^2\chi)\{2\cos^2\chi(m-1)[mS^2-T^2-(m-1)\cos^2\chi]+ \\ &\quad +(T^2-\cos^2\chi+2m\cos^2\chi)[m(S^2-\cos^2\chi)+2\cos^2\chi]\}, \\ V &= (S^2-\cos^2\chi)^2[mS^2-T^2-(m-1)\cos^2\chi][m(S^2-\cos^2\chi)+2\cos^2\chi]+ \\ &\quad +8N^2S^2\cos^2\chi(m-1)(T^2-\cos^2\chi+2m\cos^2\chi), \\ W &= -2NS\{2\cos^2\chi[mS^2-T^2-(m-1)\cos^2\chi][m(S^2-\cos^2\chi)+2\cos^2\chi]+ \\ &\quad +(S^2-\cos^2\chi)^2(m-1)(T^2-\cos^2\chi+2m\cos^2\chi)\}. \end{aligned}$$

Formula (10) can be viewed as an equation for finding h when the frequency, slip angle of the incident wave, and the parameters of the materials are all given. The equation has a solution only in the case when $|U|$ is at least less than one of the quantities $|V|$ or $|W|$. This requirement is the condition which is stipulated in Section 1. In the case when a solution exists it is not the only solution – by increasing the thickness of the layer it is possible to obtain an infinite series of solutions; however, a practical significance can only be assigned to the first set of these solutions, i.e., to those which correspond to the minimum layer thicknesses.

3. In view of the complexity of the equation, it must be solved graphically by calculating the values of the left-hand side of Equation (10) for various values of h and finding the intersection point between the resulting graph and the axis of abscissas. However, by this means it is possible to find only the thicknesses of the layers which cause the reflected transverse wave to become zero. If it is desired to obtain the frequency characteristic of the effect of suppressing transverse waves, then it is necessary to conduct a more complete calculation; this is accomplished by calculating the values of $|B|$ according to Equation (8) for a series of values of the layer thickness or for a series of values of the sound frequency.

As an example, Fig. 2 gives the results of such a calculation for a layer of cadmium deposited upon steel. In this calculation the following parameter values were used:

$$\rho = 7.8 \text{ г/см}^3,\ c_l = 5.85\cdot 10^5 \text{ см/sec},\ c_t = 3.23\cdot 10^5 \text{ см/sec},$$
$$\rho' = 8.6 \text{ г/см}^3,\ c_l' = 2.78\cdot 10^5 \text{ см/sec},\ c_t' = 1.5\cdot 10^5 \text{ см/sec}.$$

The graph is plotted for values of the angle χ which were respectively 30, 45 and 60°. In this case it is proven that the requirement necessary for the amplitude of the reflected transverse wave to become zero is that the thickness of the layer be identical for all of the examined angles of incidence (about 0.45 of a wavelength of a longitudinal wave in cadmium; for a frequency of 1 megacycle a layer thickness of about 1.3 mm is required). The width of the band within which the amplitude does not exceed 0.1 changes from 6.5 to 10%. The broadening of the band is possible by means of utilizing several layers of various materials, deposited upon the surface of the body in succession.

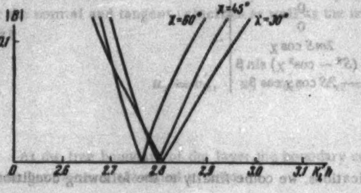

Fig. 2

Let us also mention the fully analogous problem of suppressing a longitudinal wave which arises when an incident transverse wave is reflected from the surface of the solid body. Here the problem is also solved by means of utilizing a solid layer which is deposited upon the surface of the body; the method of solution in this case is completely similar to the method used above.

In conclusion I express my appreciation to N. S. Kanevskaia, who carried out the entire computation involved in this paper.

Acoustics Institute of the Academy of Sciences U.S.S.R.
Moscow

Received February 21, 1956

EXPERIMENTAL INVESTIGATION OF ULTRASONIC TRANSITION LAYERS

G. I. Kaminir, B. D. Tartakovskii

The paper experimentally investigates a method for producing acoustic "penetration" ("translucence") at the boundaries of acoustically different media by means of transition layers. It is shown that it is possible to increase the coefficient of sound penetration of a boundary between aluminum and water by up to 98-99%, and the coefficient sound penetration of steel plates in water by up to 0.90-0.92. The utilization of double transition layers permitted a substantial widening of the "translucent" band of steel plates.

One of the authors investigated the conditions for creating complete "translucence" at the boundary of two acoustically different media and worked out a theory for acoustic transition layers [1, 2].

Thereafter, experiments were conducted whose purpose was to verify experimentally the theoretical conclusions and the possibility of affecting transition layers which permitted the penetration of the boundaries of several frequently encountered pairs of acoustical media in the field of ultrasonic engineering. Below we give a portion of the data obtained by us.[*]

EQUIPMENT AND METHOD OF MEASUREMENT

The measurements were conducted in the frequency range 500-2,000 kc. We investigated transition layers which were deposited upon plane, cylindrical and spherical surfaces. We utilized plane-parallel plates, as well as cylindrical and spherical focusing lenses in the capacity of the specimens which were made "translucent". For the purpose of making an accurate quantitative evaluation of the effectiveness of the acoustic transition layers, optical methods of observing ultrasonic fields, regardless of their convenience and simplicity, are inapplicable. Therefore the measurements were conducted by means of an air electroacoustic measuring channel. The mean random error comprised 0.1 db. The emitter, the investigated specimen and the receiver probe with an acoustic focusing lens (Fig. 1) were installed in a brass vessel whose dimensions were 100 x 25 x 25 cm, and which was filled with water. The plane emitter (1) with a diameter of 40 mm was placed at a distance of 20 cm from the measured specimen (2); within these limits the wave front at frequencies of 1,000-2,000 kc still retained a plane shape. In measuring plane specimens the receiver was located at the focus of an auxiliary ultrasonic plane-spherical focusing lens 3. This permitted us to suppress interference which was produced because of reflected acoustic waves from the incompletely deadened walls of the vessel. The utilization of the lens also permitted us to "automatically" average the results of the measurements over the entire cross section of the wave beam. Let us note that if instead of a lens we had utilized an ultrasonic plane receiver of the same diameter as the lens, the suppression of interference and the process of averaging would have been exactly the same as they are when the lens is used. However without the lens standing waves would have appeared as a consequence of the reflections from the receiver; these standing waves would have distorted the results of the experiment. The acoustic lens used was made of plexiglass whose reflection coefficient was 0.01 when under the pressure of water. For the purpose of weakening the standing waves between the emitter and the specimen, a plate was installed which was made out of material possessing a high ultrasonic absorption coefficient. The coefficient of sound penetration D of plane plates with transition layers deposited upon them was determined by means of comparing the sound pressures measured with and without the plate.

---

[*] This work was carried out during the years 1951-1955.

The measurements conducted with transition layers deposited upon prisms and lenses were of a relative character: specimens which were "translucent" and specimens which for the sake of comparison were non-translucent were successively placed in the field of a plane sound wave. The advantage added by translucence was determined by the ratio of the measured electrical voltages V_1/V_0 where V_1 is the magnitude of the electrical voltage at the output of the measuring channel (this voltage is proportional to the acoustic pressure) when measuring the translucent specimen, and V_0 is the voltage resulting from the non-translucent specimen. When the transition layers which had been deposited on the lenses were measured, the receiver was placed at the focus of the corresponding lens, and the advantage was determined by means of comparing it with a standard lens (a lens without a transition layer).

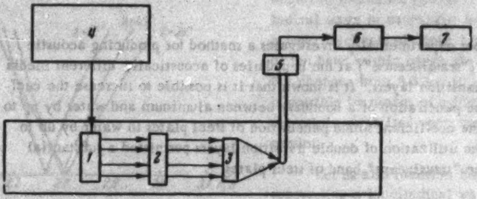

Fig. 1. Diagram of the installation: 1) emitter; 2) measured specimen; 3) lens; 4) generator; 5) probe; 6) amplifier; 7) indicator.

PREPARATION OF THE TRANSITION LAYERS

Various materials can be used for making the solid transition layers: metals, plastics, lacquers. The shape of the penetrated specimen and the design frequency of penetration are the controlling factors in the various methods of preparing transition layers. In working at frequencies of 1000 kc and below, when the thickness of a $\lambda/4$ penetrated layer comprises several tenths of a millimeter, the transition layers can be manufactured in the form of plates which are glued to the specimen.

Such flat plates with a thickness of 0.2-1.2 mm were manufactured of plexiglass; plates of a thickness 0.25-0.7 mm were manufactured of aluminum and elektron. As calculation shows, the thickness of the glue layer at a frequency of 1,000 kc has practically no effect if it does not exceed a thickness of 0.02 mm. In our experiments this was achieved by utilizing carbinole glue or B F-2 glue with polymerization under pressure. Several difficulties were encountered in manufacturing transition layers of plexiglass for spherical surfaces. The hot-press method proved to be inapplicable, since the thin transition layers warped when they cooled. Better results were obtained by utilizing the following cold-working method. A pair of lenses (one plane-concave metallic lens and one plane-convex plexiglass lens) with identical radii of curvature were made on a lathe. After they had been glued together under pressure, the plexiglass lens was turned down until a spherical layer of the specified thickness remained. Layers of thicknesses up to 1 mm were prepared with an error of ± 0.01 mm. A shortcoming of this method is the complexity of the manufacture and the appreciable losses of material which limit the application of this method to the manufacture of transition layers for large specimens. In order to deposit transition layers upon large spherical surfaces we tested powdering methods by means of a pulverizer using various lacquers and depositing them by means of a brush with subsequent drying and polymerization. The powdering method was inapplicable because air bubbles appeared in the interior of the layer. Brush depositing was successful in attaining layers of satisfactory quality up to a thickness of 0.005 mm and larger. However, this method requires the expenditure of a large amount of time for preparing layers with a thickness of 1 mm. Layers obtained by means of this method from a bakelite lacquer and B F-2 glue are easily cold-worked on lathes and milling machines after polymerization; the resulting error does not exceed ± 0.02 mm.

RESULTS OF THE EXPERIMENTAL INVESTIGATIONS

Two series of measurements were made. In the first series we investigated the increase of the acoustic permeability of the boundary between two different media with respect to a traveling wave; this is analogous to the propagation of light through the surfaces of optical lenses. For these measurements the specimen was prepared in the form of a trihedral prism or in the form of a plane-spherical lens; this weakened the effect of interference inside the specimen upon the results of the measurements. Such a device permitted us to make an independent examination of the action of each of the penetrated layers which were deposited upon both sides of the specimen. In the second series of measurements we determined the increase in the acoustic permeability of solid plane-parallel plates which were placed in a liquid medium. This phenomenon is characteristic only for acoustical problems, since here a resultant interference between waves takes place from all of the boundaries of the unit consisting of the penetrated plate and the transition layer deposited on both sides of it.

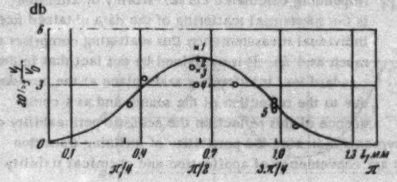

Fig. 2

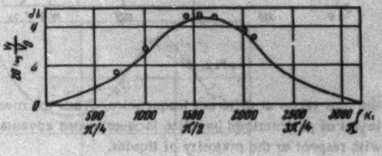

Fig. 3

The first series of measurements was carried out with transition layers made of plastic. Initially we investigated the penetration of an aluminum trihedral prism. For this purpose a plexiglass plate was glued onto one of its sides; the thickness of the plate was 0.65 ± 0.01 mm and was designed for penetration at a frequency of 1,000 kc (the solid curve in Fig. 2). When a plain prism was replaced by a prism which allowed penetration, the level of the acoustic pressure at the design frequency increases on the average by 4.3 ± 0.3 db (points 1, 2, 3 in Fig. 2). Then the same type of plexiglass plate was glued onto the other side of the prism; when this was done, the advantage increased by up to 7.7 ± 0.1 db. In accordance with the calculations [2], this advantage should have been equal to 8.5 db. The penetration effect in plexiglass plates of various thickness was measured. For this purpose plates with thicknesses of from 0.3 mm to 1.1 mm were successively applied to the plane surface of a plane-spherical lens. In Fig. 2 the circles in the upper half of the graph denote the experimental data, and the solid curves denotes the calculated values. The agreement between the calculated and experimental values can be considered to be satisfactory. During the process of experimentation it was noticed that the effect of the increase in acoustic permeability can be obtained with direct contact between the plexiglass plate and the lens by placing the plate at a distance of several half-wavelengths from the lens (points 4 and 5 in Fig. 2).

Further we investigated the penetration effect in spherical surfaces of aluminum lenses. When wave beams were slantingly incident upon the layer the wave thickness of the layer diminished, and therefore the frequency corresponding to the maximum penetration effect increased. Correspondingly, a layer with a thickness of 0.47 ± ± 0.0005 mm which was deposited upon the spherical surface yielded the maximum penetration effect at a frequency of 1570 kc, whereas for normal incidence upon a plate the penetration frequency should comprise 1400 kc (Fig. 3). Taking these facts into account, a plexiglass plate with a thickness 0.43 mm was glued to the plane side of this same lens (for this plate the maximum acoustic permeability occurred at a frequency of 1570 kc for normal incidence). The measured total advantage of 8.3 ± 0.8 db agreed satisfactorily with the calculated value of 8.5 db which took into account losses in both plates.

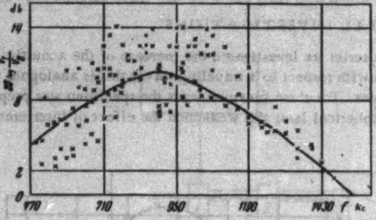

Fig. 4

Figure 4 shows the experimental values for the advantage (indicated by crosses) when the aluminum lens is made "translucent" on both sides by means of a bakelite lacquer deposited by means of a brush. The thickness of the plane layer was 0.76 mm, and the thickness of the spherical layer was 0.79 mm. The average measured advantage at the frequency of f = 900 kc (without taking attenuation into account) comprises 10.5 db. The solid line indicates the corresponding calculated curve. Worthy of attention is the substantial scattering of the data obtained from individual measurements; this scattering comprises as much as 4 db. It is explained by the fact that in the standard lens interference takes place at the boundaries due to the reflection of the sound, and as a consequence of this reflection the acoustic permeability of the lens varies at different frequencies. Thus the measurements indicated the possibility of utilizing transition layers of polymerized bakelite lacquer whose advantages are convenience of application and chemical stability with respect to the majority of liquids.

In the second series of measurements three units (Fig. 5) were prepared for the purpose of studying the increase in the acoustic permeability of plane-parallel plates: I. An aluminum plate with plexiglass transition layers. II. A steel plate with transition layers made of elektron (the wave impedance of elektron is close to the optimum value necessary for making the boundary of steel and water "translucent"). III. A steel plate with double transition layers consisting of plexiglass and aluminum.

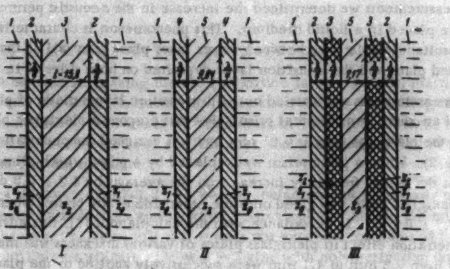

Fig. 5. 1) water; 2) plexiglass; 3) aluminum; 4) elektron; 5) steel.

As calculation shows, the application of double transition layers for a specified relationship between the wave impedances of the transition layers and of the semi-infinite media permits a broadening of the frequency band within whose limits the coefficient of acoustic permeability of the plate increases [2].

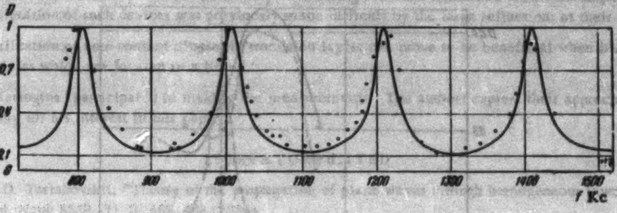

Fig. 6

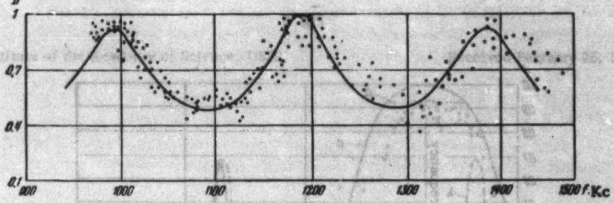

Fig. 7

Figure 6 gives the results of measurements of the acoustic permeability coefficient for an aluminum plate in water before the application of the transition layers. The calculated curve and the experimental points (the averages of five measurements) agree well. The maximum coefficient of acoustic permeability D_{max} is close to unity, and the minimum coefficient of permeability D_{min} obtained at points where the thickness of the plate contains an odd number of quarter-wavelengths is about 0.2.

Figure 7 shows analogous results for unit I. The minimum values of the coefficient of acoustic permeability have increased to a value of 0.5. The acoustic pass band has broadened by a factor of three to four. In the vicinity of the calculated frequency of maximum "translucence" (f = 1200 kc) the magnitude of D_{max} is equal to unity as before. At frequencies of f = 1000 kc and f = 1400 kc, D_{max} has become somewhat less than unity (at these frequencies the wave thicknesses of the plexiglass layers are not exactly equal to $\lambda/4$). The experimental points are well grouped around the calculated curve.

In Fig. 8 results of measurements on unit II are given. The experimental frequency characteristic for D in a steel plate without transition layers is given by the curve a. As a consequence of the attenuation of ultrasonic waves in steel D_{max} is only 0.6. In order to obtain convenient results, the frequency of penetration was selected in the region of the minimum translucence of the steel plate (f = 520 kc). The experimental values of D for the units as a whole are given by the curve b, and the corresponding calculated data (without taking losses into consideration) are represented by the curve c. The coefficient of acoustic permeability has increased to a value of 0.9; the translucent band of the unit has broadened by approximately a factor of three.

Figure 9 shows the results of the measurements on unit III. The experimental values of the coefficient of acoustic permeability for a steel plate are denoted by triangles (a); the results of calculation, taking ultrasonic losses in the steel into account, are given by curve b; the crosses indicate the frequency characteristic for D of a

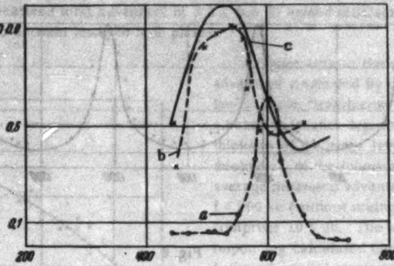

Fig. 8

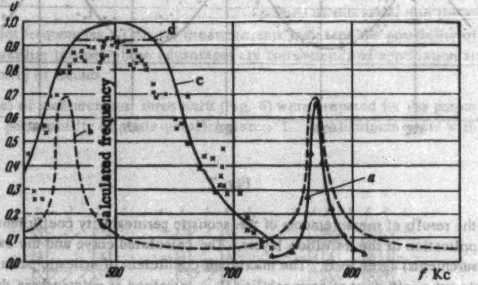

Fig. 9

steel plate with quarter-wavelength aluminum and plexiglass plates glued onto it on both sides. Curve c shows the calculated characteristic for the acoustic permeability of the unit as a whole without taking attenuation into account; the horizontal straight line d indicates the magnitude of D calculated while taking attenuation in all of the plates into account.

The pass band has widened by more than a factor of ten. It is important that D_{max} in both cases of penetration of the steel plates attains values of 0.9 to 0.92. The increase in the maximum coefficient of acoustic permeability as a result of making the unit translucent can be explained by the fact that due to the transition layers multiple ultrasonic reflection inside the plates is eliminated, and therefore the effective path length over which attenuation takes place in the steel is diminished.

The results of the experimental investigations of acoustic transition layers show that by means of such layers, it is possible to raise substantially the acoustic permeability of boundaries between acoustically different media. For example, utilizing plastic and metallic layers it is possible to raise the coefficient of acoustic permeability of the boundary between aluminum or steel and water to 98-99%.

The utilization of double transition layers consisting of materials with correspondingly selected wave impedances also permits a substantial widening of the frequency band of acoustic permeability [3]. When operating at a fixed frequency the utilization of a double layer in order to effect "translucence" permits the range of working angles to be widened.

Acoustic "translucence" yields the possibility of utilizing metallic lenses and prisms which possess small losses; the utilization of such devices was previously made difficult by the large reflections at their boundaries.

The utilization of non-contact ultrasonic transition layers can prove to be beneficial when irradiating metallic particles which are located in a liquid.

A. P. Kariugina participated in making the measurements. The authors express their appreciation to L. D. Rozenberg for his interest in this paper.

LITERATURE CITED

[1] B. D. Tartakovskii, "Theory of the propagation of plane waves through homogeneous layers," Doklady Akad. Nauk SSSR 71, 3, 465-468 (1950).

[2] B. D. Tartakovskii, "Acoustic transition layers," Doklady Akad. Nauk SSSR 75, 1, 29-32 (1950).

[3] B. D. Tartakovskii, A Method for Increasing the Transparency of Acoustic Lenses, Authors Certification No. 90182, June 25, 1949.

Acoustics Institute of the Academy of Science, USSR,
Moscow

Received February 25, 1956

THE PULSE METHOD OF FIXED DISTANCES; ITS PHYSICAL BASIS AND PRACTICAL APPLICATION

N. I. Koshkin, V. F. Nozdrev, V. D. Sobolev,
M. G. Shirkevich and V. F. Iakovlev

The paper provides the fundamentals of a newly developed pulse method for measuring ultrasonic absorption. In contrast to the widely utilized method where it is necessary to displace the emitter and reflector with respect to one another, the emitter and reflector remain stationary in this method. This fact not only simplifies the construction of the measuring chamber to a substantial degree and accelerates the measuring process, but it also permits the pulse method to be utilized more successfully for absorption measurements at high temperatures and pressures, as well as for various types of phase transitions.

In this paper we give the results of measuring the ultrasonic absorption coefficient; these measurements were conducted by means of the method of fixed distances and the experimental data are compared with the results obtained from other methods; the paper indicates the possibility of utilizing the pulse method of fixed distances as a monitoring means in industry.

In the existing papers on the investigation of ultrasonic absorption in liquid media by the pulse method, one type of method is usually proposed: the measurement is conducted for variations in the distance between a reflector and a quartz emitter. The investigation of the properties of the substance in the critical region and in the region of solidification is a very real experimental problem. The utilization of the usual pulse method for investigating absorption in the critical region encounters many engineering difficulties, and in the region of solidification of the substance this method in principal cannot be utilized. Below we discuss the investigation of ultrasonic propagation by the pulse method at fixed values of the acoustic path.

Starting from the general theory of transducers and from the analysis of ultrasonic delay lines [1], an equivalent circuit may be created to describe the transfer of energy through the medium. The circuit for the transmission of a pulse of energy from the generator to the receiver can be depicted by an electrical circuit (Fig. 1); when calculations are made according to this circuit, an exponential multiplier should be introduced which takes into account the scattering of the energy in the medium. In Fig. 1, I is the quartz coupled to the generator, II is the quartz coupled with the receiver, U_0 is the generator voltage, R_t is the input resistance of the generator, R_r is the input resistance of the receiver, R_1, R_2 are the acoustic resistances of the media on the two sides of the quartz, expressed in electrical units, U_r is the voltage at the input of the receiver, III is the transmitting medium which is equivalent to an electrical line with exponential attenuation. In accordance with this circuit, the losses which occur when the pulse is transmitted are determined in the following manner:

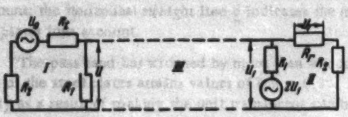

Fig. 1

$$\frac{U_r}{U_0}=\frac{2kR_1R_r}{(R_1+R_2+R_t)\,(R_1+R_2+R_r)}\cdot e^{-\alpha l}, \qquad (1)$$

where l is the length of the acoustic path, k is the amplitude reflection coefficient at the boundary between the medium and the reflector.

Relationship (1) served as the basis for solving the problem of measurements which are made at fixed values of the acoustic path. In the case of a symmetrical load upon the quartz ($R_1 = R_2$) for the condition $R_r \ll R_1$ and $R_t \ll R_1$ (this condition usually obtains during the experiment) Expression (1) can be written in the form

$$\frac{U_r}{U_0} = \frac{kR_r}{2R_1} e^{-\alpha l}. \tag{2}$$

In determining the relative variation of the attenuation coefficient, the necessity of measuring the values of the generator voltage and of the voltage at the input of the receiver is eliminated. The initial value of the attenuation coefficient can be determined for a variable value of the acoustic path under ordinary conditions. The further investigation of the variation of the absorption coefficient can be conducted in a closed system for a fixed acoustic path over a wide range of temperatures and pressures including the critical region and the region of solidification of the substance.

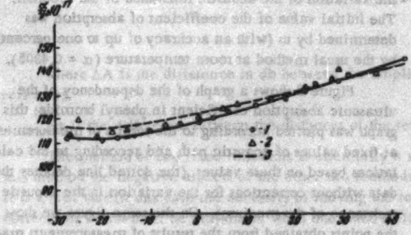

Fig. 2. Phenyl bromide (frequency ν_{av} = 17.9 megacycles): 1) fixed-distance method; 2) variable-distance method; 3) fixed-distance method without corrections.

In the proposed method the variation in the ultrasonic attenuation ΔA (in db) is measured for a fixed acoustic path. This variation can be caused by a variation in temperature, concentration, pressure etc.

Practically speaking, the quantity ΔA is determined by means of a voltage divider which is placed at the input of the receiver. Then the variation in the attenuation coefficient ($\alpha_2 - \alpha_1$) for the case of a symmetrical load or for the case where the medium loads the quartz on one side is equal to

$$\alpha_2 - \alpha_1 = \frac{\Delta A}{20 \cdot l \cdot \log e} + \frac{1}{l \cdot \log e} \log \frac{k'' R_1'}{k' R_1''}, \tag{3}$$

where k″/k′ is the relative variation of the reflection (the amplitude of this reflection) at the boundary of the separation between the reflector and the medium (k′ is the initial reflection), R_1''/R_1' is the relative variation of the acoustic resistance of the medium (R_1' is the initial acoustic resistance).

When a steel reflector is present and when the acoustic resistance of the medium varies by a factor of 1.8, a negligibly small variation in the reflection of energy takes place. In that case it is possible to neglect the second term of Expression (3). The effect of a variation in temperature upon the parameters of the quartz can be taken into account during calculations of the variation of the acoustic resistance of the medium (expressed in electrical units); this correction is negligibly small in the interval ± 50°).

The experimental verification of the method described was carried out by measuring the temperature coefficient of ultrasonic absorption in phenyl bromide. The measurements were conducted at a frequency of 17.9 megacycles with impulses with a duration of 2 microseconds in the temperature range of from –27.5 to 43°. The values of ultrasonic velocity in phenyl bromide in the given interval of temperatures were determined according to data obtained by the diffraction method [2]; the values of the density for temperatures above zero were taken from tables [3], and for temperatures below zero they were calculated by means of extrapolation.

In the interval of temperatures investigated by us the maximum relative variation of the acoustic resistance of the medium was 1.2; in this case the maximum correction for the variation in the reflection during the calculation of the attenuation coefficient was equal to 0.03%. Therefore we neglected the effect of the variation in the reflection and utilized the simplified formula:

$$\alpha_2 - \alpha_1 = \frac{\Delta A}{20 \cdot l \cdot \log e} + \frac{1}{l \cdot \log e} \log \frac{R_1'}{R_1''}. \tag{4}$$

for the purpose of calculating variations in the attenuation coefficient.

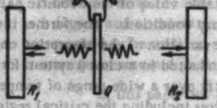

Fig. 3

Fig. 4

The component $\frac{1}{l \cdot \log e} \log \frac{R_1'}{R_1''}$ is a correction for the variation of the acoustic resistance of the medium. The initial value of the coefficient of absorption was determined by us (with an accuracy of up to one percent) by the usual method at room temperature ($\alpha = 0.4305$).

Figure 2 shows a graph of the dependency of the ultrasonic absorption coefficient in phenyl bromide; this graph was plotted according to the results of measurements at fixed values of acoustic path and according to the calculations based on these values (the dotted line denotes the data without corrections for the variation in the acoustic resistance of the medium). On the same figure we show the points obtained from the results of measurements made by the usual method. The distribution of the points on this graph for two different methods of measurement allows us to draw the following conclusions:

1. Both methods yield an identical picture of the variation of absorption as a function of temperature.

2. The method of fixed distances yields a smaller scattering of the points (the points are within the limits of one percent).

Thus we have verified the principle that both methods of measurement yield equal values and that the method of fixed distances, from the point of view of accuracy, results in a practical advantage.

A further development of the pulse method of measuring ultrasonic absorption was achieved when the method of two fixed reflectors was developed. In this method of making measurements the quartz emitter Q (Fig. 3) is excited by a pulse generator and emits ultrasonic pulses which are propagated in both directions from the surfaces of the quartz plate. Having reached the reflectors R_1 and R_2 which are located at different distances from the emitter, the ultrasonic pulses return to the quartz which transduces them into electrical pulses. The latter pulses are fed to the y-plates of a cathode-ray tube after amplification, and as a result a system of deflection appears on the screen of the oscilloscope tube; these deflections correspond to the reflected pulses from both reflectors.

Figure 4 shows one of the oscillograms. Deflection 1 corresponds to the fundamental pulse which is fed from the generator to the quartz emitter Q; deflections 2 and 3 correspond to the first and second reflected pulses from the reflector which is located closest to the emitter; deflection 4 corresponds to the first reflected pulse from the second reflector; deflection 5 corresponds to the simultaneous effect of the two reflected pulses from the different reflectors at the input of the receiver, and therefore its amplitude is greater than the amplitude pulse 4; further, the system of deflections follows a system which corresponds to the pulses obtained after multiple reflections. When measurements are made of the absorption, the first reflected pulses from both reflectors are utilized.

When the condition obtains that the magnitudes of the ultrasonic pulses sent in both directions from the quartz emitter are identical and that both reflectors are strictly parallel to the surfaces of the quartz plate, then the absorption is calculated according to the same formula as the formula used in the method of movable reflectors:

$$\alpha = \frac{\Delta A}{40 \cdot \log e \cdot \Delta x}, \tag{5}$$

where ΔA is the difference in db between the amplitudes of the two first reflected pulses from the different reflectors.

Δx is the difference between the distances of the reflectors from the quartz emitter.

The method of two fixed reflectors is essentially a synthesis of the two methods utilized earlier; in using this method the negative aspects of the other two methods are eliminated and the positive aspects are retained. It is a fact that in this case the necessity of moving the reflector is eliminated along with the necessity for the corrections which must be introduced when one fixed reflector is utilized.

Attention should be given to the fact that when the method of two fixed reflectors is used the guarantee of an identical intensity of radiation from the quartz emitter in both directions and of a strict parallel relationship between the surfaces of the quartz plate and the reflectors is not a necessary condition. Let the quartz emitter radiate an intensity I_1 in one direction and an intensity I_2 in the other direction; let the loss in intensity be k_1 when reflection takes place from the first reflector, and let this loss be k_2 when reflection takes place from the second reflector. Then the intensity of the first reflected pulse from the first reflector will be $I_1k_1e^{-\alpha \underline{l}^{1}}$ at the surface of the quartz, where $\underline{l}_1$ is the length of the acoustic path of the first pulse; correspondingly for the first reflected pulse from the second reflector the intensity will be $I_2k_2e^{-\alpha \underline{l}^{2}}$. Here the coefficients k_1 and k_2 characterize the intensity losses caused not only by reflection but also by the non-parallel relationship between the reflectors.

Then

$$\alpha = \frac{\Delta A - 10 \log \frac{I_1k_1}{I_2k_2}}{20 \cdot \log e \Delta l}, \tag{6}$$

where $\Delta A = 20 \log \frac{V_1}{V_2}$ is the difference in db between the amplitudes of the two first reflected pulses from different reflectors, $\Delta \underline{l}$ is the difference in acoustic paths for the ultrasonic pulses.

From this it is evident that in this case it is necessary to introduce the correction $\Delta A_1 = 10 \log \frac{I_1k_1}{I_2k_2}$. The magnitude of this correction for a given quartz-holder construction and a given installation of the reflectors will not depend upon other factors which vary during the course of the experiment (for example, upon variations in temperature, pressure, or variations in the intensity of radiation associated with the variation of the acoustic properties of the medium). The magnitude of this correction can be determined by measuring the magnitudes of the quantity ΔA in a standard liquid for which α is measured to a high degree of accuracy. Let us also take note that the method of two fixed reflectors cannot completely replace the method using one fixed distance. This situation may obtain during the investigation of the absorption coefficient in the states of the substance which are in the critical region and in regions beyond the critical, when the reflected pulse from the more distant reflector becomes small in amplitude (because of the large absorption); in such cases it becomes necessary, practically speaking, to make use of one fixed reflector.

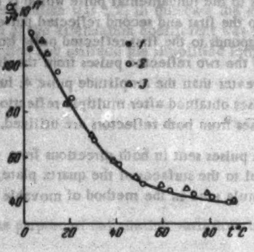

Fig. 5. 1) The variable-distance method; 2) method of two fixed distances; 3) optical method.

TABLE

Ethyl Acetate (frequency 5.1 megacycles)

t (°C)	$\frac{\alpha}{\nu^2}\cdot 10^{17}\ \frac{\text{sec}^2}{\text{cm}}$	t (°C)	$\frac{\alpha}{\nu^2}\cdot 10^{17}\ \frac{\text{sec}^2}{\text{cm}}$	t (°C)	$\frac{\alpha}{\nu^2}\cdot 10^{17}\ \frac{\text{sec}^2}{\text{cm}}$	t (°C)	$\frac{\alpha}{\nu^2}\cdot 10^{17}$ sec²
60	261	140	558	230	2170	260	2645 reheated vapors
70	281	150	632	240	2581	264.5	2449, the same
80	305	170	800	245	2852	270	2279, the same
90	332	180	908	248	3646		
100	359	190	1050	249	4095		
110	392	200	1250	250	critical temperature		
120	435	210	1500	253	3302, reheated vapors		
130	493	220	1801	256	2917, reheated vapors		

The results of measuring the absorption coefficient by the method of two reflectors are in good agreement with the results obtained by other methods. Figure 5 shows the results of measurements made of the absorption coefficient in n-butyl alcohol, using the method of two fixed reflectors, the method of a movable reflector and the optical method which employs a photo-element. The maximum deviation of the results is less than 5%, and this deviation lies within the limits of the accuracy attained in the measurements we conducted.

The method of one and two fixed reflectors was successfully utilized by one of the authors of this paper [4] for investigating the ultrasonic absorption along the saturation line when a transition took place through the critical point.

The table gives several results of measurements in ethyl acetate at the frequency of 5.1 megacycles. As can be seen from this table, the new methods of measurement permit the continuous investigation of ultrasonic absorption in the critical region of transition from liquid to vapor.

Undoubtedly the pulse method using one and two fixed reflectors will find wide application in scientific research practice when it is necessary to conduct investigations in hermetically-sealed volumes of a medium; this method can also be utilized in a number of practical problems associated with the determination of the physical and chemical characteristics of a medium. In particular, we can indicate the possibility of utilizing the method of fixed reflectors for determining the amount of dissolved gases in oil.

LITERATURE CITED

[1] H. B. Huntington, A. G. Emslie and V. W. Hughes, "Ultrasonic delay lines," J. J. Franklin Institute, 245, 1, 1-24, (1948); G. Emslie, H. B. Huntington, H. Shapiro and A. E. Benfield, "Ultrasonic delay lines II," J. Franklin Institute 245, 2, 101-115 (1948).

[2] Z. I. Avdus, Investigation of the Propagation of Ultrasonic Waves in Organic Liquids in the Vicinity of their Freezing Temperatures (Dissertation) (Moscow Regional Pedagogical Institute, 1950) p. 84.

[3] Technical Encyclopedia: Handbook of Physical, Chemical and Engineering Quantities (1930) Vol. 5, p. 160.

[4] V. D. Sobolev, Measurement of the Absorption of Ultrasonic Waves in Ethyl Acetate along the Saturation Line by Means of the Method of Two Fixed Distances (Dissertation) (Moscow Regional Pedagogical Institute, 1955), pp. 88-92.

Moscow Regional Pedagogical Institute Received February 15, 1956

THE VELOCITY OF SOUND IN LIQUIDS, LIQUID MIXTURES AND SOLUTIONS

B. B. Kudriavtsev

The paper derives an expression for the velocity of sound, in which the internal energy and several physical characteristics of the substance are included. In the previous paper [4] the velocities of sound for a series of binary mixtures of organic liquids were calculated, and these values were compared with experimental data. The observed variation in the velocity of sound with a variation in the concentration is explained. In this paper the equation which is obtained is used for calculation of velocities of sound in aqueous solutions of electrolytes. The theoretically calculated velocities of sound are in good agreement with the experimental data. The adiabatic compressibilities of aqueous solutions of alkali-metal halogen salts are theoretically calculated. On the basis of an equation obtained earlier the velocity of sound in pure water at various temperatures is calculated while taking into consideration the molecular association of the water. The paper discusses the acoustic properties of electrolyte solutions and the possibilities of utilizing acoustic measurements for calculating various physical and chemical parameters which characterize both the solution and the dissolved substance.

In contemporary physics literature there is not a unified point of view concerning the problem of how to calculate the velocity of sound in so-called ideal liquid mixtures. Several researchers consider that ideal mixtures are characterized by the additiveness of the adiabatic compressibilities [1, 2]. In such a case the relationship:

$$c^{-2} = n_1 \frac{\rho}{\rho_1} c_1^{-2} + n_2 \frac{\rho}{\rho_2} c_2^{-2}, \tag{1}$$

would be valid for the velocity of sound c in the mixture; in this expression n represents the molar fractions, ρ represents the density, c represents the velocity of sound, and the indices 1 and 2 respectively refer to the first and second components of the mixture.

Along with this point of view there exists the paper [3] in which the additiveness of the sound velocities c is considered to be characteristic of ideal mixtures (i.e., it is assumed that

$$c = (1 - \nu) c_1 + \nu c_2, \tag{2}$$

holds, where c_1 and c_2 are the velocities of sound in the first and second components of the mixture respectively, and ν is the fraction of the second component). The indicated contradiction is partially caused by the indeterminate nature of the very concept of an ideal liquid mixture. If it is assumed that the distinguishing feature of

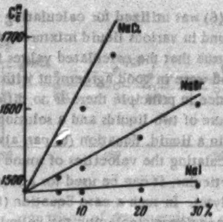

Fig. 1. Velocities of sound in aqueous solutions of halogen salts of sodium. Abscissa—percent salt by weight.

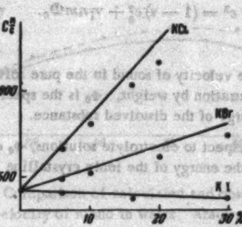

Fig. 2. Velocity of sound in aqueous solutions of halogen salts of calcium. Abscissa—percent salt by weight.

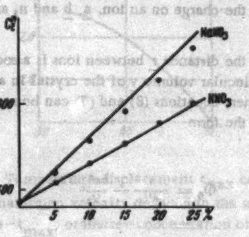

Fig. 3. Velocities of sound in aqueous solutions of nitrates of sodium and calcium. Abscissa—percent salt by weight.

an ideal liquid mixture is the additiveness of the internal energy U of the system (i.e., if it is postulated that

$$U = (1 - n)\,U_1 + nU_2, \tag{3}$$

holds, where n is the molar fraction of the second component, and U_1 and U_2 are the molecular internal energies of the first and second components of the mixture respectively), then it is easy to show that the squares of the sound velocities must be additive in this given case [4]. In fact, the internal energy Φ of the liquid, (this component is caused by the potential interaction of the molecules in the liquid) is a function of the molecular volume v; this function can be analytically described by the equation

$$\Phi = \frac{A_1}{v^n} - \frac{B_1}{v^m}. \tag{4}$$

Here n and m are certain constants which are assumed to be identical for all liquids, while A_1 and B_1 are quantities which have their own particular characteristic values for each liquid (these values are also dependent upon the temperature). If we limit ourselves to temperatures which are not very high (temperatures at which the kinetic component of the internal energy of the liquid can be neglected in comparison to the component caused by the potential interaction between the molecules of the liquid), then the following expression will be valid for the velocity of sound:

$$c^2 = \gamma nm\Phi_0, \tag{5}$$

in which γ is the ratio of the specific heat at constant pressure to the specific heat at constant volume, and Φ_0 is the potential energy of interaction between the molecules of the liquid which is in equilibrium with its own vapor. Substituting the value for Φ from Equation (5) into Equation (3) in place of the quantity U, and assuming that the values of γ in the individual components and in the mixture are close to each other in absolute value, it is easy to obtain the following expression for the velocity of sound in the mixture:

$$c^2 = (1 - \nu)\,c_1^2 + \nu c_2^2, \tag{6}$$

where ν is the fraction by weight of the second component.

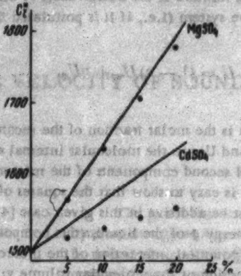

Fig. 4. Velocities of sound in aqueous solutions of sulfates of magnesium and cadmium. Abscissa—percent salt by weight.

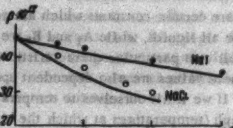

Fig. 5. Compressibilities of halogen solutions of salts of alkali metals. Abscissa—percent salt by weight, ordinate—adiabatic compressibility in cm²/dyne.

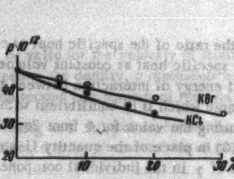

Fig. 6. Compressibility of halogen solutions of alkali metal salts. Abscissa—percent salt by weight, ordinate—adiabatic compressibility in cm²/dyne.

Equation (6) was utilized for calculating the velocities of sound in various liquid mixtures [4], and it proved to be true that the calculated values for the velocity of sound were in good agreement with the experiment. Since in principle there is no difference between a mixture of two liquids and a solution of a solid substance in a liquid, Equation (6) can also be utilized for calculating the velocities of sound in various solutions; in particular, it can be used for aqueous solutions of electrolytes. In such a case Equation (6) can be rewritten for convenience, replacing the velocity of sound c_2 in the dissolved substance by its value expressed in terms of the potential energy of the substance Φ_0, namely:

$$c^2 = (1-\nu)c_0^2 + \nu\gamma nm\Phi_0. \tag{7}$$

Here c_0 is the velocity of sound in the pure solvent, ν is the concentration by weight, Φ_0 is the specific potential energy of the dissolved substance.

With respect to electrolyte solutions, Φ_0 can be replaced by the energy of the ionic crystalline lattice [5].

$$\Phi_0 = \frac{a}{r^{n_1}} - \frac{be^2}{r}, \tag{8}$$

where r is the distance between ions in the crystalline lattice, e is the charge on an ion, a, b and n_1 are constants.

Since the distance r between ions is associated with the molecular volume v of the crystal in a single-valued manner, Equations (8) and (7) can be respectively rewritten in the form

$$\Phi_0 = \frac{a}{v^{n_1/3}} - \frac{be^2}{v^{1/3}} \tag{9}$$

and

$$c^2 = (1-\nu)c_0^2 + \nu\gamma\frac{n_1}{9}\Phi_0. \tag{10}$$

For solid solutions γ may be placed equal to 1. As far as the magnitude of n_1 is concerned, a situation exists which is indeterminate to a certain degree [5]. In calculating the energies of crystalline lattices for ions with a different electron structure, values of n_1 were used which were equal to 5, 7, 9, 10. In further calculations

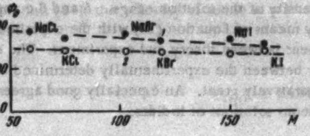

Fig. 7. Comparison of the energies of crystalline lattices calculated on the basis of acoustic data with the values found by other methods. Abscissa—molecular weight, ordinate— in kcal/mole. 1) Experiment; 2) calculation.

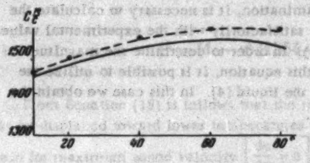

Fig. 8. Comparison of calculated and observed values of the velocity of sound in water. Abscissa—temperature, ordinate—velocity of sound in m/sec. The solid curve is plotted according to Equation (15).

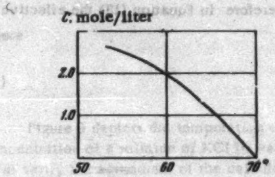

Fig. 9. Temperature displacement t_{max} corresponding to the maximum velocity of sound in the solutions. Abscissa—t_{max}, ordinate—concentration of the solution.

It was assumed that $n_1 = 5$ so that the final equation used for calculation when the potential energy in cal/g was substituted appeared in the following form:

$$c^2 = (1 - \nu) c_0^2 + \nu 2.32 \cdot 10^7 \Phi_0. \qquad (11)$$

Making use of tables to obtain data concerning the energy of crystalline lattices, [5, 6], we calculated the velocities of sound in aqueous solutions of halogen salts of alkali metals with the aid of Equation (11). Figures 1 and 2 show the calculated values for the velocities of sound compared to the values observed experimentally [9]. It can easily be verified that the former and latter values are in good agreement. The same good agreement between the calculated and experimental values of the velocities of sound [10] is observed for solutions of nitrate salts of sodium and calcium (Fig. 3). The agreement between theory and experiment is considerably worse in the case of aqueous solutions of sulfates. This can be verified from Fig. 4 in which the results of calculations using Equation (11) are compared with the results of the experimental determination of the velocity of sound. In these calculations it was assumed $n_1 = 3$. The indicated discrepancy can be explained, on the one hand, by the unreliability of the data concerning the energies of the crystalline lattices of the sulfates of di-valent metals, and on the other hand by the fact that the character of the interaction of the molecules in such a solution is substantially different from the character of the interaction in pure components.• Equation (11) provides the possibility of calculating the adiabatic compressibilities β of the aqueous solutions of electrolytes on the basis of data concerning the energies of the crystalline lattices of the corresponding substances. The equation for calculating β in this case will be of the following form:

$$\beta = \{[(1 - \nu) c_0^2 + \nu .2.32 \cdot 10^7 \Phi_0] d\}^{-1}. \qquad (12)$$

• A more rigorous relationship for the velocity of sound in a mixture [more rigorous than Equation (6)] is the expression

$$c^2 = \frac{\gamma_{mix} n_{mix} m_{mix}}{\gamma_1 n_1 m_1} (1 - \nu) c_1^2 + \frac{\gamma_{mix} n_{mix} m_{mix}}{\gamma_2 n_2 m_2} \nu c_2^2. \qquad (6a)$$

Here the symbols with the indices "mix" denote the values of the physical quantities which are characteristic of the mixture; the symbols with the indices 1 and 2 denote those same quantities for the first and second components respectively, taken separately. Equation (6a) becomes Equation (6) for the condition:

$$\gamma_{mix} n_{mix} m_{mix} = \gamma_1 n_1 m_1 = \gamma_2 n_2 m_2.$$

Here Φ_0 is the energy of the crystalline lattice in cal/g, c_0 is the velocity of sound in pure water, ν is the concentration by weight of the dissolved substance, $\underline{d}$ is the density of the solution. Figs. 5 and 6 compare the results of the calculation of the adiabatic compressibilities by means of Equation (12) with the experimental values. It can be observed that there is a satisfactory agreement between theory and experiment. The exception is represented by solutions of NaCl, for which the discrepancy between the experimentally determined and calculated values of the adiabatic compressibilities are comparatively great. An especially good agreement between theory and experiment is observed in the case of aqueous solutions of iodides.

The agreement of the values of sound velocity calculated by means of Equation (11) with the quantities determined experimentally for aqueous solutions of electrolytes permits us to utilize the experimental values for calculating the energies of crystalline lattices of dissolved salts according to data concerning the velocity of sound in the corresponding solutions. The values found by this method are compared graphically in Fig. 7 with data obtained on the basis of experiment. The calculated values for Φ_0 are in all cases somewhat less than the values found by means of experiment. This discrepancy can be explained by the variation in the character of the molecular interaction (the values of $\underline{n}$ and $\underline{m}$) which undoubtedly takes place when the salts are dissolved.

The attempt to calculate the velocity of sound in solutions without resorting to any acoustic data is of great interest. For the purpose of doing this in the case under examination, it is necessary to calculate the velocity of sound in water in such a manner that the values agree satisfactorily with the experimental values. It is possible to accomplish this by means of utilizing Equation (5). In order to determine the magnitude of the potential component Φ_0 of the internal energy, which appears in this equation, it is possible to utilize the relationship which exists between Φ_0 and the surface tension σ of the liquid [4]. In this case we obtain the following expression for the velocity of sound:

$$c^2 = \frac{[2mn\gamma N^{1/3}]\,\sigma}{M^{1/3}\rho^{2/3}}, \tag{13}$$

where N is Avogadro's number, ρ is the density, M is the molecular weight.

However, it cannot be forgotten that water is an associated liquid. According to Eucken [7], water is a mixture of monomer, diner, quadrimer and octomer molecules, and therefore in Equation (13) the effective value M_{eff} of the molecular weight should be utilized:

$$M_{\text{eff}} = Mi, \tag{14}$$

where $\underline{i}$ is the degree of association of the water.

Taking what has been said above into account, we obtain the following expression for calculating velocities of sound in water:

$$c^2_{H_2O} = \frac{[2mn\gamma N^{1/3}]\,\sigma}{[Mi]^{1/3}\rho^{2/3}}. \tag{15}$$

Utilizing the data given by Eucken [7] concerning the association of water, the values obtained from tables [8] for the coefficient of surface tension σ and for γ, ρ, and assuming m = 2, n = 3, we calculate the velocities of sound in water at various temperatures. The results of this calculation are depicted in Fig. 8. As can be proven, the calculation gives a qualitatively correct picture of the variation of the velocity of sound in water when the temperature varies. In particular, the calculation correctly predicts the position of the maximum of the velocity of sound in water at a temperature which is approximately 70°. In accordance with the latest measurements [11], the velocity of sound in water at various temperatures can be calculated according to the equation

$$c_{H_2O} = 1554 - 0.0305\,(68.4 - t)^2. \tag{16}$$

If we assume as a first approximation that in the dissolved substance the velocity of sound decreases linearly with temperature according to the relationship

$$c_1 = c_1^0\,(1 - \alpha t), \tag{17}$$

then the following relationship will be valid for the velocity of sound in aqueous solutions at various temperatures:

$$c^2 = (1 - \nu)\,[1554 - 0.0305\,(68.4 - t)^2]^2 + \nu\,[c_1^0\,(1 - \alpha t)]^2. \tag{18}$$

From Equation (18) it follows that the temperature t_{max} at which the maximum sound velocity is observed, must be displaced toward lower temperatures in solutions. In fact, on the basis of the condition which must obtain for maximum sound velocity $\left[\frac{dc}{dt} = 0\right]$ we find the following expression for a solution with the concentration ν:

$$t_{max} = 68 - b\,\frac{c_1^0\alpha(c_1^0 - 70.c_1^0\alpha)}{93 - b\,(c_1^0)^2\alpha^2}, \tag{19}$$

where

$$b = \frac{\nu}{1 - \nu}.$$

Figure 9 depicts the temperature displacement which corresponds to the maximum sound velocity when the concentration of a solution of KCl in water is varied. The absence of experimental data makes it impossible for us to verify the agreement of the calculated values with the experimental values. However, similar data [12] concerning the displacement of t_{max} in a solution of $MgSO_4$ prove the fact that in any case an agreement exists, as far as the order of magnitude is concerned, between the calculated and experimental values of the temperatures at which the velocity of sound in solutions of various concentrations has a maximum value.

LITERATURE CITED

[1] F. Danusso, "Velocita ultrasonora e compressibilita adiabatiche di niscele liquide atemiche o ideali," Atti. Accad. Naz. Lincei, Rend. classe sci. fis. mat. e nat. 10, 235-242 (1951).

[2] I. V. Persianova, Investigation of the Adiabatic Compressibility of Binary Liquid Systems (Dissertation), (Moscow Chemical Engineering Institute, 1955).

[3] W. Schaaffs, "Die Schallgeschwindigkeit von Lösungen und ihre Beziehungen zur Schallgeschwindigkeit des gelösten Stoffes," Z. physik 1937, No. 105, 658-675.

[4] B. B. Kudriavtsev, "Sound velocities in individual liquids and in liquid mixtures," J. Acoustics (USSR) 2, 1, 39-50 (1956) [Soviet Physics — Acoustics, p. 36].

[5] O. K. Rice, Electron Structure and Chemical Bonding (Foreign Lit. Press, Moscow, 1949).

[6] Abbreviated Handbook of Physico-Chemical Quantities (State Chemical Press, Moscow, 1955).

[7] A. Eucken, "Weiteres zur Assoziation des Wassers," Z. Elektrochem. 53, 3, 102-106 (1949).

[8] Landolt-Börnstein, Physikalisch-chemische Tabellen, 1923-1936.

[9] E. B. Freyer, "Sonic studies of the physical properties of liquids-II," J. Am. Chem. Soc. 53, 1313-1320 (1931).

[10] P. Prozorov, "Compressibility of aqueous solutions of strong electrolytes," J. Phys. Chem. (USSR) 14, 384-391 (1940).

[11] R. A. McConnel, and W. F. Mruk, "Microacoustic interferometer using 30-Mc pulses," J. Acoust. Soc. Am. 27, 4, 672-676, (1955).

[12] K. Tamm, and H. G. Haddenhorst, "Measurements by optical methods of the sound velocity in aqueous solutions of electrolytes," Acustica 4, 6, 653-657 (1954).

Moscow Regional Pedagogical Institute **Received February 5, 1956**

THE TRANSITION TO A GEOMETRIC APPROXIMATION IN THE THEORY OF ELASTICITY

M. L. Levin and S. M. Rytov

It is shown that the law of variation of shear-wave polarization along corresponding rays follows from the linearized equations of the theory of elasticity in a geometric approximation, along with the equation of the eikonal and the laws of conservation of energy flow in the compression and shear-waves. This polarization law proves to be the same as that which applies to electromagnetic waves.

As one of the authors of this paper has shown earlier [1], the transition to an approximation of geometric optics from the Maxwell equations, instead of from a scalar wave equation, permits us to obtain an additional result which pertains to the variation of the polarization of the electromagnetic oscillation along a ray. The use of the Wentzel-Kramers-Brillouin method with vector equations leads to the eikonal equation in the null approximation, and from the conditions for solving the equations of the first approximation (the conditions of orthogonality) there follows not only the law of conservation of light flux, but also the polarization law. Namely:

$$\frac{d\varphi}{ds} = \frac{1}{T}, \tag{1}$$

where φ is the angle between the electrical intensity and the chief normal to the ray, ds is an element of length of the ray and T is the radius of torsion of the ray.

An analogous result can be obtained in wave mechanics if we begin not with the Schroedinger equation but with the Dirac equations. As we know, this was first done by Pauli [2] who nevertheless discussed only one of the conditions of orthogonality (conservation of charge). The full analysis of this problem was conducted both for an electron and for a meson (the Prok equations) by A. D. Galanin [3], who showed that the remaining conditions of orthogonality yield the laws of rotation (and procession) for the spin when a particle moves along a classical trajectory.

In this paper the same problem is solved for linearized equations of the theory of elasticity, which encompass both compression waves and shear waves. It is precisely for the shear waves that the law of variation of the polarization along a ray is clarified in an approximation of geometric acoustics; such an analysis has not been made before as far as we know.

We start from the equations of motion

$$\rho \ddot{u}_\alpha = \frac{\partial \sigma_{\alpha\beta}}{\partial x_\beta}, \tag{2}$$

where $\mathbf{u} = (u_1, u_2, u_3)$ is the displacement vector and $\sigma_{\alpha\beta}$ is the stress tensor:

$$\sigma_{\alpha\beta} = \lambda \frac{\partial u_\gamma}{\partial x_\gamma} \delta_{\alpha\beta} + \mu \left(\frac{\partial u_\alpha}{\partial x_\beta} + \frac{\partial u_\beta}{\partial x_\alpha} \right) \tag{3}$$

The density ρ of the medium and the Lame coefficients λ and μ are sufficiently smooth functions of the point.

Let us substitute (3) into (2), and let us assume that:

$$u_\alpha = A_\alpha e^{i\omega(t-\Phi)}.$$

Converting to vector notation and using the definition

$$\mathbf{p} = \operatorname{grad} \Phi, \tag{4}$$

for the sake of brevity, we obtain the following result:

$$\begin{aligned} &\omega^2 \{(\rho - \mu p^2)\mathbf{A} - (\lambda + \mu)(\mathbf{p}, \mathbf{A})\mathbf{p}\} - \\ &- i\omega \{(\lambda + \mu)(\operatorname{grad}(\mathbf{p}, \mathbf{A}) + \mathbf{p} \operatorname{div} \mathbf{A}) + \mu(\mathbf{A} \operatorname{div} \mathbf{p} + 2(\mathbf{p}, \nabla)\cdot\mathbf{A}) + \\ &+ (\mathbf{p}, \mathbf{A}) \operatorname{grad} \lambda + (\operatorname{grad} \mu, \mathbf{p})\mathbf{A} + (\operatorname{grad} \mu, \mathbf{A})\mathbf{p}\} + \ldots = 0. \end{aligned} \tag{5}$$

The terms which do not contain ω are not written here, since they will not be needed further on.

Expanding **A** in the inverse powers of $i\omega$, we obtain

$$\mathbf{A} = \mathbf{U} - \frac{1}{i\omega}\mathbf{V} - \ldots,$$

we then obtain the equations for the null approximations from Equation (5):

$$(\rho - \mu p^2)\mathbf{U} - (\lambda + \mu)(\mathbf{p}, \mathbf{U})\mathbf{p} = 0 \tag{6}$$

and the equations for the first approximation:

$$(\rho - \mu p^2)\mathbf{V} - (\lambda + \mu)(\mathbf{p}, \mathbf{V})\mathbf{p} = \mathbf{X}, \tag{7}$$

where

$$\begin{aligned} \mathbf{X} = (\lambda + \mu)(\operatorname{grad}(\mathbf{p}, \mathbf{U}) + \mathbf{p} \operatorname{div} \mathbf{U}) + \mu(\mathbf{U} \operatorname{div} \mathbf{p} + 2(\mathbf{p}, \nabla)\cdot\mathbf{U}) + \\ + (\mathbf{p}, \mathbf{U}) \operatorname{grad} \lambda + (\operatorname{grad} \mu, \mathbf{p})\mathbf{U} + (\operatorname{grad} \mu, \mathbf{U})\mathbf{p}. \end{aligned} \tag{8}$$

The condition for the existence of a solution which is different from zero for the system of homogeneous Equations (6) is the requirement that the determinant of that system must be equal to zero; this condition yields the "equation of the eikonal" (i.e., the equation which determines p^2):

$$(\rho - \mu p^2)^2 [\rho - (\lambda + 2\mu) p^2] = 0. \tag{9}$$

Thus we have one simple root which corresponds to the compression wave:

$$p = \sqrt{\frac{\rho}{\lambda + 2\mu}} = \frac{1}{c_l}, \quad \mathbf{p} = \frac{\mathbf{t}_l}{c_l}, \tag{10}$$

and one double root which corresponds to the shear wave:

$$p = \sqrt{\frac{\rho}{\mu}} = \frac{1}{c_l}, \quad \mathbf{p} = \frac{\mathbf{t}_l}{c_t}. \tag{11}$$

The velocities of the compression and shear waves are denoted by c_l and c_t; the unit vectors obtained from the tangents to the corresponding rays are denoted by $\mathbf{t}_l$ and $\mathbf{t}_t$. In the geometric approximation the compression and shear waves are independent of one another.

The condition for solving the system of inhomogeneous equations of the first approximation (7) whose determinant is equal to zero is, as we know, the orthogonality of the right-hand portion $\mathbf{X}$ to each of the linearly-independent particular solutions of the transposed homogeneous system. Since the matrix of the homogeneous Equation (6) is symmetrical (for the sake of simplicity we assume that the medium is non-absorbing and that λ and μ are real), the solutions of the transposed system coincide with the solutions of the original system.

In the compression wave the displacement is subject only to the condition of colinearity of the ray (i.e., the general solution for Equation (10) is of the form:

$$\mathbf{U} = U\mathbf{t}_l. \tag{12}$$

It is not difficult to verify the fact that this is the sole form of the solution of the System (6) in the case under examination where the route of the eikonal equation is a simple one; this can be done by substituting Equation (10) into Equation (6). Therefore we have only one condition of orthogonality for $(\mathbf{X}, \mathbf{t}_l) = 0$, or

$$(\mathbf{X}, \mathbf{U}) = 0.$$

Introducing Expression (8) into the above expression and taking Expressions (10) and (12) into account, it is easy to reduce this condition to the form

$$\operatorname{div} \{U^2 (\lambda + 2\mu) \mathbf{p}\} = \operatorname{div} \{\rho U^2 \mathbf{c}_l\} = 0, \tag{13}$$

i.e., we obtain the law of conservation of energy flux in the compression wave.

It follows from Equations (6) and (11) that in the shear wave the displacement is subject only to the condition that it be transverse:

$$(\mathbf{p}, \mathbf{U}) = 0, \tag{14}$$

i.e., two linearly independent particular solutions which are orthogonal to $\mathbf{p}$ correspond to the double root of Equation (11). We can take the unit vectors of the chief normal ($\mathbf{n}$) and of the binormal ($\mathbf{b}$) to the ray in the capacity of these solutions:

$$\mathbf{U}_1 = \mathbf{n}, \qquad \mathbf{U}_2 = \mathbf{b}.$$

Then the general solution of Equations (6) is written in the form

$$\mathbf{U} = P\mathbf{n} + Q\mathbf{b}, \tag{15}$$

where for the time being P and Q are arbitrary functions of a point on the ray. The form of P and Q is determined by the conditions of the orthogonality of $\mathbf{X}$ to both of the particular solutions of $\mathbf{n}$ and $\mathbf{b}$:

$$(\mathbf{X}, \mathbf{n}) = 0, \qquad (\mathbf{X}, \mathbf{b}) = 0, \tag{16}$$

where the general Solution (15) must be substituted into $\mathbf{X}$.

Having carried out the substitution of (8) and (15) into (16), we may reduce the conditions of orthogonality to the form

$$\begin{aligned} P\,\mathrm{div}\,\mu\mathbf{p} + 2\mu p\left(\mathbf{n}, \frac{d\mathbf{U}}{ds}\right) &= 0, \\ Q\,\mathrm{div}\,\mu\mathbf{p} + 2\mu p\left(\mathbf{b}, \frac{d\mathbf{U}}{ds}\right) &= 0, \end{aligned} \tag{17}$$

Here we utilize the relationship

$$(\mathbf{p}, \nabla) = p\,(\mathbf{t}_l, \nabla) = p t_{l\alpha} \frac{\partial}{\partial x_\alpha} = p\,\frac{d}{ds},$$

where ds is the length element of the ray.

Having multiplied the first of Equations (17) by P and the second equation by Q, we then add and obtain ($P^2 + Q^2 = U^2$):

$$\mathrm{div}\,\{U^2\mu\mathbf{p}\} = \mathrm{div}\,\{\rho U^2 \mathbf{c}_l\} = 0, \tag{18}$$

(i.e., we obtain the law of conservation of energy flux in the shear wave.)

Multiplying the first of Equations (17) by Q and the second equation by P, we add and obtain

$$\left(Q\mathbf{n} - P\mathbf{b},\ \frac{d(P\mathbf{n} + Q\mathbf{b})}{ds}\right) = 0,$$

where

$$P\frac{dQ}{ds} - Q\frac{dP}{ds} = Q^2\left(\mathbf{n},\ \frac{d\mathbf{b}}{ds}\right) - P^2\left(\mathbf{b},\ \frac{d\mathbf{n}}{ds}\right).$$

By means of the Fresnel formulas, we obtain:

$$\frac{d\mathbf{n}}{ds} = -\frac{\mathbf{t}_l}{R} - \frac{\mathbf{b}}{T},\quad \frac{d\mathbf{b}}{ds} = \frac{\mathbf{n}}{T} \tag{19}$$

(R is the radius of curvature of the ray). The previous equation is reduced to the form of Equation (1)

$$\frac{d\varphi}{ds} = \frac{1}{T}, \tag{20}$$

where $\varphi = \text{arc}\tan\frac{Q}{P}$ is the angle between the displacement vector **U** in the shear wave and the chief normal **n** to the ray.

Thus the law of variation of polarization along the ray in the shear wave is the same as it is in an electromagnetic wave: when torsion is present in the ray, the displacement vector **U** rotates relative to a natural trihedron according to the Law (20). The fact that Expressions (1) and (20) coincide is rather natural if we turn our attention to the fact that the Maxwell equations (for a wave field) are formally equivalent to the equations for elastic waves, but in a special medium which possesses elasticity only when torsion is present [4].

Making use of (19) and (20), we can calculate the rotation of a unit vector directed along **U**:

$$\mathbf{u}_1 = \mathbf{n}\cos\varphi + \mathbf{b}\sin\varphi,$$

i.e., we can find the law of rotation for **U** with respect to a certain independent fixed system of coordinates:

$$\frac{d\mathbf{u}_1}{ds} = -\mathbf{t}_l\frac{\cos\varphi}{R}.$$

From this it follows that when s increases the rotation of **U** ceases at those points of the ray at which the displacement is colinear with the binormal ($\varphi = \pm\ \pi/2$).

Let us note in conclusion that taking into account the weak absorption which is caused by replacing $\lambda + \frac{2}{3}\mu$ and μ by complex moduli which contain the volume and shear viscosity ($\lambda + \frac{2}{3}\mu + i\omega\zeta$ and $\mu +$ $+ i\omega\eta$, where $\eta_1 = \eta\omega^2$ and $\zeta_1 = \zeta\omega^2$ are considered to be quantities of zero order) leads to the usual change in the appearance of the laws for the intensities (13) and (18), but does not affect (20).

LITERATURE CITED

[1] S. M. Rytov, "The transition from wave to geometric optics," Doklady Akad. Nauk SSSR 43, 4-5, 263-266 (1938).

[2] W. Pauli, "Diracs Wellengleichung des Elektrons und geometrische Optik," Helv. Phys. Acta 5, 3, 179-199 (1932).

[3] A. D. Galanin, "Untersuchung der Eigenschaften des Elektronen-und Mesonenspins in der klassischen Nährung," J. Phys. (USSR) 6, 1-2, 35-47 (1942).

[4] J. MacCullagh, "An essay towards a dynamical theory of crystalline reflexion and refraction," Trans. Roy. Irish Acad. 21, 17-62 (1848); Coll. works (Dubl. Univ. Press, 1880), 145-193; see also E. Whittaker, History of the Theories of Ether and Electricity I (1951), ch. V. pp. 142-144.

Pedagogical Institute of the City of Ivanovo,
P. N. Lebedev Physics Institute of the
Acad. Sci. USSR, Moscow

Received January 26, 1956

SCATTERING OF SOUND WAVES BY SINUSOIDAL AND SAW-TOOTH SURFACES

A. N. Leporskii

The results of experimental investigations on the scattering of acoustic waves by sinusoidal and saw-tooth surfaces are compared with the Lysanov theory [7]. In the region where the theory can be utilized for relative amplitude values of acoustic pressure in spectral beams, a satisfactory agreement is observed between the experimental and the calculated data.

Almost all of the experimental papers known that deal with the investigation of scattering on periodically-uneven surfaces (see, for example, [1, 2]) do not provide the possibilities of conducting a quantitative comparison of the obtained experimental data with the existing approximate theories [3-7]. The experimental data which we have obtained permit us to make such a comparison rather simply.

The purpose of this paper is the comparison of experimental data with the theory of Iu. P. Lysanov, as well as a comparison of experimentally determined angular positions of spectral beams with theoretical data. The experimental equipment and the method of measurement have been described by us in earlier papers [8].

We investigated an acoustic field which was scattered by models of sinusoidal and saw-tooth shape whose parameters and wavelengths for the incident sound are given in Table 1.

The angles of incidence of the sound upon the scattering area varied in steps of 10° from 0 to 60°. In the course of this work we investigated seven different models and we obtained more than one hundred indicators of scattering.

It is known that in order to observe the diffractional subdivision of an acoustic field into individual maxima and minima it is necessary to get far away from the object upon which the diffraction occurs; the distance R from the object, which satisfies the relationship:

$$R \gg \frac{D^2}{\lambda}, \tag{1}$$

is satisfactory, where D is the linear dimension of the object upon which the diffraction takes place, λ is the wavelength of the acoustic wave. In the case of periodically-uneven surfaces with finite dimensions, which have a period of unevenness L, the diffractional separation of the acoustic field into individual spectral beams will occur for the considerably less rigorous condition:

$$R \gg \frac{DL}{\lambda}, \tag{2}$$

where D is the length of the scattering area. This assumption presupposes that $D \gg L$ and $L \gg \lambda$. At these distances the separation of the acoustic field into separate spectral beams is dependent on the magnitude of the period L of the roughnesses. The diffractional divergence of each of the spectral beams at these distances is still insignificant and can be observed only when Condition (1) is fulfilled.

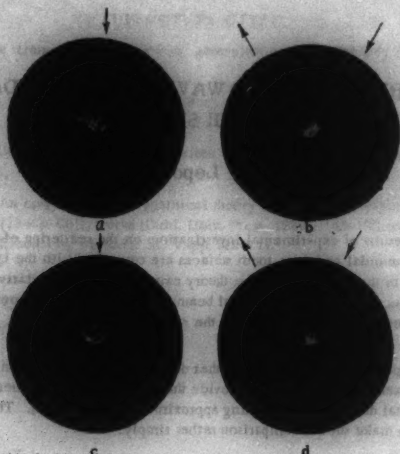

Fig. 1

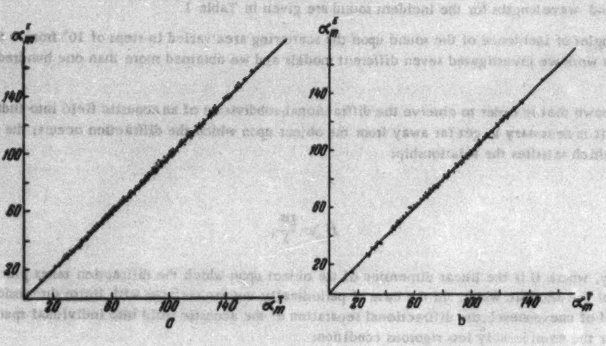

Fig. 2

Relationship (2) was initially obtained by us from the simple geometric concepts in [8] and was later rigorously derived analytically by Iu. P. Lysanov [7].

As an example, Fig. 1 shows the experimental indicators of scattering in the case of sinusoidal (a, b) and saw-tooth (c, d) surfaces. The arrows directed toward the center indicate the direction of incidence for the acoustic wave; the arrows directed away from the center indicate the direction of propagation for the spectra of zero order (mirror-reflected waves). In the figure it is evident that there is a sharp separation of the field into

TABLE

Shape of the unevenness	L — period of the roughnesses in millimeters	a — amplitude of the roughnesses in millimeters	λ — wavelength of the incident sound in millimeters
Sinusoidal	15.2	1.05	4.94; 3.57
"	15.2	1.37	4.94; 3.61; 2.60
"	15.2	1.08	4.71
Saw-tooth	15.0	0.5	4.95; 3.60; 2.88
"	15.0	1.50	4.95; 3.20; 2.60
"	15.0	0.95	2.90
"	15.0	5.00	4.95; 3.60

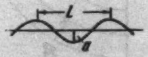

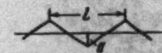

separate spectral beams. The fine structure of the spectra, as expected, cannot be detected. From the resulting scattering indicators it is possible to conclude that for the purpose of fulfilling inequality (2) it is sufficient that R be 4-6 times greater than DL/λ.

The angular position of the spectral beams with respect to the median plane of the uneven surface can easily be determined from the experimental scattering indicators. In accordance with the above-cited theories [3-7], the angular position of the diffraction spectra is determined by the expression

$$\cos\alpha_m = \cos\alpha_0 + m\frac{\lambda}{L}, \tag{3}$$

where α_0 is the angle of slip for the incident wave, α_m is the angle of slip for the spectra of the m-th order, m = 0, ±1, ±2, ..., λ is the wavelength of the incident wave, L is the period of the roughnesses.

We attempted to compare the experimental angular position of the spectra with their angular position which was calculated according to Equation (3). The results of this comparison are shown in the graphs of Fig. 2, where the experimentally determined angles of slip α_m^E for the spectra of order m are plotted along the axes of ordinates, and the values of α_m^T calculated according to Equation (3) are plotted along the axes of abscissas. Graph a refers to the case of sinusoidal surfaces, Graph b refers to the case of saw-tooth surfaces. As can be seen from the graphs, Expression (3) for determining the angular position of the diffraction spectra is well verified by the experiment, both for sinusoidal and for saw-tooth surfaces.

The experimental indicators of scattering which were obtained by us permitted us to evaluate the relative magnitudes of the acoustic pressure in the directions of propagation of the diffraction spectra. The results of the experiment were compared with the calculated data obtained on the basis of the derivations in the paper by Iu. P. Lysanov [9].

We plotted graphs which were of the following nature: the values of A_m^E which were proportional to the acoustic pressure in the directions of propagation of the experimentally-obtained m-th order spectra were plotted along the axes of ordinates; the corresponding values of A_m^T which were theoretically calculated were plotted along the axes of abscissas. Such a graph was plotted for each investigated surface for a given wavelength of incident sound and for seven different angles of incidence. On each of these graphs straight lines were drawn

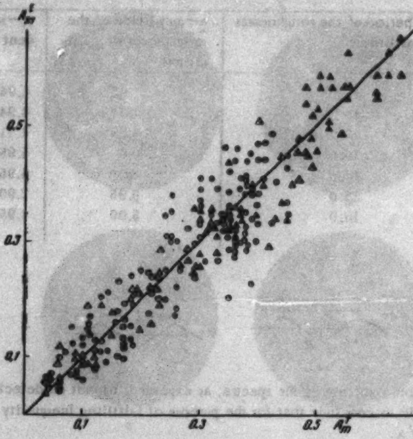

Fig. 3

through the resulting points and the origin; these straight lines had different slopes in each separate case. It is not difficult to vary the scale along the axis of ordinates in such a way that these straight lines coincide with the bisector of the coordinate angle. The graphs obtained in this manner for the sinusoidal and saw-tooth surface models listed in the table (with the exception of the last of the saw-tooth models) were reduced to a single graph shown in Fig. 3. Here the circled points refer to the case of sinusoidal models; the points denoted by triangles refer to the case of saw-tooth models. It is evident from the graphs that the experimental points are well grouped near the bisector of the coordinate angle, if we take into account the fact that the accuracy of the experiment was approximately 25%. This indicates satisfactory agreement between experiment and theory.

For greater convenience Figs. 4 and 5 show the scattering indicators in a polar system of coordinates in a certain arbitrary linear scale for the purposes of an example; these indicators are plotted in accordance with the data on the graph in Fig. 3. Here the solid straight lines coincide with the direction of propagation of the corresponding diffraction spectra. The crosses indicate the relative amplitude values of the spectra, calculated according to the theory; the circles indicate the corresponding experimental values. The arrows directed away from the center indicate the direction of propagation for the zero-order spectra.

Figure 4 shows three indicators of scattering for a sinusoidal model having L = 15.0 mm, a = 1.08 mm for an incident sound wavelength of λ = 4.71 mm. Figure 5 illustrates scattering from a saw-tooth model having L = 15.0 mm, a = 0.50 mm for λ = 3.60 mm.

Without showing the scattering indicator for a saw-tooth model with the parameters L = 15.0 mm, a = 5.00 mm (the last model in the table), we shall indicate that there is no correlation between the experimental and theoretical data because the theory is inapplicable in this particular case.

In conclusion I express my appreciation to L. M. Brekhovskikh and V. S. Grigor'ev for their advice and remarks, as well as to Iu. P. Lysanov for his participation in the discussion of the experimental data.

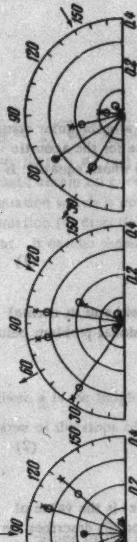

Fig. 4

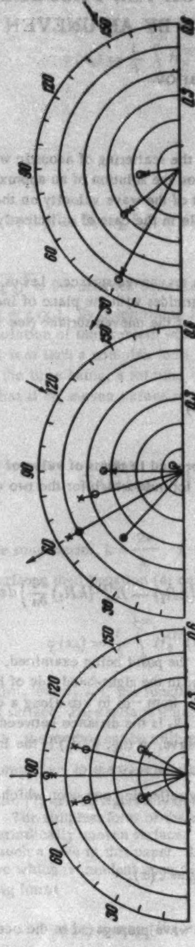

Fig. 5

LITERATURE CITED

[1] F. Conac and V. Gavreau, "Ultrasonore ondes en air et les applications," Acustica 1951, No. 1, 3-16.

[2] Meyer and Bohn, "Schallreflexion an Flächen mit periodischer Struktur," Akustische Beihefte 1952, No. 4, 195-207.

[3] Raleigh, Theory of Sound (State Tech. and Theor. Lit.Press, 1955) pp. 94-101.

[4] Raleigh, "On the Dynamical Theory of Gratings," Sci. Papers (1912) 388.

[5] L. M. Brekhovskikh, "Diffraction of waves by an uneven surface, I. general theory," J. Exptl.-Theoret. Phys. (USSR) 23, 275-288 (1952).

[6] L. M. Brekhovskikh, "Diffraction of waves by an uneven surface," J. Exptl.-Theoret. Phys. (USSR) 23, 289-304 (1952).

[7] Iu. P. Lysanov, The Theory of the Scattering of Waves by Uneven and Inhomogeneous Surfaces, (Dissertation) (Acoustical Institute Acad. Sci. USSR, 1955).

[8] A. N. Leporskii, "Experimental investigation of the diffraction of acoustic waves by periodic structures," J. Acoustics (USSR) 1, 1, 48-571 (1955).

[9] Iu. P. Lysanov, "One approximate solution for the problem of the scattering of ultrasonic waves by an uneven surface," J. Acoustics (USSR) 2, 2, 182-187 (1956) [Soviet Physics — Acoustics, pp. 190-197]

Acoustics Institute of the Acad. Sci. USSR, Moscow

Received February 13, 1956

ONE APPROXIMATE SOLUTION FOR THE PROBLEM OF THE SCATTERING OF ACOUSTIC WAVES BY AN UNEVEN SURFACE

Iu. P. Lysanov

A method is proposed for calculating the scattering of acoustic waves on an uneven surface; this method is based on the solution of an approximate integral equation for the normal component of the wave velocity on the scattering surface. The method is applicable in the case of sufficiently flat absolutely reflecting surfaces.

Let a plane wave be incident at a certain angle upon an uneven surface. Let us select a rectangular system of coordinates (x, y, z) in such a way that the xz plane coincides with the plane of incidence for the acoustic wave, and the plane $z = 0$ coincides with the median level of the uneven surface (see figure) whose equation is given in the form

$$z = \zeta(x). \tag{1}$$

The total field at an arbitrary point (x, z) can be expressed in terms of value of the field and its normal derivative on the scattering surface according to the Green formula which for the two dimensional problem being examined in this case is written in the form

$$\Phi(x, z) = \Phi_i(x, z) + \frac{i}{4}\int\limits_S \left(\Phi \frac{\partial}{\partial n} H_0^{(1)}(kR_1) - H_0^{(1)}(kR_1)\frac{\partial \Phi}{\partial n}\right) ds_1, \tag{2}$$

where $\Phi(x, z)$ is the total value of the velocity potential at the point being examined, $\Phi_i(x, z)$ is the value of the velocity potential in the incident wave; the second term in the right-hand side of Equation (2) describes the scattered field. Integration is conducted within the limits of from $-\infty$ to $+\infty$ along a curve which is obtained as a result of cutting the uneven surface by the plane $y = 0$. R_1 is the distance between the point of observation (x, z) and the variable point x_1, $\zeta(x_1)$ on the integration curve. $n(n_x, 0, n_z)$ is the internal normal to this curve.

Let us assume that the uneven surface is an absolutely reflecting one upon which the following condition is fulfilled:

$$\Phi = 0 \quad \text{for} \quad z = \zeta(x). \tag{3}$$

This case is realized, in particular, when an acoustic wave propagated in the ocean is reflected from the water-air boundary.

Having required that Expression (2) satisfy boundary Condition (3), we obtain a precise integral equation for the function f(x):

$$\varphi(x_2) = \frac{i}{4}\int_{-\infty}^{+\infty} H_0^{(1)}(kR_{12})\, f(x_1)\, dx_1, \tag{4}$$

where

$$\varphi(x_2) \equiv \Phi_i(x_2, \zeta_2); \quad f(x_1) \equiv \frac{\partial \Phi}{\partial n}\frac{1}{n_z}, \quad dx_1 = ds_1 n_z; \tag{5}$$

$R_{12} = \sqrt{(x_2 - x_1)^2 + (\zeta_2 - \zeta_1)^2}$ is the distance between two points lying on the integration curve and it is also true that $\zeta_2 \equiv \zeta(x_2)$ and $\zeta_1 \equiv \zeta(x_1)$. By determining f(x) from Equation (4) and substituting it in Equation (2), we would obtain an accurate solution of the problem which has been posed. However, the core of the integral equation which is obtained is of such a complex form that it is evidently impossible to find the solution of Equation (4) directly. For the time being, a solution can be obtained only for a surface which is sufficiently flat. It can be shown [1] that if an uneven surface satisfies the following two conditions:

$$\frac{1}{2}\left(\frac{\partial\zeta}{\partial x}\right)^2_{\max} \ll 1, \quad ka\left|\frac{\partial\zeta}{\partial x}\right|_{\max} \ll 1. \tag{6}$$

where a is the height of the roughnesses, $k = \frac{2\pi}{\lambda}$, λ is the wavelength of the sound, $\left(\frac{\partial\zeta}{\partial x}\right)_{\max}$ is the maximum value of the slope of the surface, then Equation (4) can be approximately written in the form*

$$\varphi(x_2) = \frac{i}{4}\int_{-\infty}^{+\infty} H_0^{(1)}(k\,|x_2 - x_1|)\, f(x_1)\, dx_1. \tag{7}$$

Since in this approximation $n_z \sim 1$, the function $f(x_1)$ yields the distribution of the normal component of velocity over the scattering surface. For a surface which is sufficiently flat $\left|\frac{\partial\zeta}{\partial x}\right|_{\max} \ll 1$ the method can be utilized for roughnesses which are large in comparison to the wavelength of the sound.

A solution of Equation (7) can be rigorously obtained by means of known methods. The simplest form of the solution occurs for the case of a periodically uneven surface. We shall limit our examination to such a case in this paper. Let us write the expression for the wave which is incident upon the scattering surface in the following form:

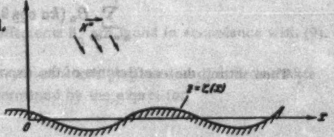

$$\varphi(x) = \exp\{ik(\sin\theta_0 x - \cos\theta_0 \zeta(x))\}, \tag{8}$$

where θ_0 is the angle of incidence.

---

* Let us note that Conditions (6) are analogous to the approximation made by E. L. Feinberg [2] in the problem concerning the propagation of radio waves along a real surface.

Expanding this expression into a Fourier series

$$\exp\left(-ik\cos\theta_0\zeta(x)\right)=\sum_{n=-\infty}^{+\infty}B_n(ka\cos\theta_0)\,e^{inqx}, \tag{9}$$

where a is the height of the roughnesses, $q=\frac{2\pi}{L}$, L is the period of the uneven surface, we obtain the following expression for $\varphi(x)$:

$$\varphi(x)=\sum_{n=-\infty}^{+\infty}B_n(ka\cos\theta_0)\,e^{ik_x^n x}, \tag{10}$$

where $k_x^n = k\sin\theta_0 + nq$.

The solution for $f(x_1)$ will then also be sought in the form of a similar series*

$$f(x_1)=\sum_{m=-\infty}^{+\infty}C_m e^{ik_x^m x_1}. \tag{11}$$

Substituting (10) and (11) into (7) and utilizing the known relationship

$$\frac{1}{2}\int_{-\infty}^{+\infty}H_0^{(1)}(k|\xi|)\,e^{ik_x^m\xi}\,d\xi=\frac{1}{\sqrt{k^2-(k_x^m)^2}}, \tag{12}$$

we obtain

$$\sum_{n=-\infty}^{+\infty}B_n(ka\cos\theta_0)\,e^{inqx}=\frac{i}{2}\sum_{m=-\infty}^{+\infty}C_m\frac{e^{imqx}}{\sqrt{k^2-(k_x^m)^2}}. \tag{13}$$

Then setting the coefficients of the exponentials with identical exponents equal to one another, we obtain

$$C_m=-2i\sqrt{k^2-(k_x^m)^2}\,B_m(ka\cos\theta_0).$$

---

* L. A. Vainshtein indicated the possibility of obtaining solutions in this form.

Then the final form of the expression for $\underline{f(x)}$ can be written as

$$f(x) = -2i \sum_{m=-\infty}^{+\infty} B_m(ka\cos\theta_0)\sqrt{k^2-(k\sin\theta_0+mq)^2}\,\exp\{i(k\sin\theta_0+mq)x\}. \tag{14}$$

Since $\left|\frac{\partial\zeta}{\partial x}\right|_{\max} \sim aq$ for the case of the periodic surface which we are examining, the second of Conditions (6) can be written in a somewhat different form, namely:

$$(ka)^2 \ll L/\lambda. \tag{15}$$

Therefore if the height of the roughnesses is great in comparison to the wavelength of the sound ($ka \geq 1$), then the method is applicable for the condition $L/\lambda \gg 1$. For small values of $\underline{ka}$, values $L/\lambda \sim 1$ are allowable.

If the surface is not periodic (for example, an individual projection on a surface), then the solution of Equation (7) can be obtained by means of generalized Fourier integrals [3].

Knowing the distribution of the normal component of the velocity over the scattering surface, it is possible to calculate the scattered field everywhere above the uneven surface by means of the formula

$$\Phi_S(x,z) = -\frac{i}{4}\int_{-\infty}^{+\infty} H_0^{(1)}(kR_1)\,f(x_1)\,dx_1, \tag{16}$$

which follows directly from Equation (2). The calculation of the integral in (16) in the case where the function $\underline{f(x)}$ is determined by Equation (14) does not present any difficulties. For $\Phi_S(x, z)$ we obtain

$$\begin{aligned}\Phi_S(x,z) = &-\sum_{m,n=-\infty}^{+\infty} B_m(ka\cos\theta_0)\,B_n(ka\cos\theta_{m+n})\,\frac{\cos\theta_m}{\cos\theta_{m+n}}\times\\ &\times\exp\{ik(\sin\theta_{m+n}x+\cos\theta_{m+n}z)\},\end{aligned} \tag{17}$$

where $\sin\theta_r = \sin\theta_0 + r\frac{q}{k}$, $r = m + n = 0, \pm 1, \pm 2, \ldots$ The coefficients B_n are found in accordance with (9).

Thus the scattered field consists of a superposition of plane waves whose propagation directions makes angles θ_r with the $\underline{z}$ axis; the amplitude of the $\underline{r}$-th wave is determined by the expression

$$A_r = \frac{-1}{\cos\theta_r}\sum_{s=-\infty}^{+\infty} B_{r-s}(ka\cos\theta_0)\,B_s(ka\cos\theta_r)\cos\theta_{r-s}. \tag{18}$$

When $|\sin\theta_r| > 1$ the plane wave corresponding to a given value of $\underline{r}$ will be an inhomogeneous wave which is attenuated when it recedes from the uneven surface. Therefore at distances from the surface which are sufficiently large, the scattered field consists of a finite number of plane waves.

From Equation (9) it is evident that for small values of the argument

$$B_s(ka\cos\theta_r) \sim (ka\cos\theta_r)^s. \tag{19}$$

The argument B_s goes to zero when $a \longrightarrow 0$, or $\cos\theta_r \longrightarrow 0$. In the first case, $A_r = 0$ if $r \neq 0$, $A_0 = -1$; this corresponds to reflection from an absolutely compliant plane. The second case corresponds to the propagation of the r-th order spectrum along an uneven surface. For the amplitude of this spectrum, we obtain:

$$A_r = -B_r(ka\cos\theta_0) + \lim_{\cos\theta_r \to 0}\left\{B_{r+1}(ka\cos\theta_0)\frac{\partial}{\partial\cos\theta_r}B_1(ka\cos\theta_r) + \right.$$
$$\left. + B_{r-1}(ka\cos\theta_0)\frac{\partial}{\partial\cos\theta_r}B_{-1}(ka\cos\theta_r)\right\}. \tag{20}$$

From (19) it follows that A_r always has a finite value. In the particular case of a sinusoidal surface $\zeta = a\cos qx$ the coefficients are $B_n = (-i)^n J_n$, where J_n is an n-th order Bessel function. Expression (18) for the amplitudes of the spectra of the scattered field have a simpler form in the case of small roughnesses. Limiting ourselves to terms of the second order with respect to ka, we obtain:

$$A_0 = -1 + (ka)^2\cos^2\theta_0; \quad A_{\pm 1} = ika\cos\theta_0; \quad A_{\pm 2} = \frac{(ka)^2}{2}\cos^2\theta_0. \tag{21}$$

The resulting expressions coincide with the results obtained by Raleigh [4] if on the basis of Equation (15) we assume that $\cos\theta_{\pm 1} \approx \cos\theta_0$.

Let us now examine the scattering of an acoustic wave on an uneven surface which has the linear dimension D in one direction (for example, along the x axis) and extends infinitely in the perpendicular direction. Taking the finite dimensions in the other direction into account does not present any additional difficulties. We thus assume that D is large in comparison to the acoustic wavelength and that it contains a sufficiently large number of periods on the uneven surface. In such a case the scattered field will, as before, be determined by Formula (16), but the integration in this formula will be conducted within the limits of from $-D/2$ to $+D/2$. In doing this we do not take into account the edge effect which will have a magnitude of the order of $\sim \frac{\lambda}{D}$. In the Frauenhoffer zone the scattered field will have the form

$$\Phi_S(x, z) = -\sum_{n=-\infty}^{+\infty} A_n \psi_n \frac{e^{i(kR_0 - \pi/4)}}{\sqrt{\lambda R_0}},$$

where

$$\psi_n = D\cos\theta_n \frac{\sin\left[(\sin\theta_n - \sin\theta)\frac{kD}{2}\right]}{\left[(\sin\theta_n - \sin\theta)\frac{kD}{2}\right]}. \tag{23}$$

A_n is determined according to Equation (18). R_0 is the distance from the center of the area to the observation point. Since $kD >> 1$, the function $\sin\left[(\sin\theta_n - \sin\theta)\frac{kD}{2}\right] : \left[(\sin\theta_n - \sin\theta)\frac{kD}{2}\right]$, (and therefore the scattered field as well) is different from zero only in the vicinity of the directions which satisfy the condition that requires the argument of this function to go to zero. In view of this, it may be said that the scattered field represents the superposition of cylindrical waves; the directivity characteristic for each of these waves is given by Expression (23).

In the Fresnel zone the scattered field has a more complex character. For a certain direction of observation $\theta \neq \theta_r$, we obtain from (16);

$$\Phi_S(x, z) = \frac{-e^{-i\frac{\nu^2}{4\mu}}}{\sqrt{2}} \sum_{m,\, n=-\infty}^{+\infty} B_m(ka\cos\theta_0)\, B_n(ka\cos\theta)\, \frac{\cos\theta_m}{\cos\theta} F(\rho_-, \rho_+), \tag{24}$$

by taking into account the terms $\sim\left(\frac{D}{R_0}\right)^2$ when we expand R_1. Here $\mu \equiv \frac{k\cos^2\theta}{2R_0}$,

$$\nu \equiv k(\sin\theta_r - \sin\theta), \quad F(\rho_-, \rho_+) = \int_{\rho_-}^{\rho_+} e^{i\frac{\pi}{2}u^2}\, du, \quad \rho_\pm = \sqrt{\frac{2R_0}{\lambda}}(\sin\theta_r - \sin\theta) \pm \frac{D\cos\theta}{\sqrt{2\lambda R_0}}.$$

We shall examine the scattered field at distances R_0 from the center of the surface which are such that at these distances the following inequality holds true:

$$\left|\sqrt{\frac{2R_0}{\lambda}}(\sin\theta_r - \sin\theta)\right| \gg \frac{D\cos\theta}{\sqrt{2\lambda R_0}}. \tag{25}$$

Since the point being examined belongs to the Fresnel zone, the right-hand side of (25) is greater than or equal to 1. Therefore

$$\sqrt{\frac{2R_0}{\lambda}}\,|\sin\theta_r - \sin\theta| \gg 1. \tag{26}$$

Under these conditions it is possible to make use of an asymptotic representation of the Fresnel integral in (24):

$$F(\rho_-, \rho_+) \approx \sqrt{\frac{i}{2}} + \frac{e^{i\frac{\pi}{2}\rho_+^2}}{\pi i\rho_+} + \ldots - \sqrt{\frac{i}{2}} - \frac{e^{i\frac{\pi}{2}\rho_-^2}}{\pi i\rho_-} - \ldots \tag{27}$$

Neglecting the small quantities in Expression (27), we obtain:

$$F(\rho_-, \rho_+) \approx 0.$$

Thus at a distance of R_0 which satisfies the Conditions (25) and (26) the scattered field for the directions $\theta \neq \theta_r$ is close to zero. It can therefore be said that the scattered field at such distances consists of individual diffraction beams which are separated in space and which are propagated in the directions $\theta = \theta_r$. We can reduce Condition (25) to a simpler form. For this purpose we shall rewrite it in the form

$$2R_0 |\sin\theta_r - \sin\theta| \gg D. \tag{28}$$

Let us write this condition for the direction θ which is a direction intermediate between the beams $\underline{r}$ and $r + 1$. Assuming that $\lambda/L \ll 1$, we have $\sin\theta \approx \sin\theta_0 + (r + 1/2)\lambda/L$. Substituting $\sin\theta$ in such a form into (28), we obtain:*

$$R_0 \gg DL/\lambda. \tag{29}$$

In the direction $\theta = \theta_r$ the scattered field for the indicated distances is determined by the expression

$$\Phi_S(x, z) = -\sqrt{2}\, A_r F(0, \gamma_r)\, e^{i\left(kR_0 - \frac{\pi}{4}\right)}, \tag{30}$$

where

$$\gamma_r \equiv \frac{D\cos\theta_r}{\sqrt{2\lambda R_0}}.$$

The values of the scattered field which are calculated satisfactorily according to Formula (30) (within the limits of the accuracy of the measurements) agree with the experimental results obtained by A. M. Leporskii [6] for the scattering of sound on uneven surfaces.

The author expresses his deep appreciation to L. M. Brekhovskikh for his valuable advice and for his discussion of the results obtained in this work.

LITERATURE CITED

[1] Iu. P. Lysanov, Theory of Wave Scattering by Uneven and Inhomogeneous Surfaces (Dissertation) (Acoustics Institute Acad. Sci. USSR, 1955).

[2] E. L. Feinberg, Investigations of Radiowave Propagation, Collection II (Acad. Sci. USSR Press, Moscow-Leningrad, 1948).

[3] E. Titchmarsh, Introduction to the Theory of Fourier Integrals. (State Tech. and Theor. Lit. Press, Moscow, 1948).

[4] Raleigh, "On the dynamical theory of gratings," Sci. Papers, 5, 388 (1912).

---

* Condition (29) was obtained earlier in [5] on the basis of purely geometric concepts of the field in the indicated region.

[5] A. N. Leporskii, "Experimental investigation of the diffraction of acoustic waves by periodic structures," J. Acoustics (USSR) 1, 1, 48-57 (1955).

[6] A. N. Leporskii, "The scattering of sound waves by sinusoidal and saw-tooth surfaces," J. Acoustics (USSR) 2, 2, 177-181 (1956) [Soviet Physics — Acoustics, pp. 185-189].

Acoustics Institute of the Acad. Sci. USSR, Moscow

Received February 13, 1956

NON-MIRRORLIKE REFLECTION OF SOUND BY A THIN CYLINDRICAL SHELL

L. M. Liamshev

By using the axially symmetric vibrations of a thin cylindrical shell as an example, it is shown that the non-mirrorlike reflection of sound from a bounded cylindrical shell is dependent on the vibrations of the shell which are excited by the external field.

In the paper cited in [1] it was stated that when a plane acoustic wave is obliquely incident upon a cylindrical shell at certain angles of incidence a strong scattering of sound is observed in the direction opposite to the direction of the incident wave; this is so-called non-mirrorlike reflection. It was also postulated in [1] that the phenomenon of non-mirrorlike reflection is associated with shell vibrations which are excited by the external field. In this paper we utilize axially symmetric vibrations of a thin cylindrical shell to show that the above postulate can be verified; we also clarify certain special features of non-mirrorlike reflection.

In the case of axially symmetric vibrations of a cylindrical shell in air or in a vacuum the equations of motion of the shell have the form [2]:

$$\frac{\partial^2 u}{\partial x^2} + \frac{\nu}{a}\frac{\partial w}{\partial x} - \frac{h^2}{3a}\frac{\partial^3 w}{\partial x^3} = \frac{1}{c_1^2}\frac{\partial^2 u}{\partial t^2} \tag{1}$$

and

$$\frac{\nu}{a}\frac{\partial u}{\partial x} + \frac{1}{a^2}w + \frac{h^2}{3}\frac{\partial^4 w}{\partial x^4} + \frac{h^2}{3a^4}w - \frac{h^2}{3a}\frac{\partial^3 u}{\partial x^3} + \frac{1}{c_1^2}\frac{\partial^2 w}{\partial t^2} = 0, \tag{2}$$

where u is the axial displacement and w is the radial displacement, a is the radius, 2h is the thickness of the shell, c_1 is the velocity of longitudinal waves in the thin plate, ν is the Poisson coefficient of the shell material.

Let a wave be propagated along the shell in the positive direction along the x axis; let the displacement of this wave be described by the expressions:

$$u = u_0 e^{ik_x x} \tag{3}$$

and

$$w = w_0 e^{ik_x x}. \tag{4}$$

Here $k_x = \frac{\omega}{c_x}$, c_x is the velocity of propagation of the vibrations in the shell.

Let us substitute Expressions (3) and (4) into (1) and (2); then the latter expressions can be rewritten in the form

$$k_x^2a^2u_0 - ik_xa\nu w_0 - ik_x^3a^3\frac{h^2}{3a^2}w_0 = k_1^2a^2u_0 \tag{5}$$

and

$$i\nu k_xau_0 + w_0 + \frac{h^2}{3a^2}k_x^4a^4w_0 + \frac{h^2}{3a^2}w_0 + i\frac{h^2}{3a^2}k_x^3a^3u_0 = k_1^2a^2w_0 \tag{6}$$

Eliminating u_0 from Expression (5), substituting its value into Relationship (6) and also neglecting the terms which are small in comparison to unity, we obtain a dispersion equation which relates the propagation velocity of the axially symmetric vibrations to parameters of the shell:

$$\frac{h^2}{3a^2}k_x^6a^6 - \left(\frac{2h^2\nu}{3a^2} + \frac{h^2}{3a^2}k_1^2a^2\right)k_x^4a^4 + (1-\nu^2-k_1^2a^2)k_x^2a^2 - (1-k_1^2a^2)k_1^2a^2 = 0. \tag{7}$$

Let us analyze Equation (7). Let us assume that the radius of the shell is large in comparison to the length of a longitudinal wave in the material of the shell, i.e., let

$$k_1^2a^2 \gg 1. \tag{8}$$

Turning our attention to Condition (8), Equation (7) can be rewritten in the following manner:

$$\frac{h^2}{3a^2}k_x^6a^6 - \frac{h^2}{3a^2}k_1^2a^2k_x^4a^4 - k_1^2a^2k_x^2a^2 + k_1^4a^4 = 0$$

or

$$(k_x^2a^2 - k_1^2a^2)\left(\frac{h^2}{3a^2}k_x^4a^4 - k_1^2a^2\right) = 0. \tag{9}$$

From Equation (9) we obtain

$$k_x^2a^2 - k_1^2a^2 = 0$$

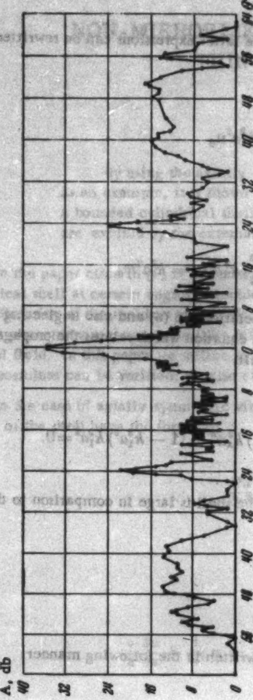

Fig. 1

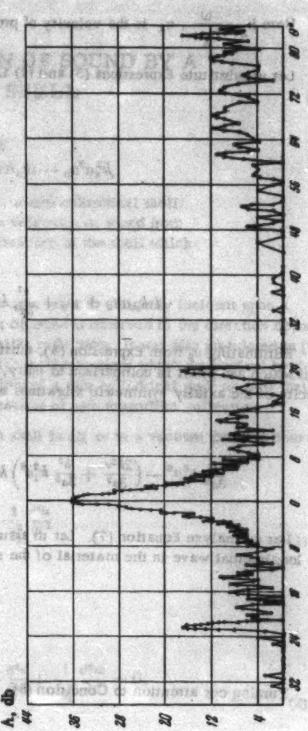

Fig. 2

and

$$\frac{h^2}{3a^2} k_x^4 a^4 - k_1^2 a^2 = 0,$$

where

$$c_x = c_1, \tag{10}$$

i.e., c_x is equal to the velocity of propagation of longitudinal vibrations in a thin sheet.

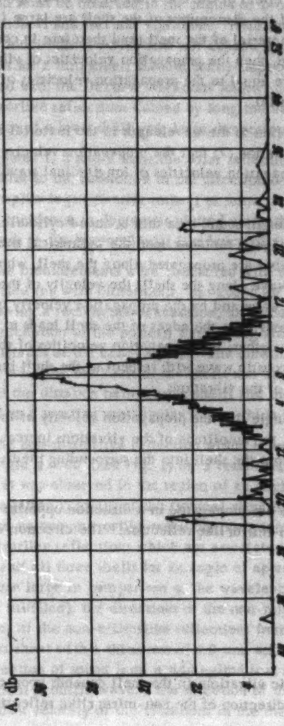

Fig. 3

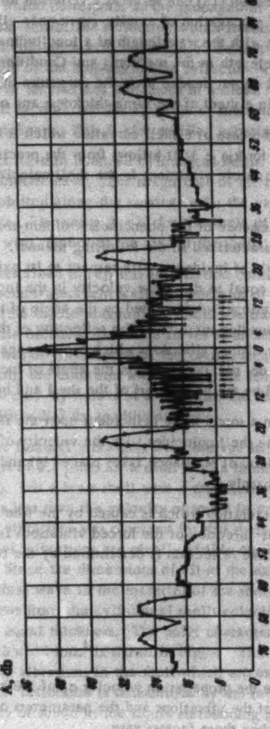

Fig. 4

Further,

$$c_x = \left[\frac{1}{3}\omega^2 c_1^2 h^2\right]^{1/4}. \qquad (11)$$

Expression (11) represents a formula for the velocity of propagation of flexural vibrations in a thin sheet.

Thus for high frequencies or large radii the vibrations in the shell are propagated with the velocities of longitudinal and flexural waves in a sheet.

From Equation (7) it can be established that the propagation velocities of the longitudinal and flexural vibrations in the shell coincide with the propagation velocities of longitudinal and flexural vibrations in a thin sheet with an accuracy of up to 1%, if

$$k_1 a > 10. \qquad (12)$$

Expression (12) can serve as a criterion for evaluating the effect of the curvature of the shell upon the velocity of propagation of axially-symmetric vibrations in it. If the dimensions of the shell are large in comparison with the wavelength of a longitudinal wave in the material of the shell (and therefore in comparison to the wavelength in the medium) and Condition (12) is fulfulled, then the propagation velocities of vibrations in the shell do not depend upon the curvature of the shell and are equal to the propagation velocities of the vibrations in a sheet of the same thickness and of the same material.

For the case of a shell curvature which is small in comparison to the wavelength in the material of the shell (i.e., for $k_1a < 1$) it follows from the precise solution of Equation (7) that the propagation velocity of axially symmetric vibrations in the shell coincides with the propagation velocities of longitudinal waves in a rod.

The essence of the phenomenon of non-mirrorlike reflection of sound by a thin bounded cylindrical shell may be characterized in the following manner. When a sound wave is incident upon the cylindrical shell at a certain angle of incidence with respect to its axis, forced vibrations are propagated along the shell, whose velocity is equal to the phase velocity in the incident acoustic wave along the shell; the velocity of these forced vibrations is determined by the angle of incidence of the wave and by the propagation velocity of sound in the surrounding medium. The reflection of the forced vibrations from the edges of the shell leads to the appearance of free vibrations which are propagated toward one another; the propagation velocities of these free vibrations do not depend upon the angle of incidence of the acoustic wave with respect to the shell but are determined by the parameters of the shell and by the frequency of the vibrations.

When a sound wave is incident upon the shell at such an angle that the propagation velocity of the forced waves in the shell coincides with the velocity of the free waves, the amplitude of the vibrations increases greatly (a certain kind of resonance takes place [1]) and the radiation from the shell into the surrounding medium increases sharply.

The radiation which is caused by the free vibrations which are propagated in a direction opposite to the propagation direction of the forced vibrations is observed as non-mirror like reflection. The direction of the non-mirrorlike reflection is determined by the relationship

$$\sin\theta = c/c_x. \tag{13}$$

Since the propagation velocity c_x of the axially symmetric vibrations in the shell depends upon the frequency of the vibrations and the parameters of the shell, the direction of the non-mirrorlike reflection will also vary when these factors vary.

If the shell is surrounded by a liquid, then the mutual interaction between the shell and the liquid can lead to a variation in the propagation velocity of the vibrations. However, in our case this interaction is not substantial. In fact, the liquid has practically no effect upon the velocity of longitudinal waves in a plate (rod) nor upon the velocity of flexural waves in a sheet, as long as the velocity of the flexural waves is substantially greater than the velocity of sound in the liquid.* The latter case is the only one which is of interest to us, since when the velocity of the flexural waves is less than the velocity of sound in liquid, the radiation (and therefore the non-mirrorlike reflection) is not observed.

Assuming that the velocity of sound in the surrounding medium (liquid) is independent of frequency, we conclude that the dispersion law for the vibration in the shell [when this law is depicted on an appropriate angular scale which is determined by Expression (13)] shows a variation in the direction of the non-mirrorlike reflection which depends upon the dimensions of the shell and upon the frequency of the vibrations.

---

* In a first approximation the radiation leads only to the attenuation of the vibrations which are being propagated in the shell.

In particular, for a cylindrical shell with large dimensions and a small thickness the non-mirrorlike reflection must be observed in the region of two critical angles which correspond to the propagation velocities of longitudinal and flexural vibrations. Here the angle of the non-mirrorlike reflection which is associated with the longitudinal waves does not depend upon frequency and coincides with the angle of the non-mirrorlike reflection for a thin sheet; the frequency-dependence of the angle of the non-mirrorlike reflection which is associated with the flexural vibrations follows the dispersion curve for flexural vibrations in a sheet. For example, non-mirrorlike reflections caused by longitudinal vibrations must be observed for an angle of incidence of $\theta = 23°$ in the case of a brass shell with large dimensions and a small thickness. This is also verified experimentally.

Figures 1, 2 and 3 show the polar reflection characteristics for thin bounded cylindrical shells. These figures refer to the reflection in the direction opposite to the incident wave. The magnitude of the reflected signal amplitude (in db with respect to some standard level) is plotted along the vertical axis; the value of the angle of incidence in degrees is plotted along the horizontal axis. The value $\theta = 0°$ for the angle of incidence corresponds to the perpendicular incidence of an acoustic wave with respect to the axis of the shell.

The measurements were conducted with the installation described in [1]; this installation consisted of a water-filled tub with dimensions of $200 \times 60 \times 60$ cm^3 with sound-absorbent walls; a generator of ultrasonic pulses having a rectangular waveshape, an X-cut quartz dipole (the dipole accomplishes both the transmission and the reception of the pulses); a receiving amplifier and a pulse oscilloscope which serves as an indicator for the amplitudes of the echo-signals. The duration of the pulses was 30 microseconds, the carrier frequency was 1 megacycle, the thickness of the shells was approximately 1 mm, the diameter was 30 mm, the length was 60 mm, and the distance between the shells and the dipole was 150 cm. By means of a fine wire the shells were attached to a rotating rectangular frame which was equipped with a dial for reading angles.

The non-mirrorlike reflection which is associated with the flexural vibrations was observed in the region of the angle $\theta = 40°$ (see Fig. 1) for a brass shell with a thickness of 1.2 mm; for a shell with a thickness of 0.6 mm it was observed in the region of an angle of 70° (Fig. 2). For a brass shell with a thickness of 0.4 mm the propagation velocity of the flexural vibrations in the shell is less than the velocity of sound in the liquid. Therefore no non-mirrorlike reflection associated with flexural vibrations was observed for this shell (Fig. 3). Non-mirrorlike reflections which are associated with longitudinal vibrations are clearly visible on the polar diagrams of all three shells for an angle of approximately 23°. Since the dimensions of all of the experimental shells were large in comparison to the wavelength of a longitudinal wave in the material of the shells (criterion (12) was fulfilled), the directions of the non-mirrorlike reflections from the cylindrical shells coincide with the directions of the non-mirrorlike reflections from brass sheets of equal thickness. The polar characteristic of a thin brass sheet with a thickness of 0.6 mm and dimensions of 15×30 mm^2 is shown in Fig. 4. Thus non-mirrorlike reflection of sound from a thin cylindrical shell is caused by vibrations in the shell which are excited by the incident acoustic wave. The direction of the non-mirrorlike reflection is determined by the ratio of the propagation velocity of the vibrations in the shell to the velocity of sound in the liquid surrounding the shell.

I express my appreciation to G. D. Maliuzhints for a number of valuable suggestions.

LITERATURE CITED

[1] L. M. Liamshev, Reflection of Sound by Thin Plates and Shells in a Liquid (Acad. Sci. USSR Press, Moscow, 1955).

[2] W. Flugge, Statik und Dynamik der Schalen, Springer, Berlin, 1934).

Acoustics Institute of the Acad. Sci. USSR, Moscow Received November 21, 1955

DIFFERENTIAL METHOD OF MEASURING THE ABSORPTION OF ULTRASONIC WAVES IN LIQUIDS

I. G. Mikhailov and G. N. Feofanov

The paper describes a method which permits the measurement of small differences in the absorption coefficients of ultrasonic waves in liquids, when these liquids are located in two vessels. The results of the tests made of the method are given, and the sensitivity of the method is determined.

It is known that by contemporary methods, the accuracy of measuring the absorption of ultrasonic waves in liquids is not very great. The methods which are most widely used at the present time are pulse methods. The best variants of the pulse methods permit measurements of the absorption with an accuracy that does not exceed several percent. As a consequence of this, the existing methods are of no use for measuring small variations in the ultrasonic absorption of liquids, variations which arise due to the various effects. At the same time it is possible to mention a number of problems which at this time are of great practical and theoretical interest and which require a method for their solution which permits the measurement of small variations in the absorption. Thus, for example, the problem of measuring absorption in dilute solutions is of great interest. Certainly these investigations are of help in understanding the molecular mechanism of ultrasonic wave absorption in solutions and mixtures. Further, it is known that in the solutions of a number of high-molecular substances the absorption differs little from the absorption in the pure solvent [1]. For the theory of such a phenomenon, it is important to know how this small difference between the absorptions of the solution and the pure solvent depends upon temperature and frequency.

For the purpose of solving such problems, we developed a differential method for measuring absorption. The principle of this method consists of the following: two identical piezo-quartz dipoles radiate high-frequency ultrasonic pulses of equal magnitude and duration in a liquid. These pulses are propagated in two different tanks: the carrier tank and the measuring tank (or in one tank which is partitioned). The ultrasonic pulses, having reached opposite walls of the tanks, are reflected from them and are received by the same piezo-quartz plates; then the received pulses are amplified and detected. The circuit for the receiver is composed in such a way that at its output the difference in the intensities of the reflected ultrasonic pulses is measured by means of a pointer instrument. If identical pure liquids are located in both tanks at identical temperatures, then the difference in the intensities of the received signals will be equal to zero. If in the second (measuring) tank the absorption varies due to any cause, then the equilibrium is violated and the pointer of the instrument shows a certain deviation which is proportional to the difference between the absorptions in the two tanks. The utilization of two tanks permits the elimination of certain factors which play a role in the absorption but which are undesirable in the given experiments. Thus, if both tanks are subjected to the same temperature conditions, then the indications of the instrument will not depend upon temperature but will depend, for example, only upon the concentration of the dissolved substance. Here it assumed, of course, that the temperature coefficients of absorption for the pure solvent and the dilute solution are equal. On the other hand, by filling both tanks with the same liquid and varying the temperature in the measuring tank, it is possible to mreaure the temperature coefficient of absorption.

A block diagram of the equipment is shown in Fig. 1.

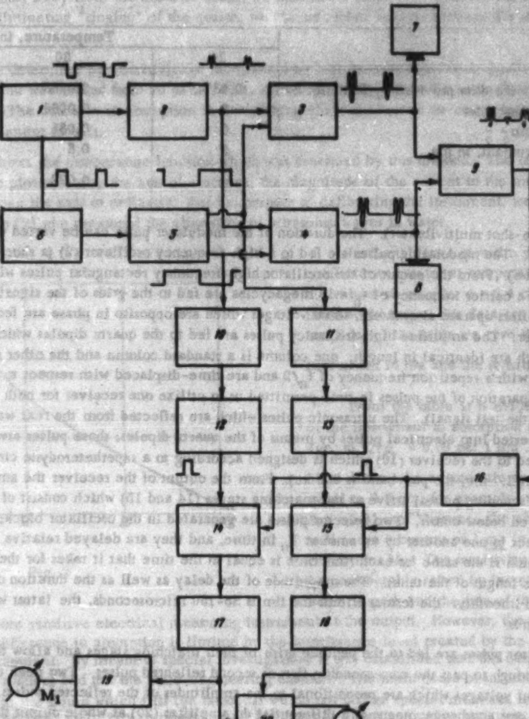

Fig. 1. Block diagram of the equipment for the differential method of measuring the absorption of ultrasonic waves:
1) Modulator; 2) high-frequency oscillator; 3 and 4) amplifiers; 5) trigger;
6) signal generator, 7) standard tank; 8) working tank; 9) mixer; 10 and 11) delay circuits of the selector pulses; 12 and 13) selector-pulse generators, 14 and 15) matching stages; 16) superheterodyne receiver; 17 and 18) peak detectors;
19) vacuum tube voltmeter; 20) dc differential amplifier.

The circuit operates in the following manner. The signal generator (6) (which is a self-excited multivibrator) produces highly unsymmetrical rectangular waves. The repetition frequency f_n of these waves is smoothly variable over the limits 1.4-14 kc. The leading positive edge of the short half-cycle (this half-cycle is of the order of 10 microseconds) sets off the trigger (5) which produces symmetrical rectangular waves with a frequency which is half the frequency f_n. The trailing negative edge of the short-half cycle sets off the

TABLE

		Temperature, in °C		
		20	30	50
α	According to the data provided by Bazhulin	0.0374	0.0288	0.0213
$\Delta\alpha$	for 12 megacycles	0	0.0086	0.0161
$x\Delta\alpha$	for x = 6.4 cm	0	0.055	0.103
Readings of the instrument, in ma		0	0.6	1.2
Sensitivity $\frac{x\Delta\alpha}{1\,\text{ma}}$		–	0.092	0.086

modulator (1) (a one-shot multivibrator). The duration of the modulator pulse can be varied within the limits of 10-15 microseconds. The modulating pulses are fed to a high-frequency oscillator (2) (a shock-excited circuit with under-excitation). From the output of the oscillator, high-frequency rectangular pulses with a repetition frequency of f_n and a carrier frequency of f_b = 12 megacycles are fed to the grids of the signal amplifiers (3) and (4). The amplifiers operate alternately, since voltages which are opposite in phase are fed to their screen grids from the trigger. The amplified high-frequency pulses are fed to the quartz dipoles which operate on two liquid columns which are identical in length: one column is a standard column and the other is a test column. These pulses arrive with a repetition frequency of $f_n/2$ and are time-displaced with respect to one another by a time T_n. Such a separation of the pulses in time permitted us to utilize one receiver for both signals (the standard signal and the test signal). The ultrasonic pulses which are reflected from the rear walls of the tanks (7) and (8) are converted into electrical pulses by means of the quartz dipoles; these pulses are then mixed in the mixer (9) and are fed to the receiver (16) which is designed according to a superheterodyne circuit (the intermediate frequency is 1.7 mc, the pass band is 200 kc). From the output of the receiver the amplified reflected pulses (and also the sounding pulses) arrive at the matching stages (14 and 15) which consist of pentode amplifiers whose grids are biased below cutoff. Two selector pulses are generated in the oscillator block; these pulses are displaced with respect to one another by an amount T_n in time, and they are delayed relative to their sounding pulses by a time which is the same for each (this time is equal to the time that it takes for the ultrasonic pulse to traverse twice the length of the tank). The magnitude of the delay as well as the duration of the selector pulses can be varied smoothly: the former within the limits 35-150 microseconds, the latter within the limits of 15-70 microseconds.

Positive selector pulses are fed to the pentode grids of their matching stages and allow the pentodes to conduct just long enough to pass the corresponding first or second reflected pulses. Two peak detectors (17) and (18) produce constant voltages which are proportional to the amplitudes of the reflected pulses. These voltages are subtracted from one another by means of a differential dc amplifier (20) at whose output the pointer instrument M_2 is placed; this instrument responds to the difference between these voltages. Thus this instrument registers the variation in the amount of ultrasonic absorption in one tank (the test tank) relative to the amount of absorption in the other tank (the standard tank).

If the amplitude of the ultrasonic wave which is incident upon the piezo-quartz plate after having been reflected from the opposite wall of the tank is equal to $A_1 = A_0e^{-\alpha_1 x}$ in the first tank and to $A_2 = A_0e^{-\alpha_2 x}$ in the second tank, then the readings of the instrument M_2 will be proportional to $(\alpha_1-\alpha_2)\, x = \Delta\alpha x$, where α_1 is the absorption coefficient of the liquid in the first tank, α_2 is the coefficient of absorption of the liquid which fills the second tank, and x is the length of the acoustic path (this path is equal to twice the internal distance between opposite walls in the tanks). Since the calibration remains reliable only for one value of signal level (at that value for which calibration was carried out), a vacuum tube voltmeter M_1 19 was introduced into the circuit; this voltmeter measures the amplitude of the standard pulse whose magnitude is maintained at one and the same level.

The tests of the installation were made with two completely identical tanks which were made from polished mirror glass 4 mm thick. The internal dimensions of the tanks were the following: widths 32 mm, height 107 mm and depth 55 mm. The piezo-quartz plates were pressed onto the walls of the tanks in such a way that the sound was propagated across the tanks. Thus the length of the acoustic path was equal to 64 mm. In the remaining portion of the tanks, away from the acoustic beam, we installed a heater, an agitator, and a thermometer. For the purpose of eliminating "ringing" of the quartz, we placed rubber washers between the rear electrode and the quartz sheets.

In order to determine the sensitivity of the method both tanks were filled with distilled water, and the water in the working tank was heated from 20 to 50°. The ultrasonic absorption in the water decreases when the temperature increases. The decrease in absorption in the working channel causes a de-compensation of the current in the pointer (instrument circuit.

Figure 2 shows the temperature function which was measured by this method. The temperature differences in both tanks are plotted along the axis of abscissas; the magnitude of the current in the measuring instrument in ma is plotted along the axis of ordinates. For the purpose of calibrating the instrument, we made use of the data cited by Bazhulin [2] who measured the absorption of ultrasonic waves in water.

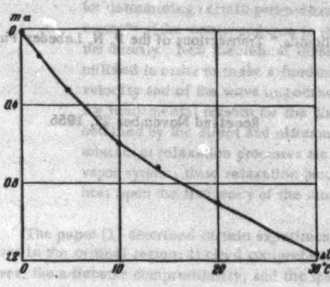

Fig. 2

In the table we give the values for the absorption coefficient in water at temperatures of 20, 30 and 50°; the values of $x\Delta\alpha$ for $x = 6.4$ cm which were calculated according to this data are also given. In the two last lines of the table we give the readings of the instrument in ma and the sensitivity $\frac{x\Delta\alpha}{1\ \text{ma}}$.

From the table it is evident that the sensitivity of the instrument to absorption is equal, on the average, to $x\Delta\alpha = 0.09$ per 1 ma.

If we take an acoustic path length which is equal to 9.0 cm, for example, then a difference of $\Delta\alpha = 0.01\ \text{cm}^{-1}$ between the absorption coefficients will cause a current of 1 ma in the circuit of the instrument M_3. The sensitivity of the installation can be considerably raised by increasing the length of the acoustic path and the gain of the dc amplifier, or by connecting a more sensitive electrical measuring instrument at the output. However, the lower limit for measuring the difference in absorption is limited by the interference level created by the instability in the operation of the equipment. By means of special investigations it was established that the basic source of interference is the acoustic channel and not the radio-engineering channel. The main cause of instability is due to the thermal thermal fluxes in the liquid which fills the tanks. If we do not utilize special measures for the purpose of making the experiment thermally stationary, then the thermal fluxes can cause variations in the readings of our instrument which can attain values of up to 0.2 ma. When the tanks are made thoroughly thermostatic, the interference level can be considerably lowered.

As far as the accuracy of the method is concerned, due to the utilization of a pointer-indicator the accuracy of measuring the difference between absorption coefficients is somewhat higher than the accuracy in measuring the absorption by ordinary pulse methods which utilize cathode-ray indicators. According to preliminary evaluations, our device accurately measures $\Delta\alpha$ to within 3-5%.

In order to illustrate the operation of our installation, we tested it with a suspension of quartz sand whose particles had an average dimension of 8 μ. It was found that the dependency of the instrument readings upon the concentration by weight of the suspension is linear. The sensitivity of the instrument with respect to concentration (in percentage by weight) of the suspension of the specified sand is 0.5% per 1 ma.

Besides the problems described, it is possible, for example, to measure small differences in the reflection coefficients of ultrasonic waves by means of this installation. In order to illustrate this we took a rectangular glass rod with the dimensions 36 × 55 × 60 mm. Two quartz sheets located some distance away from one another were pressed onto one of the surfaces of this glass rod; these two quartz sheets created the working and standard acoustic channels. A column of castor oil 5-6 mm in height was placed upon the surface facing the quartz of the working channel. As a consequence of the difference between the coefficients of reflection from the glass-air and glass-castor oil boundaries, the intensity of the reflected pulses in the two channels becomes different; this causes the de-compensation of the current in the circuit of the instrument M_3. Calculations show that for the glass-castor oil boundary, the coefficient of reflection is equal to 0.655, and for the glass-air boundary the reflection coefficient can be considered equal to 1. This difference in reflection coefficients gives rise to a current of 2 ma in the circuit of the instrument. If we assume that the decrease in the reflection coefficient of the working channel simulates the absorption in this channel, then the sensitivity of the circuit can be calculated in this manner. The sensitivity proved to be $x\Delta\alpha = 0.1$ per 1 ma, and this agrees sufficiently well with the sensitivity found directly according to the temperature dependence of the absorption in water.

LITERATURE CITED

[1] I. G. Mikhailov and L. A Shagalova, "Propagation of ultrasonic waves in solutions of polymers," Doklady Akad. Nauk SSSR 89, 5, 829-832 (1953).

[2] P. A. Bazhulin, "Absorption of ultrasonic waves in liquids," Transactions of the P. N. Lebedev Physics Institute Acad. Sci. USSR 1950, No. 5, 263-338.

Leningrad State University

Received November 22, 1955

THE PROBLEM OF APPLYING ULTRASONIC METHODS IN THE INVESTIGATION OF ORGANIC SUBSTANCES IN THE CRITICAL REGION

V. F. Nozdrev

The paper shows that hysteresis phenomena are absent in the propagation velocity of ultrasonic waves in the critical region of the liquid-vapor system and discusses the problem concerning the possibility of utilizing ultrasonic methods for determining certain parameters of the critical state (T_{cr}, ρ_{cr}). The "diameter"* of the wave impedance is verified by utilization of new data concerning the density. New theoretical investigations of the liquid and gaseous states are utilized in order to make a fundamental analysis of the diameters of the sound velocity and of the wave impedance. It is experimentally shown that one of the fundamental reasons for the discrepancy between the data on specific heat obtained by the direct and ultrasonic methods is the fact that in several substances relaxation processes are present in the critical region of the liquid-vapor system; these relaxation processes lead to a dependence of the specific heat upon the frequency of the ultrasonic waves.

The paper [1] described certain experimental features of the investigation of propagation of ultrasonic waves in the critical region; it cited comprehensive experimental material on the velocity of the ultrasonic waves, the adiabatic compressibility, and the specific heat for that case. The experimentally established mechanisms and rules were explained on the basis of the theory of thermodynamics. This paper is devoted to a clarification of certain new methodological and theoretical problems which arise in connection with further study of the ultrasonic properties in a critical region.

1. In a number of papers [2, 3] devoted to the investigation of the critical state it is indicated that hysteresis phenomena are present in the behavior of certain most important physical parameters (density, viscosity, permittivity, etc.) in the critical region. Here we are speaking of the presence of various values for said parameters at one and the same value of temperatures in the critical region, depending on whether or not the process flows with an increase of temperature or in the opposite direction. From the point of view of method as well as from the point of view of scientific research, it is important to verify whether or not such hysteresis phenomena take place in the behavior of the ultrasonic velocity and the absorption coefficient in the critical region. For this purpose we measured the ultrasonic velocity in many of the substances which we had investigated, increasing the temperature and measuring the ultrasonic velocity simultaneously in the liquid, its saturated vapor, and (during the transition through the critical state) in its reheated vapors. The same type of measurements were also obtained (when the temperature was lowered) for the transition from the reheated steam region to the region of the two-phase state. In certain cases such experiments were repeated many times.

However, we did not observe hysteresis phenomena in the variation of the ultrasonic velocity in any one of the series of such experiments. Within the limits of the error incurred during our experiment (1-2%), the experimental points fall satisfactorily along one curve when measurements are made in the forward and reverse directions.

Figure 1 shows the results of such measurements in the critical region of n-hexane for a transition through the critical state (1) and when critical conditions are not observed (2) (triangles indicate the points which are obtained when the system is cooled). The investigation conducted in our laboratory [4, 5] on the absorption of ultrasonic waves in the critical region (utilizing the pulse, optical and mechanical methods) also failed to lead to the detection of hysteresis phenomena. Schneider's very thorough measurements of the velocity and absorption of ultrasonic waves in sulfur hexafluoride also convincingly demonstrate the absence of hysteresis phenomena in the values of ultrasonic velocity and absorption in the critical region.

---

*["diameter" – double the absolute value, i.e., the diameter of the circle representing the variation of the quantity in the complex plane. Translator's note].

A natural question arises with respect to the results of our experiments as well as with respect to the results of other authors [2, 6]; this question concerns the causes for the appearance of hysteresis phenomena when investigating some parameters (density, viscosity, etc) and the absence of these phenomena when investigating other parameters (velocity and absorption of ultrasonic waves). Our analysis of this question shows that hysteresis phenomena are detected in those cases when the method of measuring the physical parameters does not permit the intermingling of the substance in the critical region [3], or in those cases where this intermingling is limited or cannot be fully effected [2].

It is known [2, 3] that in the critical region of the gradients of density, temperature, and of other quantities are especially evident. This is most noticeable when there is an absence of intermingling in the liquid [3]. Here a very important factor is the temperature regime of the investigated system [3, 6]. Thus the hysteresis phenomena in the critical region arise as a result of the fact that during the measurement of many physical parameters it is difficult methodically to realize the statistically most probable states for which the averaged values of the physical parameters can be measured.

In our view it is just such favorable conditions for measuring the average statistical values that are created in ultrasonic measurements of various kinds, where the element of intermingling (with the aid of the ultrasonic waves) is an organic part of the method of procedure. It is understandable that here it is necessary to utilize the minimum ultrasonic intensity so that the measurements may be made in the region of small amplitudes. In all of our investigations these conditions were rigorously observed [1].

These specifics of the ultrasonic methods substantially broaden their possibilities. In particular, these methods may be successfully used for measuring the parameters of the critical state (i.e., the density and temperature). The density in the critical state can be determined to a sufficient degree of accuracy according to the diameter of the wave impedance which we have proposed [1], and the critical temperature can be determined according to the minimum ultrasonic velocity in the critical state, when the measurements are conducted along the saturation line with a transition through the critical point to the gaseous phase. This can prove especially valuable when applying this method to binary, ternary and other multiple-component mixtures. As an example, we cite the critical temperatures which were measured by the ultrasonic method for several substances (Table 1).

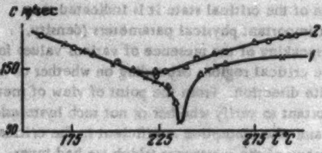

Fig. 1

As can be seen, our data is in good agreement with the tabular values of the critical temperatures. Here it is important to stress that within the limits of the experimental error the minimum for the ultrasonic velocity occurs for one and the same temperature, both during the transition from the reheated steam region to the 2-phase region though the critical point and for the transition from the 2-phase region into the single-phase region (gaseous region).

2. When experimentally establishing the diameter (ρc) of the wave impedance [1], we utilized our experimental data for the ultrasonic velocity. The densities were taken from tables [7].

It is known [7] that the densities in the liquid and the saturated vapor in a critical region were determined on the basis of the postulate that when the meniscus disappears, $\rho_{\text{liq}} = \rho_{\text{sat vap}}$; this method has been used right up to the present time. In actual fact, as the latest investigations have shown, at the temperature where the meniscus disappears $\rho_{\text{liq}} \neq \rho_{\text{sat vap}}$ and the curves for the dependence of density upon temperature along the saturation line for the liquid and especially for the vapor phases deviate from the parabolic law [3].

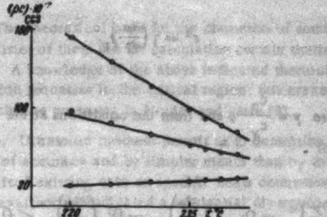

Fig. 2

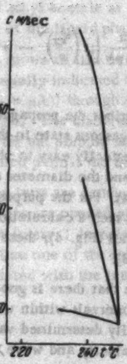

Fig. 3

It became necessary to verify whether or not the rule concerning the diameter of the wave impedance retained its validity when we utilized the newest data concerning the density of the liquid and gaseous phases in the critical region. We were able to do this for two substances: hexane and ethyl alcohol. As we can see from Fig. 2 (ethyl alcohol), the rule postulating a straight-line diameter for the wave impedance retains its validity when we utilize the newest data concerning the density. The curves, naturally, do not come together at the temperature where the meniscus disappears, since here $\rho_{\text{liq}} \neq \rho_{\text{sat vap}}$ and the joining of the curves must evidently occur at a higher temperature. Let us note that we were especially interested in verifying the rule concerning the diameter of the wave impedance in the vicinity of the critical point, when the newest data concerning the density is utilized. In regions far from the critical state, the values of density obtained from the tables and the values obtained in these latest investigations are in good agreement [3].

When new experimental data is obtained concerning the velocity of sound and the density, and when this data verifies the rule concerning the diameter of the wave impedance, the necessity of providing a theoretical basis for this rule becomes a problem which is posed even more sharply. In the papers cited [1] we showed that such a theoretical basis may be obtained by starting from thermodynamic relationships. There we indicated the limited nature of the results we obtained for the region which was directly adjacent to the critical point.

It was important to find such a theoretical basis by starting from the molecular-kinetic concepts. In our laboratory we carried out such a project [8].

TABLE 1

Substance	t_{cr}(°C), obtained from the tables	t_{cr}(°C) determined by the ultrasonic method
Methyl alcohol [11]	240	240
Ethyl alcohol	243.1	243.5
Isobutyl alcohol	282.7	283.5
Ethyl acetate	250	251
Sulfur hexafluoride [6]	45.55	45.65

Starting from the equation describing the state of the substance,

$$p = \frac{kT}{v} - \frac{\partial \varphi}{\partial v}, \tag{1}$$

where $\varphi = \alpha v^{-\mu} + \beta v^{-\nu}$; from the relationship

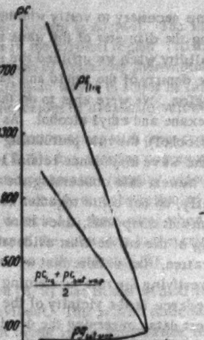

Fig. 4

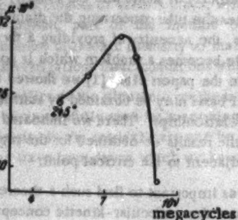

Fig. 5

$$c^2 = \gamma \left(\frac{\partial p}{\partial \rho}\right)_T, \tag{2}$$

where $\gamma = \frac{c_p}{c_v}$, **and from the conditions at the critical point**

$$\left(\frac{\partial p}{\partial v}\right)_{T_{cr}} = 0; \quad \left(\frac{\partial^2 p}{\partial v^2}\right)_{T_{cr}} = 0; \quad \left(\frac{\partial^3 p}{\partial v^3}\right)_{T_{cr}} < 0, \tag{3}$$

we obtain an expression for the velocity of sound*

$$c = \left[\frac{5}{3}\frac{RT}{M} + \frac{RT_{cr}}{M(v-\mu)}\left\{\mu\left(\frac{v_{cr}}{v}\right)^{\nu} - \nu\left(\frac{v_{cr}}{v}\right)^{\mu}\right\}\right]^{1/2}, \tag{4}$$

which satisfactorily describes the propagation of acoustic waves in the liquid and gaseous state in the critical region. In particular, it is theoretically easy to obtain the diameter of the wave impedance and the diameter of the sound velocity [1] from Equation (4). For the purposes of illustration, let us give the results of such a calculation for ethyl acetate (Fig. 3) and propyl alcohol (Fig. 4); these calculations were made by L. Belinskaia [8].

It is characteristic that there is good agreement between the temperature intervals within which the experimentally and theoretically determined values of the diametes of the acoustic velocity and wave impedance are applicable. This can be proved by examining Table 2.

TABLE 2

Substance	Experimental data [12]		Theoretical data [8]	
	t_{cr} -t from the diameter of the sound velocity	t_{cr}-t from the diameter of the wave impedance	t_{cr}-t from the diameter of the sound velocity	t_{cr}-t from the diameter of the wave impedance
Methyl alcohol	15	116	6	
Ethyl alcohol	20	137	10	
Propyl alcohol	20	139	14	129
Ethyl acetate	15	100	10	125
Butyl alcohol	20	124		
Isobutyl alcohol	30	120		5

*** The definition of the quantities which appear in Formulas (1-4) complies with the accepted standard. μ, ν, α, β are constant coefficients in the formula for the potential of interaction φ.**

The theoretical basis for the diameters of sound velocity and wave impedance substantially enhances the possibilities of their use for calculating certain thermodynamic parameters in the critical region (c_p, c_v, β_{ad}, p etc). A knowledge of the above indicated thermodynamic parameters is necessary when investigating relaxation processes in the critical region; this creates great possibilities for the investigation of intramolecular and exchange processes in liquids and gases [9].

3. Ultrasonic methods permit us to determine the specific heats c_p and c_v in the critical region to a high degree of accuracy and by simpler means than by the direct determination of the specific heats [1]. However, the limited existing data on specific heats determined by direct and ultrasonic methods [10] (carbon dioxide, sulfur hexafluoride) indicated a substantial divergence between the data obtained by these two methods. The authors [10] postulate that these divergences are caused by the fact that the velocity of sound is not only a thermodynamic quantity but is also masked by the dispersion effect.

In our laboratory we conducted a study of the possible causes for the discrepancy between the specific heat data obtained by the two above indicated methods [4].

We used ethyl acetate as the object for investigation. In fact, we detected relaxation phenomena in the critical region of the liquid phase of ethyl acetate.*

Figure 5 shows an illustration of the complete relaxation region in ethyl acetate when $t = 245°$ ($t_{cr} = 250°$) this region is usually indicated by passage of the ultrasonic absorption [the absorption is normalized to the wavelength, i.e., ($\mu = \alpha\lambda$)] through a maximum [9]. The measurement of α was carried out in the frequency range 5-15 megacycles. The discovery of relaxation phenomena in ethyl acetate in the critical region permits us to conclude that for the purpose of determining the specific heats by the ultrasonic method it is necessary to utilize frequencies which permit the investigation to be conducted outside of the relaxation region.

When the tests are conducted utilizing frequencies which guarantee the appearance of relaxation regions broad possibilities are opened up for utilizing ultrasonic means to determine the specific heats which are associated with the internal degrees of freedom. For example, in relaxation processes of the exchange type it is possible to utilize one of the relaxation-theory formulas from [9] in order to calculate the specific heat (c_i) which is associated with the internal degrees of freedom:

$$\frac{\alpha}{\nu^2} = \frac{2\pi^2 c}{c_0^2} \cdot \frac{c_p c_i \Delta}{(c_p - \Delta)\,[c_p^2 - (c_p - c_i)^2 \omega\tau^2]}, \tag{5}$$

where α is the absorption coefficient, c is the velocity of sound at the given frequency, c_0 is the velocity of sound when $\omega\tau << 1$, τ is the relaxation time, ω is the angular frequency, $\Delta = c_p - c_v$, and c_p is the specific heat at constant pressure. All of the quantities included in Equation (5) can be found from the experimental determination of the velocity of sound [1] and the absorption coefficient [9] by utilizing the frequencies of the relaxation and non-relaxation regions and the quantities ρ, $\left(\frac{\partial p}{\partial T}\right)_v$ and $\left(\frac{\partial p}{\partial v}\right)_T$. Thus the present state of ultrasonics permits us to propose a method for determining both the overall specific heats (c_p, c_v), as well as the specific heats which are associated with the external and internal degrees of freedom.

LITERATURE CITED

[1] V. F. Nozdrev, "Investigation of the propagation of ultrasonic waves in the critical region of a liquid-vapor system," J. Acoustics (USSR) 1, 3, 235-248 (1955).

[2] V. K. Semenchenko, "Phase transitions of the II kind as generalized critical phenomena," J. Phys. Chem. (USSR) 21, 1461 (1947).

---

* The gaseous region has not yet been investigated.

[3] A. P. Gritsenko, Investigation of the Density of Substances Which Are in a Critical State (Dissertation) (Kiev State Univ., 1956).

[4] V. D. Sobolev, Measurement of the Absorption of Ultrasonic Waves in Ethyl Acetate Along the Saturation Line by Means of the Two-Fixed-Distances Pulse Method (Dissertation) (Moscow Regional Pedagogical Institute, 1955).

[5] A. P. Osadchii, "Investigation of ultrasonic absorption in certain alcohols at high temperatures ranging right up to critical temperatures," Collection: Application of Ultrasonics to the Investigation of Matter, (Moscow Regional Pedagogical Institute, 1956) p. 4.

[6] W. G. Schneider, "Sound velocity and sound absorption in the critical temperature region," Can. J. Chem. 29, 3, 242-252 (1951).

[7] Technical Encyclopedia: Handbook of Physical, Technical and Engineering Values, 1930, Vol. 5, 395-405.

[8] L. Belinskaya, " The theory of sound propagation in liquids," Archives of the Physics Faculty of Moscow Regional Pedagogical Institute, Jubilee Issue, 1956.

[9] I. G. Mikhailov. "Absorption of ultrasonic waves in liquids and the molecular mechanism of volume viscosity," Progress Phys. Sci. (USSR) 50, 1, 1-50 (1953).

[10] C. F. Curtiss, C. A. Boyd and H. B. Palmer, "Thermodynamics of the critical point," J. Chem. Phys. 19, 6, 801 (1951).

[11] I. V. Rozhdestvenskii, Diplomate paper (Physics Faculty, Moscow State Univ., 1953).

[12] A. S. Povalishnikova, Investigation of the Velocity of Ultrasonic Waves in Monoatomic Alcohols and Their Saturated Vapors Over a Wide Range of Temperatures and Pressures Including the Critical Region (Dissertation) (Moscow Regional Pedagogical Institute, 1954).

Moscow Regional Pedagogical Institute

Received February 21, 1956

CERTAIN RESULTS OF THE ANALYSIS OF A SINGER'S VOICE

S. N. Rzhevkin

In the voice of a highly qualified singer it is possible to detect the presence of sharply expressed "singer's formants" in the regions near 500 and 2500 cps; these "singer's formants" are identical for all vowels over the entire range from low notes to high notes. A comparison with the voice of an inexperienced singer shows that in the case of the latter the "singer's formants" are not sharply defined and are not stable; the upper formant, which controls the degree to which the voice sounds metallic, is absent. A hypothesis is offered concerning the rapid readjustment of the voice of an experienced singer from the speech position at the beginning of a vowel sound to the singing position which is characteristic of the steady-state extended portion of the sound.

Up to this time, a singer's voice as an acoustic phenomenon has seldom been examined, and then only superficially. The first important investigations in this field were made by V. D. Zernov [1], who determined the strength of the sound produced by a voice and the law according to which it varied with the height of the tone in singers with different kinds of voice training (F. Shaliapin, G. Pirogov, et. al).

In 1927 V. S. Kazanskii and the author [2] recorded the voices of a number of singers by means of a mechanical oscillograph; we discovered that for well-trained singers' voices there is a characteristic region of amplified overtones (a singer's formant) which lies in the vicinity of 500 cps. Our data were then verified in papers by Bartholomew [3], as well as Wolf, Stanley and Sette [4]. Bartholomew discovered a second singer's formant in the region 2800-3200 cps, in addition to the singer's formant in the region of 500 cps.

The cause of the insufficient study of a singer's voice by the field of acoustics results from the fact that only random individual work is being done in this field, i.e., no systematic investigations are being conducted. The utilization of the methods of modern acoustics is completely inadequate in vocal pedagogy as well as in the study of the physiological and psychological aspects of the singing voice. A survey of papers on the study of the singing voice is given by Hutton and Bell [5]. Up to this time there is actually no theory of the singing voice. In order to create a voice theory, it is necessary to correlate the anatomic physiological characteristics of the vocal apparatus with the resulting acoustic effect. A deep acoustic-physiological investigation of the singing voice is a problem of great complexity and scope. In this paper we have only attempted to illuminate a small group of problems related to the analysis of the sound of a singing voice.

The material which is subjected to analysis in this paper was obtained as a result of recording a number of singers in one of the studios of the Moscow Radio Center. The recording of the curves which are characteristic of the acoustic pressure was accomplished by means of a loop oscillograph. We utilized a high-quality condenser microphone which permitted us to record sounds of frequencies from 50 to 6000 cps without distortion. The microphone was located approximately 2 m from the singer. The recordings were made during a brief time interval of approximately 0.2 sec; this interval was selected to coincide with the instant when the sound of the voice was completely steady. The curves for the majority of the sounds go throuth a certain variation with the passage of time; their amplitudes alternately increase and decrease, and this phenomenon is the result of "vibrato".

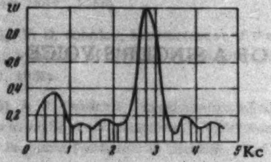

Fig. 1. Bass D., la-217 cps, the vowel a, forte.

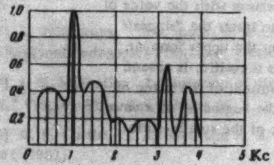

Fig. 2. Baritone R., la-217 cps, the vowel a, forte.

Basically, this paper provides detailed data resulting from the analysis of recordings which were made of just one singing voice – that of the bass, D., a gifted singer with a very beautiful voice timbre; the range of his voice extended from sol-94 cps to sol-386 cps (47 recordings were made). For the purposes of comparison certain data for an inexperienced singer, R., are given (6 recordings); the voice of singer R. was quite powerful, but it dropped in richness on high notes (above re-288 cps).

The analysis of the recordings was accomplished by means of magnifying one cycle of the curve by means of magnifying one cycle of the curve by means of an epidiascope to an amplitude of 8-15 cm and then decomposing it into its harmonics by means of a mechanical analyzer using the Madier system; this device permits analysis to be made up to the 25-th harmonic. Not nearly all of the recordings were analyzed in view of the difficulty in this work. The most interesting recordings were investigated in several places, since the character of the curve often varied radically and it was thus essential to investigate the spectrum at various instants of sonority. Such repeated analyses, notwithstanding the difference in the shape of the curve, as a rule yielded similar results. The maximum number of the analyzed curves (49) was made for the voice of the bass D; 7 analyses were carried out for the baritone R.

Figures 1 and 2 show two spectra for the sounds of different singing voices for the vowel a* at a frequency of 217 cps (la_1). The scales of the graphs are plotted on a relative scale along the ordinates; one unit was everywhere considered to be the amplitude of the greatest harmonic. The envelopes of the curves were drawn through the tops of the ordinates of the spectra. The maximums of the envelopes determine the position of the formant regions which characterize the resonant frequency of the coupled system consisting of the throat and mouth cavities. In the voice of bass D. (Fig. 1), an amplification of harmonics is observed in the region near 500 cps and near 2800 cps; in the spectrum of the voice of Baritone R., there is a maximum amplification in the region of 1100 cps and a number of secondary maxima in the regions of 500, 1600, 3400 and 3700 cps. The difference in nature of these spectra is very substantial.

The resultant data given below in the graphs represents only a portion of the material that we have obtained; from among all of the spectra obtained we selected the typical and most characteristic ones. However, the general conclusions which are given below are based upon the entire experimental material. We did not observe any substantial deviations from the data provided.

The results of the analysis of a male singer are illustrated by means of graphs (Fig. 3-8) upon which several spectra are depicted at once; these results can be briefly formulated in the following manner:

1. In the sound of a high-quality singing voice (male) a sharp amplification of the overtones is observed in a narrow band of the high frequencies; the width of this band is approximately 1 tone (Fig. 3 for the vowel a, Figs. 4-7 for various vowels). The center of this band lies in the interval 2500-3000 cps ($re_4^{\#}$ – sol_4). It is convenient to call this characteristic region of amplified overtones the "upper singing formant".

---

* [Translator's Note: The most probable phonetic values for the Russian vowels mentioned in this article are, according to Webster's New Int. Dict., 2nd Ed., Unabridged, (1949) p. 75; a = ă, e = ĭ, i = ē, o = ō, u = o͞o].

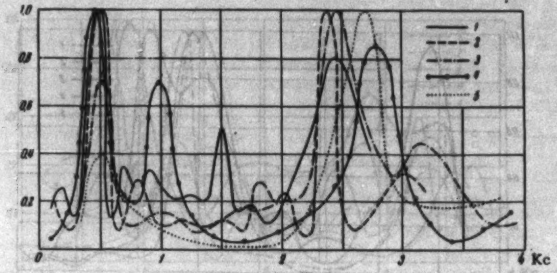

Fig. 3. Bass D., the vowel a, forte. 1) sol-94 cps; 2) do-129 cps; 3) la-169 cps; 4) do-259 cps; 5) re-288 cps.

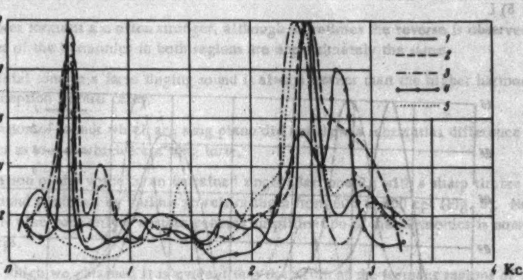

Fig. 4. Bass D., do-129 cps, forte. Vowels: 1) u; 2) o; 3) a; 4) e; 5) i.

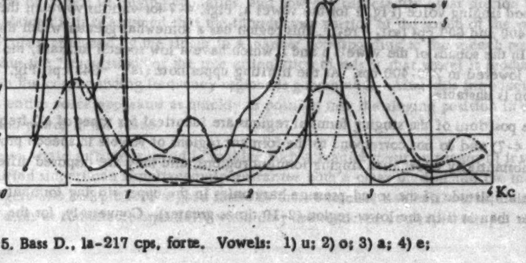

Fig. 5. Bass D., la-217 cps, forte. Vowels: 1) u; 2) o; 3) a; 4) e; 5) i.

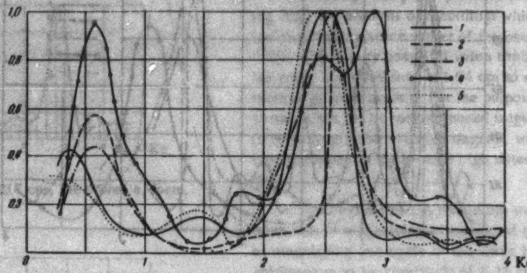

Fig. 6. Bass D., re-288 cps, forte, closed sound. 1) u; 2) o; 3) a; 4) e; 5) i.

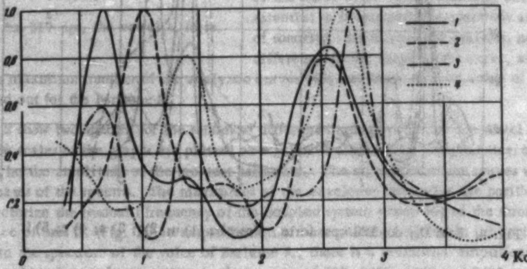

Fig. 7. Bass D., fa-345 cps, forte; closed found. 1) o; 2) a; 3) e; 4) i.

2. In addition to the upper formant region a lower formant region is observed in the majority of sounds made by a good singing voice (Fig. 3 for the vowel a, Figs. 4-7 for various vowels); the center for this region lies between 400 and 600 cps (sol$_1$ – re$_2$). This region has a somewhat greater width than the upper region (2-3 tones). In the sounds of the vowels u and i which have a low speech formant, the lower singing formant sometimes is lowered to 250-400 cps. At the limiting upper note (fa$^{\#}$ –345 cps, Fig. 7) the position of the lower formant region is unstable.

3. The positions of the singing formant regions are identical for tones of all frequencies used and for all vowels (Figs. 4-7) and do not correspond to the formant regions of vowels in speech pronunciation. Speech formant regions are substantially wider than singing formant regions, and they are disposed differently.

4. The amplitude of the sound-pressure harmonics in the upper singing formant region for the vowel i is always greater than it is in the lower region (2-10 times greater). Conversely, for the vowel u the harmonics

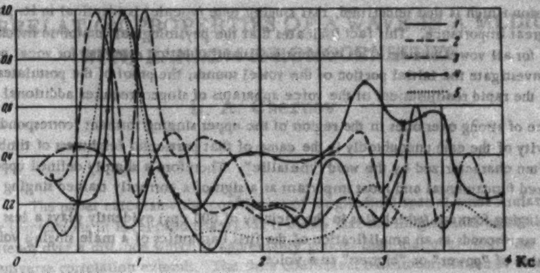

Fig. 8. Baritone R., vowel a, forte. 1) do-129 cps; 2) mi-167 cps; 3) la-217 cps; 4) re-288 cps; 5) mi-325 cps.

in the region of the lower formant are often stronger, although sometimes the reverse is observed. For the vowels o, and e the amplitudes of the harmonics in both regions are approximately the same.

5. The fundamental tone in a forte singing sound is always weaker than the higher harmonics. The vowel u presents an exception in rare cases.

6. The investigation of sounds which are sung piano did not show a substantial difference in terms of their spectrum in comparison to sounds which were sung forte.

7. The investigation of the voice of an untrained singer (Baritone R.) with a sharp timbre showed that the lower formant in the sound produced by various vowels changes from 600 to 900 cps (Fig. 8). No sharply defined upper formant region is observed; only a certain general amplification of the harmonics is noted in the region of from 2500 to 3500 cps.

From the results which we obtained it is evident that the width of the formant regions of the singing voice is small in comparison to the speaking voice. This can be explained by the greater rigidity of the walls in all of the cavities of the voice apparatus in singing phonetics, in comparison to the situation for speech phonetics. This rigidity is evidently caused by the tension of the musculature of the larynx, throat and mouth cavity and produces a sharper tuning of the resonant cavities.

The other essential feature of the singing voice in comparison with the speaking voice is the fact that the singing formant regions are practically identical for all vowels and do not correspond to the formant regions which occur in speech pronunciation. In this connection the following question arises: In what manner is it possible to guarantee the articulation of vowels in singing phonetics, and how can sufficiently clear diction be achieved? This paradox can be explained if it is assumed that the introductory portion of the sound of the vowels (the period of "sound attack") is reproduced by the singer in a manner corresponding to the speech position of the resonant cavities, and thus the "impression" of the true articulation of this or that vowel is produced (i.e., the sound of the overtones in the corresponding frequency regions is guaranteed). After this introductory period the singer must readjust his entire voice apparatus as quickly as possible into the singing position in order to guarantee the necessary sonority and power in his voice.

It is only possible to attain sufficient speed in making such a readjustment by means of intensive training, and therefore only qualified singers can simultaneously guarantee both a clear diction and the mastery of singing tone. Beginning singers who can produce a good sound in their exercises can easily lose their singing tonal quality when rendering arias or romances, especially when they are rendered at a rapid tempo.

The conclusion which is thus underlined, that singing tone (vocale) is identical in its physical structure for all vowels, is of great importance. This fact indicates that the physiological-anatomic mechanism of a singer's voice is the same for all vowel sounds. This concept is without question essential for vocal pedagogy. In our work we did not investigate the initial portion of the vowel sounds; the proof of the postulates which we have stated concerning the rapid readjustment of the voice apparatus of singers requires additional investigation.

The presence of strong overtones in the region of the upper singing formant (corresponding to the region of maximum sensitivity of the ear) undoubtedly is the cause of that particular brightness of timbre in good singing voices which is often characterized by the word "metallic". Therefore a sharply defined upper singing formant should be considered fundamental and most important as a sign of a correctly trained singing voice.

The lower singing formant (which lies in the vicinity of 500 cps) evidently plays a less important role than the upper one. It corresponds to an amplification of the first harmonics of a male singing voice and most probably causes the impression of "power" or "bigness" in a voice.

The results we obtained here are based, for the time being, upon extremely tentative material. However, our results permitted us to note certain working hypotheses and paths for further investigations which must, in our opinion, be carried out in the future. The results of such investigations, undoubtedly, would have great scientific and practical significance.

LITERATURE CITED

[1] V. D. Zernov, Absolute Measurement of Sound Intensity (Moscow, 1909).

[2] V. S. Kazanskii and S. N. Rzhevkin, "Investigation of the sound timbre of the voice and of bow instruments," J. Appl. Phys. 1928, No. 5, 87-103.

[3] W. Bartholomew, "A physical definition of good voice quality in the male voice," J. Acoust. Soc. Am. 1934, 6, 25-33.

[4] S. Wolf, D. Stanley and W. Sette, "Quantitative studies on the singing voice," J. Acoust. Soc. Am. 1935, 6, 255-266.

[5] Hutton and Bell, Central States Speech Journ, 1954.

Acoustics Faculty Moscow State University

Received January 29, 1956

CORRELATION PROPERTIES OF A WAVE IN A MEDIUM WITH RANDOM INHOMOGENEITIES

L. A. Chernov

The paper calculates the coefficient of longitudinal spatial autocorrelation for fluctuations in level (and phase). It is shown that the longitudinal correlation extends over a distance which is appreciably greater than that over which the transverse correlation extends. The time coefficient of autocorrelation is determined for fluctuations of level (and phase). An attempt is made to explain certain experimental data taken from the field of hydroacoustics relative to the time correlation of level fluctuations.

The paper cited in [1] examines the problem concerning the spatial autocorrelation of level (or phase) fluctuations during the process of wave propagation in a randomly inhomogeneous medium for the case when both receivers are located in a plane which is perpendicular to the direction of wave propagation (transverse autocorrelation). It was shown that the transverse autocorrelation between fluctuations of level (or phase) extends approximately over the same distance as does the correlation between the random inhomogeneities of the medium itself, if the scale of the inhomogeneities is great in comparison with the wavelength. However, the transverse autocorrelation does not provide a full representation of the correlation properties of a wave field. It is still necessary to investigate the longitudinal spatial autocorrelation of the fluctuations in level (and in phase). A knowledge of the spatial correlation properties of a wave field permits us to determine easily its time correlation properties in a coordinate system which is moving with respect to the medium. The problem of longitudinal spatial and time autocorrelation of level (and phase) fluctuations is examined in this paper on the basis of the same assumptions as those used in discussing transverse spatial autocorrelation in [1]. The following assumptions are made: regular inhomogeneities are not present in the medium; random deviations of the index of refraction of the medium from its average value are small and the scale of these deviations is large in comparison to a wavelength. The spatial distribution of inhomogeneities is quasi-static.

Utilizing these assumptions, A. M. Obukhov [2] obtained the following formulas for the phase fluctuations S and the level fluctuations L of a wave which traverses the path x' in an inhomogeneous medium:

$$S(x',y',z') = \int_0^{x'}\int_{-\infty}^{+\infty}\int_{-\infty}^{+\infty} \Phi_1(x'-\xi',\rho')\cdot\mu(\xi',\eta',\zeta')\cdot d\xi'\,d\eta'\,d\zeta' \tag{1}$$

$$L(x',y',z') = \int_0^{x'}\int_{-\infty}^{+\infty}\int_{-\infty}^{+\infty} \Phi_2(x'-\xi',\rho')\cdot\mu(\xi',\eta',\zeta')\cdot d\xi'\,d\eta'\,d\zeta'. \tag{2}$$

Here x', y', z' are dimensionless coordinates of the observation point; ξ', η', ζ' are the dimensionless coordinates of an elementary scattering volume, and they are related to the dimensioned coordinates by the relationships $x' = kx$, $y' = ky$, $z' = kz$, $\xi' = k\xi$, $\eta' = k\eta$, $\zeta' = k\zeta$, where k is the wave number; $\mu(\xi', \eta', \zeta')$ is the fluctuation of the index of refraction; $\rho'^2 = (y' - \eta')^2 + (z' - \zeta')^2$.

$$\Phi_1(x'-\xi', \rho') \equiv \frac{1}{2\pi(x'-\xi')} \cdot \sin\frac{\rho'^2}{2(x'-\xi')}, \tag{3}$$

$$\Phi_2(x'-\xi', \rho') \equiv \frac{1}{2\pi(x'-\xi')} \cdot \cos\frac{\rho'^2}{2(x'-\xi')}. \tag{4}$$

By means of Equations (1) and (2) the various correlation functions of the wave field can be calculated if the correlation coefficient for the fluctuations of the index of refraction is given.

Let us pass on directly to an examination of the problems concerning the longitudinal autocorrelation of the fluctuations in level (and phase) and various reception points. Let us assume that the receivers are distributed along the line of propagation. The coordinates of the receivers are $(L_1', 0, 0)$ and $(L_2', 0, 0)$. The autocorrelation function of the fluctuations of level and phase are determined by the following formulas on the basis of Equations (1) and (2):

$$\overline{S_1S_2} = \overline{\mu^2} \int_0^{L_1'}\int_0^{L_2'}\iiiint_{-\infty}^{+\infty} \Phi_1(L_1'-\xi_1', \rho_1')\Phi_1(L_2'-\xi_2', \rho_2')\, N(r')\, d\xi_1' d\xi_2' d\eta_1' d\eta_2' d\zeta_1' \zeta_2', \tag{5}$$

$$\overline{L_1L_2} = \overline{\mu^2} \int_0^{L_1'}\int_0^{L_2'}\iiiint_{-\infty}^{+\infty} \Phi_2(L_1'-\xi_1', \rho_1)\Phi_2(L_2'-\xi_2', \rho_2)\, N(r')\, d\xi_1 d\xi_2 d\eta_1' d\eta_2' d\zeta_1' d\zeta_2, \tag{6}$$

where $N(r')$ is the correlation coefficient for the fluctuations of the index of refraction, $r'^2 = (\xi_1' - \xi_2')^2 + (\eta_1' - \eta_2')^2 + (\zeta_1' - \zeta_2')^2$.

In these formulas the upper limit of integration with respect to ξ_2' can also be placed equal to L_1'. In fact, due to the fact that the character of the scattering is directional, waves which are scattered by the layer bounded by the planes $\xi' = L_1'$ and $\xi' = L_2'$ are incident upon the second receiver and are not incident upon the first receiver. Therefore in examining the problem concerning the correlation of levels (or phases) we can neglect the scattering by the layer $L_2 - L_1$. By making a conversion to relative coordinates $\eta = \eta_1' - \eta_2'$, $\zeta = \zeta_1' - \zeta_2'$ and to center-of-gravity coordinates $y = \frac{1}{2}(\eta_1' + \eta_2')$ $z = \frac{1}{2}(\zeta_1' + \zeta_2')$, it is possible to carry out integration with respect to the variables $\underline{y}$ and $\underline{z}$. Then we obtain

$$\overline{S_1S_2} = \frac{1}{2}\overline{\mu^2}(I_1 + I_2), \tag{7}$$

$$\overline{L_1L_2} = \frac{1}{2}\overline{\mu^2}(I_1 - I_2), \tag{8}$$

where

$$I_1 = \int_0^{L_1'}\int_0^{L_1'}\iint_{-\infty}^{+\infty} \Phi_1\left[L_2' - L_1' - (\xi_2' - \xi_1'),\ \rho\right] \cdot N(r')\, d\xi_1' d\xi_2' d\eta d\zeta, \tag{9}$$

$$I_2 = \int_0^{L_1'}\int_0^{L_1'}\iint_{-\infty}^{+\infty}\Phi_1\,[L_2' + L_1' - (\xi_2' + \xi_1'),\ \rho]\cdot N(r')\,d\xi_1' d\xi_2' d\eta d\zeta. \tag{10}$$

The formulas (7-10) yield the solution for the problem concerning the longitudinal autocorrelation of the fluctuations of level (and phase) in its general form.

The further simplification of the integrals I_1 and I_2 is possible in the case where the range is great in comparison to the scale of the inhomogeneities. Introducing the relative coordinate $\xi = \xi_1' - \xi_2'$ and the center-of-gravity coordinate $x = \frac{1}{2}(\xi_1' + \xi_2')$, we have the right in this case to integrate with respect to ξ from the limits of $-\infty$ to $+\infty$. Integrating with respect to x within the limits of from 0 to L', we obtain the following formulas by making use of Equations (3) and (4):

$$I_1 = L_1'\iiint_{-\infty}^{+\infty}\frac{1}{2\pi\,(\Delta L' - \xi)}\cdot\sin\frac{\rho}{2\,(\Delta L' - \xi)}\cdot N(r')\,d\xi d\eta d\zeta, \tag{11}$$

$$I_2 = -\frac{1}{4\pi}\iiint_{-\infty}^{+\infty}\left\{\operatorname{si}\frac{\rho^2}{2\,(L_2' - L_1')} - \operatorname{si}\frac{\rho^2}{2\Delta L'}\right\}N(r')\,d\xi d\eta d\zeta, \tag{12}$$

where $\Delta L' = L_2' - L_1'$. Since the integrands of these formulas are axially symmetrical, it is convenient to convert to polar coordinates $(\rho,\ \varphi)$ on the plane $(\eta,\ \zeta)$. Then we obtain

$$I_1 = L_1'\int_{-\infty}^{+\infty}d\xi\int_0^{\infty}\frac{1}{\Delta L' - \xi}\cdot\sin\frac{\rho^2}{2\,(\Delta L' - \xi)}\cdot N(r')\,\rho d\rho, \tag{13}$$

$$I_2 = -\int_0^{\infty}d\xi\int_0^{\infty}\left\{\operatorname{si}\frac{\rho^2}{2\,(L_2' + L_1')} - \operatorname{si}\frac{\rho^2}{2\Delta L'}\right\}\cdot N(r')\,\rho d\rho \tag{14}$$

(in the process involved in the conversions of I_2 it is also taken into account that the correlation coefficient N(r') is an even function with respect to ξ).

Let us assume that the correlation coefficient N(r') can be expressed in Gaussian form:

$$N(r') = e^{-\frac{\xi^2+\eta^2+\zeta^2}{a'^2}},$$

where a' is the dimensionless correlation radius for fluctuations of the index of refraction (the scale of the inhomogeneities) and is related to the dimensioned correlation radius a by the relationship a' = ka (it also satisfies the condition a' >> 1 in the case of large-scale inhomogeneities).

In this case the problem reduces to integrals which are available in tables, and the calculation of these integrals yields

$$I_1 = L'_1 \int_{-\infty}^{+\infty} \frac{e^{-\frac{\xi^2}{a'^2}} d\xi}{1 + 4\,\frac{\Delta L'^2 - 2\Delta L'\xi + \xi^2}{a'^4}}, \tag{15}$$

$$I_2 = \sqrt{\pi} \cdot a' L'_1 \left\{ \frac{1}{D} \operatorname{arctan} D - \frac{2}{D} \operatorname{arc\,tg} \left(\frac{1}{2} \frac{\Delta L'}{L'} D \right) \right\}. \tag{16}$$

The last expression is obtained on the basis of assuming that the distance between receivers $\Delta L'$ is small in comparison to the distance L'_1. The dimensionless parameter $D = 4L/ka^2$ which appears in this expression was called the wave parameter by G. S. Gorelik [3].

In the region of large values of the wave parameter ($D \gg 1$) the integral I_2 can be neglected in comparison with the integral I_1. Then we obtain

$$\overline{L_1L_2} = \overline{S_1S_2} = \frac{1}{2}\,\overline{\mu^2} L'_1 \int_{-\infty}^{+\infty} \frac{e^{-\frac{\xi^2}{a'^2}} d\xi}{1 + 4\,\frac{\Delta L'^2 - 2\Delta L'\xi + \xi^2}{a'^4}}. \tag{17}$$

If the distance between receivers $\Delta L'$ is of the order of the correlation radius a', then the second term in the denominator can be neglected in comparison to unity. In fact, the region of real values of ξ is of the order of a'. In this region the second term in the denominator will be of the order of $\frac{1}{a'^2} \ll 1$. In this case we obtain

$$\overline{L_1L_2} = \overline{S_1S_2} = \frac{\sqrt{\pi}}{2}\,\overline{\mu^2} k^2 a L, \tag{18}$$

and this coincides with the expression for the mean-square of the fluctuations of level $\overline{L^2}$ and phase $\overline{S^2}$. Thus at a distance ΔL which is of the order of the correlation radius $\underline{a}$ the fluctuations of level and phase are fully correlated.

Let us therefore examine distances ΔL which are large in comparison with the correlation radius $\underline{a}$: $\Delta L' \gg a'$.

In the region of real values of ξ the terms $\Delta L'\xi$ and ξ^2 are respectively of the order of $\Delta L'a'$ and a'^2. They can be neglected in comparison to the term $\Delta L'^2$. Formula (17) then acquires the form:

$$\overline{L_1L_2} = \overline{S_1S_2} = \frac{\frac{\sqrt{\pi}}{2} \cdot \overline{\mu^2} k^2 a L}{1 + \left(\frac{2\Delta L}{ka^2}\right)^2}. \tag{19}$$

For the autocorrelation coefficients

$$R_l = \frac{\overline{L_1 L_2}}{\overline{L^2}};\ \ R_s = \frac{\overline{S_1 S_2}}{\overline{S^2}}$$

we obtain

$$R_l = R_s = \frac{1}{1 + \left(\frac{2\Delta L}{ka^2}\right)^2}. \tag{20}$$

on the basis of Formulas (18) and (19).

With a growth in ΔL the correlation coefficient decreases. Assuming that the distance ΔL_k equals the correlation radius (at this distance the correlation coefficient increases by a factor of two), we obtain the following formula for determining the correlation radius:

$$\frac{2\Delta L_k}{ka^2} = 1. \tag{21}$$

Comparing the left-hand side of Equation (21) with the expression for the wave parameter $D = \frac{4L}{ka^2}$, we come to the following conclusion. If the distance between receivers does not exceed the range within whose limits the ray method of analysis is applicable, the fluctuations of level (or of phase) are, practically speaking, completely correlated. The longitudinal correlation extends over a distance which is appreciably greater than that over which the transverse correlation extends. With regard to the above discussion, it ceases to be necessary to examine the other limiting case which corresponds to small values of the wave parameter ($D \ll 1$): in this region complete longitudinal autocorrelation of the level (and phase) fluctuations takes place.

After the above it is easy to determine the time coefficient of level (or phase) autocorrelation for a receiver which moves at a constant velocity with respect to the medium. If the receiver passes through the point A at the instant of time t_1, and passes through the point B at the instant of time t_2, then the level (or phase) at the instant of time t_1 will be determined by the level (or phase) at the point A; at the instant of time t_2 it will be determined by the level (or phase) at the point B. As a consequence of this the coefficient of time autocorrelation for the moving receiver will be equal to the coefficient of space autocorrelation at the two points, i.e.,

$$R(\tau) = R_1(l), \tag{22}$$

where $\tau = t_2 - t_1$, $l = AB$, and $l = v \cdot \tau$ if v is the velocity of the receiver.

During the time τ (which is of the order of a/v) the longitudinal displacement cannot cause an appreciable weakening of the correlation. Therefore in Formula (21) it is sufficient to take into account the transverse displacement $l_z = v_z \cdot \tau$ (the coordinate system is so oriented that the velocity lies in the plane xoz). Then we obtain:

$$R(\tau) = R_1(l_z). \tag{23}$$

Now it is possible to make use of the formulas for the coefficients of transverse correlation which were obtained by the author [1]. This yields.

$$R_{l,s} = \frac{\exp\left(\frac{v_z^2}{a^2}\tau^2\right) \pm \frac{}{2iD}\left[Ei\left(\frac{-i\,\frac{v_z^2}{a^2}\tau^2}{D+i}\right) - Ei\left(\frac{i\,\frac{v_z^2}{a^2}\tau^2}{D-i}\right)\right]}{1 \pm \frac{1}{D}\operatorname{arc\,tg} D}. \tag{24}$$

The upper sign is the one which must be used when calculating the coefficient of autocorrelation R_s for the phases; the lower sign must be used when calculating the coefficient of autocorrelation R_l for the levels. In the Frauenhofer zone ($D \gg 1$) Formulas (24) acquire a particularly simple form:

$$R_l(\tau) = R_s(\tau) = e^{-\frac{v_z^2}{a^2}\tau^2} \tag{25}$$

The correlation interval $T = \frac{a}{v_z}$ depends upon the transverse components of the receiver velocity.

The results must not change if the receiver is quiescent and the medium moves with a velocity $-v$.

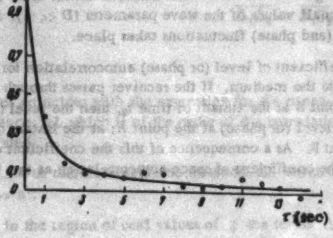

In the paper by Minzer [4] hydroacoustic data is given concerning the autocorrelation of fluctuations in level with respect to time; this data had been obtained by Sheehey. Analyzing this data, Minzer came to the conclusion that the time coefficient of autocorrelation does not depend upon the distance. Along with this, experiments conducted for one and the same distance produced radically differing graphs for the autocorrelation coefficient. Since the experiments were conducted on moving ships, the variability of the autocorrelation coefficient can be explained by its strong dependence upon the velocity of motion of the receiver; this dependence can be seen from Formula (25).

The average values of the autocorrelation coefficient are denoted by circles in the figure. The dependency of the autocorrelation coefficient upon time can be explained theoretically if we average the autocorrelation coefficient (25) over all the possible values of ship velocity, assuming that the ship velocity varies from experiment to experiment in a random manner and that the velocity distribution of the ship obeys the normal law:

$$W(v_z) = \frac{1}{\sqrt{2\pi}\cdot v}\cdot e^{-v_z^2/2v}. \tag{26}$$

Then we obtain

$$R_l(\tau) = \frac{1}{\sqrt{1 - \tau^2/T^2}}, \qquad (27$$

where $T = l/\sqrt{2} \cdot a/v$. If we assume that T = 0.33 sec, then Function (27) can be depicted by a curve which satisfactorily describes the relationship between the experimental points.

LITERATURE CITED

[1] L. A. Chernov, "Correlation of fluctuations of amplitude and phase when a wave is propagated in a medium with random inhomogeneities," J. Acoustics (USSR) 1, 1, 89-95 (1955).

[2] A. M. Obukhov, "The effect of weak atmospheric inhomogeneities upon the propagation of sound and light," Bull. Acad. Sci. USSR Geophys. Ser. 2, 155-165 (1953).

[3] G. S. Gorelik, Oscillations and Waves (State Tech. and Theor. Lit. Press, Moscow-Leningrad, 1950).

[4] D. I. Minzer, "Wave propagation in a randomly inhomogeneous medium-III, J. Acoust. Soc. Am. 26, 2, 186-190 (1954).

Iaroslav State K. D. Ushinsky Pedagogical Institute

Received February 19, 1956

THE PROBLEM OF THE BIOLOGICAL EFFECT OF ULTRASONIC WAVES

I. E. El'piner

The paper provides data which shows that due to the effect of ultrasonic waves, the output of ergosterol from yeast cells is increased, the sacharase enzyme is activated in these cells (this enzyme inverts the sucrose), and finally the activity of the cholinesterase enzyme (which participates in the transmission of nerve pulses) in the nerve tissue is accentuated. An analysis of this phenomenon verifies the fact that ultrasonic waves have the ability to "shatter" the molecular complexes of the submicroscopic structures of the cell elements even in those cases when the death of living cells is not observed.

Ultrasonic waves can produce intense biological effects. Animal and plant cells (both the simplest types and microorganisms) die in an ultrasonic wave field. In addition to this it has been rigorously established that different biological objects differ in their sensitivity to the action of this physical agent (the selective effect of ultrasonic waves). The selective action was judged on the basis of data concerning the survival of the irradiated objects. It was assumed that when they were subjected to the action of ultrasonic waves biological objects which were suspended in an aqueous medium were either subjected to coarse mechanical damage or were completely unharmed.

However, the effect of ultrasonic waves does not reduce only to mechanical destruction of cells and cell structure; as a result of ultrasonic effects we often observed subtle biochemical and functional changes which do not lead to the death of the organism [1]. As will be shown, such variations occurred even in those cases where the biological object was considered to be resistant to the effect of ultrasonic waves.

It is difficult to bring to light such subtle biochemical and functional variations, variations which appear in animal cells due to the effects of one or another physical factor. Such variations may arise as a result of the disruption of the multiple interconnections which exist in the cell between the biocatalyzers, substrata, and inhibitors, as well as between the molecular complexes which lie at the basis of submicroscopic structures and which determine the physico-colloidal state of the cell, its individual elements and its functional direction.

Physical phenomena which are genetically associated with the processes of the propagation of elastic mechanical vibrations in a liquid medium (a variable pressure, the acceleration and displacement of particles, cavitation, etc.) can cause disruptions of the physico-chemical state of a heterogeneous system (a living cell is such a system), such that some of these systems can be restored to their original state, whereas others are irreparably damaged. One of the criteria of physico-chemical disruption in microstructures is a shift in the state of the cellular biocatalysts – a shift in their amounts and degrees of activity. Such shifts were observed by us in a number of cases, and this is the subject of the present paper.

First of all, let us dwell upon several experimental results which we obtained by means of cytological investigations [2]. These results show convincingly that the effect of ultrasonic waves upon a yeast culture cannot be reduced solely to the coarse destruction and disruption of cells. As a result of the effects of ultrasonic waves, physico-colloidal changes are observed in the intracellular structures which do not always lead to the death of the irradiated organism. Such variations were observed for comparatively insignificant exposures to ultrasonic waves in the case of irradiation of Endomyces magnusii. A concave piezo-quartz sheet of 55 mm diameter

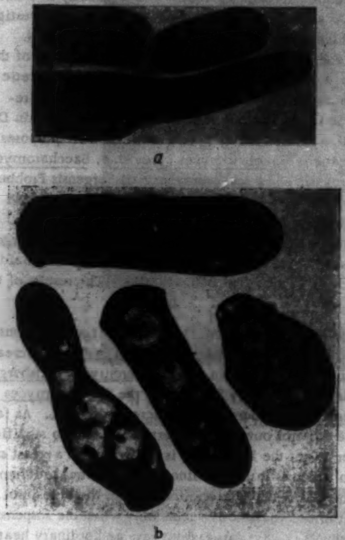

Fig. 1. a) Non-irradiated yeast cells of *Endomyces magnusii*; b) cells of *E. magnusii*, irradiated for a period of 30 seconds.

served as the ultrasonic emitter. The focal length of the plate was 8 cm, the power supplied to the quartz plate was 250 w, the vibration frequency of the ultrasonic waves was 1,200,000 cycles. It was found that at 30 seconds or 1 minute of exposure time "foaming" of the protoplasm was observed in some cells, and in other cells the gelatinization of the protoplasm was observed (Figs. 1 and 3). Coloring the living cells with Janus green and with neutral red points up the presence of Brownian particles in a number of cases (these particles consist of pieces of chondriosomes and very small granules of volutin. Certain of the rapidly moving particles are lipoid and fat formations which are brought to light by sudan and scarlet. According to the data obtained by ultra-microscopic investigations the affected cells lose the ability to absorb fluochromes. The volutin and the nucleii which are so well detected by fluochroming normal cells with orange acridine are not evidenced here at all. More valuable information would be obtained by using microscopy in a dark field. When this method is used the membranes and tonoplast are detected in the undamaged cells as well as the fat and lipoid inclusions; the protoplasm, nuclei and vacuoles are optically represented as empty space (Fig. 2, *a*). The appearance and intensification of the opalescence which is detected in microscopic observation of the irradiated yeast cells in a dark field (Fig. 2, *b*), can be explained by the lowered dispersion of the colloids and by the change in physico-chemical state of the proteins in the protoplasm.

When the irradiation time of the yeast suspension of endomyces is extended to five minutes, it is possible to establish the presence of coarse mechanical destruction of the cells. The nature and location of the damage differs: sometimes the ends of the cells are torn off, giving the cell a cylindrical shape; at other times the cell is torn into two parts (this occurs predominantly at places where partitions are ordinarily located), at still other times funnel-shaped defects are formed at various places along the cell wall. In such cells there is a practical absence of protoplasm. Under the microscope only "shadows" ("sheaths") of the cells are visible (Fig. 3).

Other changes, more subtle and rapidly transient, occur when ultrasonic waves react upon yeast cells; these changes are associated with the cultures of saccharomycetes. In this particular case coarse mechanical damage does not occur even when the yeast suspension is irriadiated for 30-60 minutes. For such a protracted irradiation the only thing that was observed was an intense dilution of the protoplasm, which was accompanied by the freeing of many drops of fat. In certain cases the protoplasm and the membranes become thinner. The latter often acquire an improper angular shape. The observed picture somewhat reminds us of the autolysis of yeast cells (Fig. 4). The irradiated culture of saccharomycetes, as a rule, yields an abundant growth when it is subsequently inoculated. More than that, even after a 1-1.5 hour irradiation the amount of oxygen absorbed by the culture (*Saccharomyces globosus*) is only lowered by 10-20%, i.e., 80-90% of the cells survive [3]. Nevertheless, data has been obtained which shows that in these cases as well physico-chemical shifts occur in the cells, and these shifts evidently lead to the "shattering" or "loosening" of the intracellular molecular complexes. This latter fact is expressed in the sense that a series of biologically active substances are released in the yeast cells (vitamins, ferments, etc) when they are subjected to the action of ultrasonic waves, and a considerable

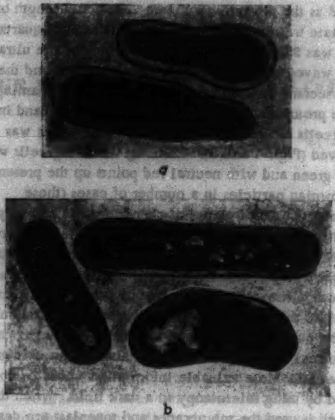

Fig. 2. a) Control cells of E. magnusii (dark field); b) cells of E. magnusii, irradiated for a period of 30 seconds (dark field).

portion of these substances is located in cells which are intact; these substances are therefore evidently in a bonded state. As an example we cite the results of the investigations which we conducted in cooperation with M. N. Meisel and R. D. Gal'tsova. We are speaking here of the effect of ultrasonic waves upon sterol saccharomycetic compounds which in these cells are predominantly represented in the form of ergosterol – the pro-vitamin D_2. We utilize the following yeast cultures for the purposes of investigation: Saccharomyces cerevisiae, Saccharomyces carlsbergensis and Saccharomyces carlsbergensis Frohberg. The saccharomycetes were irradiated in glass bulbs 45 minutes, the vibration frequency was 740 kc, and the ultrasonic intensity was 10 w/cm². The amount of ergosterol was determined according to the method of Gaidushka and Lindner as modified by Proskuriak. The results of the investigation are given in Table 1.

As can be seen from Table 1, the ergosterol content in the irradiated Saccharomyces cerevisiae cells increases approximately by 60%; in the Saccharomyces carlsbergensis cells it increases by 30% and in the Saccharomyces carlsbergensis Frohberg cells it increases by 45%. As far as the ergosterol output is concerned, it is of no significance whether or not the irradiation is performed in a yeast suspension which is in an alkaline or in a neutral medium. It is important to note that the increase in the ergosterol content in the yeast cells occurs only when the suspension is subjected to the effect of ultrasonic waves. Other physical agents (x-rays, ultraviolet rays and ordinary heat) do not directly cause an increase in the ergosterol content in the studied yeast cultures (Table 2).

TABLE 1

Ultrasonic Effect upon the Egosterol Content in Various Cultures of Yeast Cells – Saccharomycetes (2-day Culture)

Yeast culture	Ergosterol content in the yeast cells (%)		Increase in ergosterol output (%)
	Before irradiation	After irradiation	
Saccharomyces cerevisiae	1.07	1.80	68
" "	1.09	1.72	58
Saccharomyces carlsbergensis	3.06	4.00	30
" "	3.06	4.00	30
Saccharomyces carlsbergensis Frohberg	2.54	3.89	53
" " "	2.75	3.89	41

Other observations also bear witness to the possibility that ultrasonic waves can affect the cellular molecular complexes. It was considered established that yeast cells of Saccharomyces globosus (349) do not contain saccharase which inverts sucrose. These cells acquire the ability to metabolize sucrose only when they are grown for a long period and re-grown many times in a medium which contains the substance named (sucrose [4]). It proved to be true that when ultrasonic waves affect cells of Saccharomyces globosus (349) an active saccharase appears (the ultrasonic intensity was 10 w/cm² [5], the frequency was 740,000 cps, and the duration of the irradiation was 30 minutes). This enzyme was discovered in condensed solutions of the irradiated suspensions of saccharomycetes, as can be seen from the chromatogram given (Fig. 5).

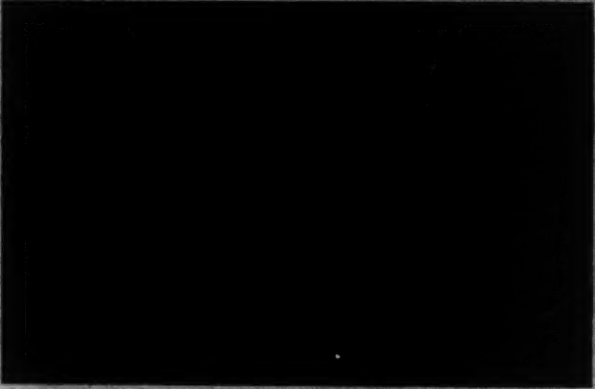

Fig. 3. Various types of damage to E. magnusii cells when a yeast suspension is irradiated for 5 minutes.

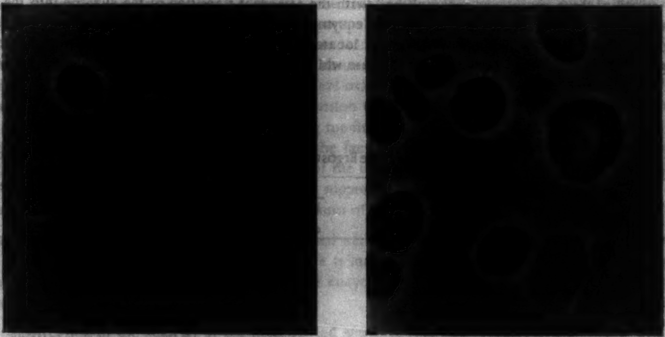

a

b

Fig. 4. a) Non-irradiated Saccharomyces cerevisiae cells; b) Saccharomyces cerevisiae cells, irradiated for 10 minutes; c) the same when irradiated for 20 minutes; d) the same when irradiated for 30 minutes.

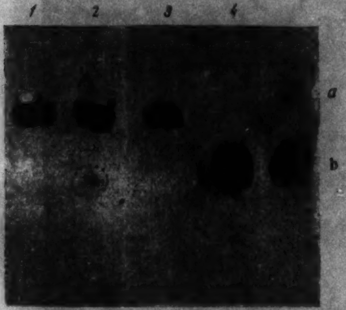

Fig. 5. 1) Original yeast suspension of Saccharomyces globosus (no enzyme); 2) appearance of enzyme after irradiation for 15 minutes; 3) inactivation of the enzyme by boiling; 4) after irradiation of the yeast cells for 30 minutes; a) sucrose; b) fructose.

The increase in the activity of saccharase was discovered by us when ultrasonic waves acted upon other yeast cultures in whose intact cells it is usually present. The activity and functional direction of these cells depend to a significant degree upon the localization of enzymes in the cell. As was shown, yeastlike cells (Endomyces magnusii) are easily destroyed by the action of ultrasonic waves; this permits us to separate the contents of the protoplasm from the membranes. This creates favorable conditions for separately determining the presence of enzymes in the protoplasmic fraction and in the membranes. By such means it was possible to show that dehydrases are cytoplasmic enzymes and that the saccharase is closely associated with the structure of the membrane. Along with this it was discovered that in the irradiated preparations of Endomyces magnusii the activity of the saccharase increases by a factor of 3-4 in comparison with the activity of this particular enzyme in non-irradiated cells of the same yeast culture. It can be postulated that the molecular complexes of the saccharase which have been stripped of their enzyme activity are also associated with the cell membrane. Only when they are subjected to ultrasonic waves is the "shattering" of these complexes accomplished (with the attendant transition of the enzyme into the surrounding medium in an active state). The raising of the enzyme activity due to the effect of ultrasonic waves was not brought out when studying enzymes which were located in the protoplasmic fraction of the irradiated Endomyces magnusii yeast cells. This also applies to maltase which was discovered in the protoplasm of the investigated cells.

TABLE 2

Direct Effect of Various Physical Agents upon the Ergosterol Content in Yeast Cells (Saccharomyces cerevisiae)

Physical agent	Amount of ergosterol (%)		Increase in the amount of ergosterol (%)
	Before action of the agent	After action of the agent	
x-Rays	1.09	1.10	0
Ultraviolet rays	1.09	1.09	0
Heating the culture in a boiling water bath for 30 minutes	1.09	1.12	0
Ultrasonic waves	1.09	1.72	48

It should be noted that there are no indications in the literature of the possibility of raising enzyme activity by means of the effects of ultrasonic waves upon purified or crystalline enzymes in an aqueous medium. In such cases the inactivating effect of the given physical agent is usually evidenced. The inactivation of the enzyme most probably occurs as a result of the interaction of this enzyme with unsaturated valence free radicals — the products of the hydrolysis of ionized water molecules: HO, HO_2, H, etc. The ionization of water molecules is accomplished in the cavitational cavities where tremendous electrical stresses arise [6]. There is a basis for thinking that the appearance of products resulting from the hydrolysis of the ionized water molecules, which are very active in the chemical sense, is caused by the dissociation of the amino acids and protein, by the depolymerization of nuclein acids, by the hydrolysis of purine compounds and of other biologically active substances [7]. More than that, by selecting appropriate substances or gases it is possible to retard or intensify one or another set of chemical reactions [8, 9, 10]. In the presence of air, aqueous solutions of polyphenol oxidase (tyrosinase) are rapidly inactivated in the field of ultrasonic waves. Hydrogen, conversely, lowers the inactivating effect of this type of energy in the specified case [11]. When carbon tetrachloride is present the inactivation of the saccharase is intensified; this enzyme is very stable under ordinary conditions of irradiation [12]. According to this data, the intensification of the inactivation process of the enzyme is also observed in the presence of potassium iodide, which oxidizes and forms atomic iodine when it is subjected to the effect of ultrasonic waves. However, the intensification of the inactivizing effect of KI and CCl_4 is not observed if albumin is present in the irradiated solution; albumin easily blocks atomic iodine and atomic chlorine. The discovery of such a mechanism of suppression and intensification of the chemical processes significantly broadens our concept concerning the nature of the processes which are caused by ultrasonic waves in an aqueous medium surrounding biological objects. Along with the mechanical forces generated by cavitation, the chemical processes which are developed as a result of the cavitational electro-chemical effect of the ultrasonic waves are evidently also of great significance with respect to the biological effects. The possibility of cavitation inside of animal or plant cells is subject to doubt. The absence of cavitation is associated with the large viscosity of the cytoplasm. In other words, the mechanical and chemical processes which are genetically associated with cavitation take place in the external medium and primarily affect the cell membranes or "sheaths" which are bounded by this medium. It is evidently not accidental that the saccharase activity which is localized in the membranes of the yeast cells is intensified. The other facts which have recently been established by us are also probably not accidental.

It is known that the cholinesterase, which is intimately associated with the processes by means of which a nerve impulse is created and transmitted, is located in the membrane of the nerve tissue and its elements. Experiments have shown that when ultrasonic waves act upon pulverized brain tissue the activity of the cholinesterase which is associated with the structures of this tissue is increased almost two-fold. The activity of the enzyme increased almost by a factor of 3 when the brain tissue was irradiated in the presence of an insignificant quality of hydrogen peroxide (H_2O_2 intensifies the chemical oxidizing processes when subjected to the effect of ultrasonic waves). When H_2O_2 is added to the tissue suspension the process of enzyme evolution flows in such a way that the transition of this enzyme into the suspending medium is made easier. However, the activity of the enzyme (which is raised in this case) does not yet verify the fact that this increase in activity is entirely caused by the chemical processes which take place in the field of the ultrasonic waves. Ethyl ether, which always brakes cavitational electro-chemical phenomena, only partially suppresses the process of the intensification of the cholinesterase activity which is associated with the structures of the nerve tissue.

The behavior of the cholinesterase which is extracted from brain tissue is different in the field of the ultrasonic waves. The cholinesterase isolated from brain tissue is inactive when subjected to the effect of this particular physical agent. Here H_2O_2 intensifies the process of enzyme inactivation, and ethyl ether completely protects it from damage.

The intensification of the activity of the investigated enzymes (the enzymes which are included in the composition of submicroscopic structures of the cell membranes) may be caused by a number of processes. Included in the latter must be the inactivation of inhibitors, the destruction of the molecular complex in which the enzyme is included, the denuding of the enzyme centers of the protein molecule, the disruption of the physical state of the biocatalyzer (the variation of the spatial configuration and orientation of the molecules), etc. All of these processes may basically be reproduced when high-intensity ultrasonic waves act upon aqueous solutions of the individual biologically active substances. These processes arise as a result of the indirect effect of the ultrasonic waves — the effect caused by the cavitational electrochemical phenomena in the aqueous medium. However, as we have said, the appearance of cavitation inside the cell is placed in doubt since the viscosity of the protoplasm is appreciable. It is logical to think that the shifts in the physico-chemical state of the biocolloids can also be caused by mechanical forces which are intimately associated with the propagation of ultrasonic vibrations (the acceleration and displacement of particles). This possibility must be especially taken into account when analyzing the phenomena described above which are primarily concentrated at the boundary between different phases. Evidently a special part is played here by the ionic and mycelial vibration potentials which arise in the biocolloids due to the effect of the ultrasonic waves. Undoubtedly the further development of investigations in the indicated direction will serve the more rapid advance of the interpretation of the mechanism of the biological effect produced by ultrasonic waves.

LITERATURE CITED

[1] I. E. El'piner, "The mechanism of the effect of ultrasonic waves upon microorganism," Microbiology, (USSR) 24, 3, 371-381 (1955).

[2] G. A. Medvedeva and I. E. El'piner, "Effect of ultrasonic waves upon yeast cells," J. Gen. Biol. (USSR) 16, 4, 315-320 (1955).

[3] A. I. Oparin, N. S. Gel'man and I. E. El'piner, "Study of the localization of enzymes in Endomyces magnusii cells by means of ultrasonic waves," Doklady Akad. Nauk SSSR 96, 3, 573-576 (1954).

[4] K. V. Kosikov, Yeast Genetics and Methods of Selecting Yeast Cultures (Acad. Sci. USSR Press, Moscow, 1954).

[5] A. I. Oparin, N. S Gel'man and I. E. El'piner, "Detection of saccharase in Saccharomyces globosus (349) by means of ultrasonic waves," Doklady Akad. Nauk SSSR 97, 2, 293-295 (1954).

[6] Ia. I. Frenkel', "Electrical phenomena associated with cavitation which is caused by ultrasonic vibrations in a liquid," J. Phys. Chem. 14, 305 (1940).

[7] I. E. El'piner, "Biological and chemical processes in a field produced by ultrasonic waves," J. Tech. Phys. (USSR) 21, 10, 1204-1212 (1951).

[8] I. E. El'piner and Ts. B. Katz, "Effect of ultrasonic waves upon purine and pyramidine bases," Doklady Akad. Nauk SSSR 82, 611-614 (1952).

[9] I. E. El'piner and M. F. Kolesnikova, "The processes of oxidizing and reducing iodine in a field produced by ultrasonic waves," Doklady Akad. Nauk SSSR 75, 837-839 (1950).

[10] I. E. El'piner, L. A. Bliumenfel'd and S. E. Krasovitzkaia, "Disintegration of a porphyritic nucleus due to the effect of ultrasonic waves," Doklady Akad. Nauk SSSR 79, 495-498 (1951).

[11] P. Grabar, I. Voinovitch and R. Prudhomme, "Action des ultrasons sur une oxydase," Biochim. Biophys. Acta 3, 412 (1949).

[12] A. I. Oparin, M. S. Bardinskaia and I. E. El'piner, "Effect of ultrasonic waves upon yeast saccharase", Doklady Akad. Nauk SSSR 99, 423-426 (1954).

Biophysics Institute of the Academy of
Sciences of the USSR, Moscow

Received February 21, 1956

CHRONICLE

IN MEMORY OF PIERRE CURIE (1859-1906)

Fifty years ago, on April 19, 1906, Pierre Curie died in Paris as a result of an accident; his name will always be cherished in the memory of scientists the world over.

Pierre Curie was born on May 15, 1859 into the family of a French doctor of modest means who was a person of high cultural aspirations and a lover of natural science. Pierre Curie inherited his father's love of experimental science; having obtained his education at home, he easily won his baccalaureate degree. In 1895 he was a professor at the School of Applied Physics and Chemistry; during that same period he married Marie Sklodowska, and his further scientific work (as a result of which radium was discovered) was carried out in co-operation with his wife. In 1903 he and his wife received a joint Nobel prize for this work.

The scientific work of Pierre Curie was carried out under difficult conditions in a poor laboratory environment. It is sufficient to recall that his work in the isolation of radium was conducted with almost no assistance, and that the chemical labors involved in the dissolving, purifying and processing of uranium ore were all conducted solely by him and his wife. But under such conditions they carried out their work and left a deep mark upon science, contributing to such basic fields of engineering as piezoelectric emitters and receivers and, of course, to modern atomic science. Along with this he clearly realized that those extraordinary possibilities which had arisen due to the discovery of radium also carried with them a danger to humanity.

It was with these words that he closed the speech which he gave when he received the Nobel Prize:

"One can imagine that in criminal hands radium can become extremely dangerous, and one can ask oneself: 'has humanity matured enough so as not to use the secrets of nature,which it discovers,for evil?' "

The discovery of piezoelectric phenomena (in cooperation with his brother, Paul Curie) was not an accidental result of his work. He was one of the first clearly to assert the importance of the idea of symmetry in the field of physics. We shall cite his formulation of the physical meaning of geometric symmetry:

"If definite causes produce definite results, then the elements of the symmetry of these causes must be detected in the symmetry of the results produced by them. If the results evidence dissymmetry, then this dissymmetry must also be evidenced in the causes which have given rise to these results. Assertions which are contrary to the two theorems formulated above are, practically speaking at least, incorrect; in other words, the results may prove to be more symmetrical than the causes."

These formulations which are so general conceal a deep vital content which has been adequately revealed only by the subsequent work of an entire generation of researchers.

The Editors

E. A. SHOLPO (1891-1951)

(On the Fifth Anniversary of His Death)

On January 5, 1956 five years had passed from the day on which E. A. Sholpo died; he was the inventor of synthetic or graphical sound (i.e., sound which is obtained by tracing the shape of the oscillations on a moving-picture film). The idea to which E. A. Sholpo devoted his whole life now has a boundless future. A tool has been placed in the hands of the composer by means of which he can write not the conventional signs (notes) but the actual sounds of any timbre, and what is most important, he can write them with all of their shadings; the tool which accomplishes this is an electroacoustic device which transmits only that which the composer has contributed. The great service which E. A. Sholpo has performed consists of the fact that he has built several variants of the device for the composer to work with: the recording of several operas was accomplished by means of this device. The possibility of realizing the idea of "graphical sound" was clear to all who heard these operas, although technically they were far from perfection. The death of E. A. Sholpo and other circumstances halted the further development of this project, but the time will undoubtedly come when these efforts will be renewed, and the ideas and experiments of E. A. Sholpo will serve as the basis for solving the problem at a new level of acoustic engineering and electronics.

LETTERS TO THE EDITOR

VISUALIZATION OF ULTRASONIC SHEAR WAVES IN TRANSPARENT SOLID BODIES

V. G. Aver'ianova, V. I. Makarov, S. N. Rzhevkin

For the purpose of observing the propagation of ultrasonic waves we utilized a high-sensitivity Tepler installation, with long-focus meniscus object glasses, which corresponded to those used in the Maksutov system. For the purpose of exciting shear waves in a glass block made of flint glass we utilized a Y-cut quartz plate which was glued on by means of stiff putty. The installation did not utilize polarization optics.

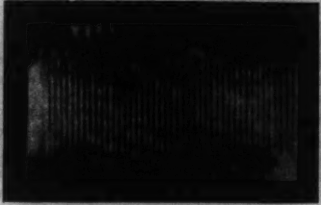

Fig. 1. Standing shear waves in flint glass; distance between the dark bands ($\lambda/2$) is equal to 1.64 mm.

Figure 1 shows a photograph of the standing shear waves at a frequency of 805.6 kc. By means of measureing the wavelength a propagation velocity of 2481 m/sec was found; this value corresponds to the velocity of a shear wave in the given type of glass. When the frequency changed by a small amount (to 808 kc), the same plate excited longitudinal waves with a velocity of 4250 m/sec in the glass block. When ultrasonic waves were normally incident upon a thin interlayer of transformer oil, longitudinal waves freely passed through it into a second identical glass block and excited standing waves in it. When shear waves were incident no penetration of waves through the interlayer was observed.

When a longitudinal wave is reflected from a plane air boundary the reflected waves are broken up into longitudinal and transverse (shear) waves. The angle of reflection of the wave is $\sin\theta_S = \frac{c_S}{c_L}\sin\theta_L$ where θ_L is the angle of incidence of the longitudinal wave, and c_S and c_L are the velocities of the shear and longitudinal waves, respectively. The appearance of a traveling shear wave when reflection occurs is evidenced in the form of a light beam (this is visible on the photographs as well) at an angle of θ_S; this beam covers the spectrum of zero order in the diffraction picture when a Fuquot knife edge is properly positioned.

In the proximity reflection zone, where the longitudinal and shear waves are still superimposed upon one another, an optical interference picture results which is caused by the effects of two waves of identical frequency (ν) which are propagated at different velocities. The interference bands must be distributed parallel to the reflecting surface at distances of

$$\Delta y = \frac{c_S}{\nu}\frac{\sin\theta_L}{\sin(\theta_L-\theta_S)}$$

from one another.

Fig. 2. Interference phenomena in the superposition zone of the shear and longitudinal wave in the glass.

Figure 2 shows a photograph of the interference bands when ultrasonic waves with a frequency of ν = = 3520 kc are reflected at an air boundary.

Sometimes the opinion is expressed that shear waves cannot be seen by the dark-field method, since for a pure shear deformation no variation of the density takes place, and therefore the index of refraction does not vary either. The theoretical concepts of Mueller [1] shows that the index of refraction must vary due not only to the effects of density variation but also due to the effect of elastic stresses, which creates an anisotropy of the molecular refraction. The intensity of the diffraction picture for shear waves must, however, be weaker than the diffraction picture for longitudinal waves, since it is determined by the difference between two photoelastic Neumann constants ($\underline{p}$ and $\underline{q}$). The diffraction effect produced by shear waves (and therefore the appearance of a visible depiction of the wave upon a dark field) must be observed in both natural light and (especially clearly) in polarized light for crossed Nicol prisms (if the plane of polarization is turned to an angle of 45° with respect to the direction of the shear deformations).

The visualization of the shear waves by means of the dark-field method when utilizing polarization optics was accomplished by Hiedemann and Hoesch [2] in 1935. In 1955 Hiedemann [3] demonstrated the possibility of forming diffraction spectra from a slit source for shear waves in glass. It should be assumed that the possibility of visualizing shear waves when utilizing natural light (as we did in our experiments) was a consequence of the high sensitivity of the installation to weak contrasts in the illumination.

It can be assumed that the use of the visual method in the study of the propagation of shear waves in solid bodies is of interest in a number of fields of physics and with respect to the solution of practical problems in ultrasonic defectoscopy.

LITERATURE CITED

[1] H. Mueller, "Theory of photoelasticity in amorphous solids," Physics 6, 179-184 (1935).

[2] E. Hiedemann and K. Hoesch, "Schubwellen als optische Gitter," Naturw. 23, 29, 511-512 (1935).

[3] M. A. Breazeale and E. A. Hiedemann, "Simple way to observe optical diffraction patterns produced by shear waves," J. Acoust. Soc. Am. 27, 6, 1220-1221 (1955).

Acoustics Chair Moscow State University

Received March 7, 1956

A NICKEL FERRITE ULTRASONIC EMITTER

I. P. Golliamina

Ferrites, which are widely known as high-frequency magnetic materials, are beginning to command attention because of their magnetostrictional properties. In recent years a series of papers have appeared on the investigation of ferrites as magnetostrictional resonators with the aim of applying them in radio engineering filters and stabilizing elements (for example, [1, 2]). It is also possible to utilize them for the purpose of electro-acoustic transducing: a reference to this is contained in [3] and [4], and the first attempt at investigating an emitter made of commercial nickel-zinc ferrite is described in [5]. The latter paper describes an emitter which attained an efficiency of 43% and indicates that ferrites were easily damaged even for the small amounts of power which were consumed when they were utilized for the purpose of making measurements.

This paper gives the results of tests made upon a nickel ferrite emitter (see also [6]). The utilization of nickel ferrites (as well as nickel-zinc ferrites with a small zinc content) is practicable, since these ferrites, as is known ([1, 2]), possess an appreciable saturation magnetostriction, a moderate amount of hysteresis, and a coefficient of magnetomechanical coupling which is comparable to that of nickel. The materials which were prepared for manufacturing the emitter were investigated in order to establish certain of their mechanical and electromagnetic parameters. A nickel ferrite emitter was found to have the highest efficiency; this emitter possessed the following properties: a specific weight of 5.0, an open porosity of the order of 1%, an initial magnetic permeability of 25, a Young's modulus of $1.6 \cdot 10^{12}$ CGSE, a Poisson coefficient of 0.34 (the latter two quantities were measured by the resonance method), a coercive force of 6 oersteds, a residual magnetization of 2300 gauss (these quantities were determined from the hysteresis loop which was obtained by the ballistic method) a resistivity of 3 kohm/cm, and a saturation magnetostriction of $26 \cdot 10^{-6}$.

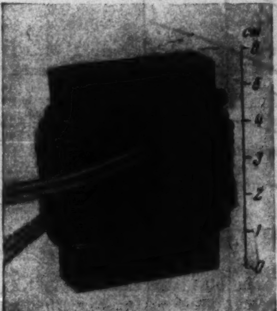

Fig. 1. Ferrite emitter.

An external view of the emitter is shown in Fig. 1. The core had a simple rectangular shape, and because of engineering difficulties it was manufactured out of two halves which were glued together; this resulted in a certain lowering of the emitter efficiency. The coil consisted of 90 turns of 0.7 mm diameter wire and served simultaneously for the excitation of oscillations and for dc magnetization. The emitter was investigated as a resonant transducer at a frequency of ~43 kc for radiation in two directions at various values of magnetization current; the magnitude of the dc field H_0 corresponding to the specified current was determined with the aid of the basic magnetization curve according to the induction measured by the ballistic method.

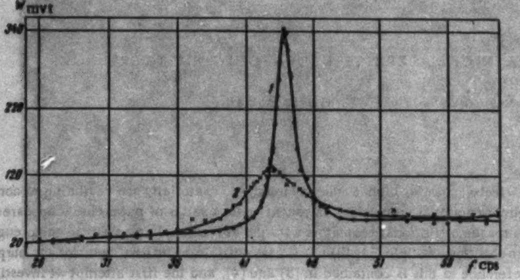

Fig. 2. Dependence of the power required by the emitter upon frequency. H_0 = 14 oersteds; 1) in air; 2) in water.

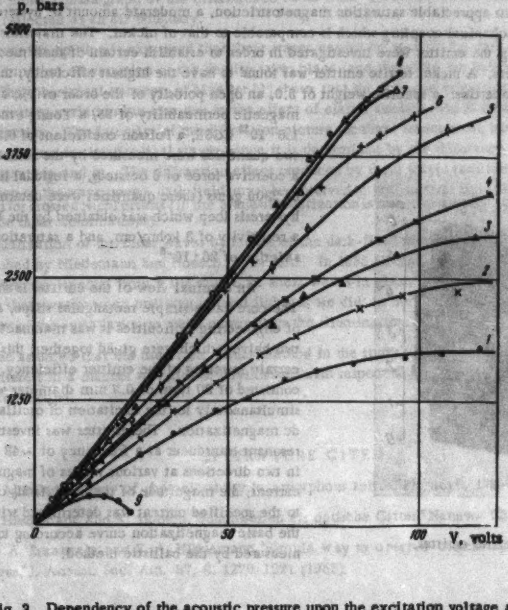

Fig. 3. Dependency of the acoustic pressure upon the excitation voltage at the resonant frequency of the emitter. The dc field H_0 is given in oersteds. 1) 2.5; 2) 5; 3) 7; 4) 9; 5) 16; 6) 20; 7) 26; 8) 29; 9) residual magnetization.

The efficiency was calculated by the known method which utilizes the frequency responses to the electrical power used by the emitter in air and in water; these responses were measured for a constant ratio of voltage to frequency (Fig. 2). The power was measured by the three-voltmeter method. The maximum electroacoustic efficiency was attained for $H_0 = 14$ oersteds (the corresponding magnetization current was 1.7 amps) and was equal to 50%; for these conditions the mechanico-acoustic efficiency was 67%.

We also investigated the field of the emitter by means of a calibrated hydrophone when the emitter operated in a pulse regime. Figure 3 shows the dependence of the acoustic pressure p (at the peak of the directionality characteristic, at a distance of 2.8 meters) upon the alternating voltage V across the emitter. From the family of curves shown in Fig. 3 it is evident that the function $p = f(V)$ retains its linear character longer for large values of H_0; this indicates that a substantial part is played by hysteresis losses during the operation of the emitter. The increase which was observed in the figure-of-merit with an increase in H_0 during our measurements in air is evidence of the appreciable losses that are due to magnetoelastic hysteresis. The evaluation of losses due to eddy currents and ohmic losses in the coil of the emitter yields negligibly small values.

The density of the core produces an appreciable effect upon the efficiency. Emitters which are made of more porous ferrite, which has a smaller specific weight, yielded a maximum efficiency of 42-44%. Evidently porosity leads to an increase in the hysteresis losses as well as in the purely mechanical losses. The maximum specific acoustic power, determined by electrical measurements made upon the emitter (it was assumed that the efficiency measured at small values of power retains the same significance in the region of a linear dependence of p upon V and constant impedance) was 3.5-4w/cm^2. The power attained was limited by the capabilities of the supply circuit. The operational stability of the emitter in a continuous regime was tested for a constant value of required power which was equal to 60 w; this value remained constant for a period of five hours. The readings of the hydrophone which monitored the radiation remained unchanged during the entire test.

Thus it can be assumed that ferrites require attention because they are materials which can be used for designing ultrasonic emitters.

I express my appreciation to N. N. Andreev for his attention to the work reported here, as well as to V. S. Belevantsev, V. K. Chulkova and L. I. Ivanova who took part in the work.

LITERATURE CITED

[1] C. W. Diethelm, "Ferrite als magnetostrictive Resonatoren und ihre Anwendung als Elemente elektrischer Filter," Technische Mitteilungen PTT 8, 281-297 (1951).

[2] Van der Burgt, "Dynamical physical parameters of the magnetostrictive excitation of extensional and torsional vibrations in ferrites," Philips Research Repts. 8, 2, 91-132 (1953).

[3] G. Bradfield, "Ultrasonic electroacoustics," Acustica 4, 1, 171-181 (1954).

[4] P. Popper, "The magnetostriction of ferrites, "Soft Magnetic Materials for Telecommunications, (London, 1954) pp. 322-332.

[5] H. Thiede, "Untersuchungen an Ferriten auf ihre Eignung als Flüssigkeitsschallwandler," Acustica 4, 5, 532-536 (1954).

[6] I. P. Goliamina et. al., Utilization of Ferrites in the Capacity of Sound Emitters (Preliminary Report) (Acoustics Institute, Acad. Sci. USSR, 1955).

Acoustics Institute, Academy of Sciences
of the USSR, Moscow

Received February 20, 1956

REFLECTION OF SOUND BY THICK BOUNDED PLATES IN A LIQUID

L. P. Liamshev, S. N. Rudakov

As a result of the investigation of the reflection of sound in water by thick bounded brass, steel and aluminum plates* in a direction opposite to the incident wave non-mirrorlike reflections were discovered whose directions do not coincide with the directions of the types of reflection known earlier [1]. It has been established that the number of these non-mirrorlike reflections increases with an increase in the thickness of the plate and the frequency of the oscillations.

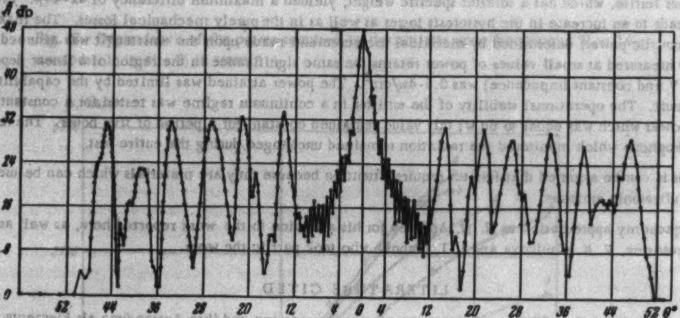

Fig. 1

The measurements of the non-mirrorlike reflection of sound by thick plates were conducted in the same manner as they were in the work described in [1], that is, with a unit consisting of a tub with dimensions of 200 × 60 × 60 cm^3 filled with water and having sound absorbent walls, a generator of ultrasonic pulses which possess a rectangular shape, a quartz dipole consisting of an X-cut quartz with a half-wavelength thickness (the dipole accomplished both the transmission and reception of pulses), a receiving amplifier, and a pulse oscilloscope which served as an indicator for the amplitudes of the echo-signals. The duration of the pulses was 30 microseconds, the repetition frequency of the pulses was 200 cps and the carrier frequency was 1 megacycle; the usual dimensions of the plate were 30 × 60 mm^2 and the distance of the plate from the dipole was 160 cm. The plates were attached by means of thin wires mounted upon a rotating rectangular frame which was equipped with a dial for reading angles.

The polar reflection diagrams of several brass, aluminum and steel plates are shown in Figs. 1, 2, 3. According to what has been said above, they refer to reflection in a direction opposite to the incident wave.

*** It is assumed that plates are used whose thicknesses are comparable to or greater than the wavelength of a longitudinal wave in the material of the plate.**

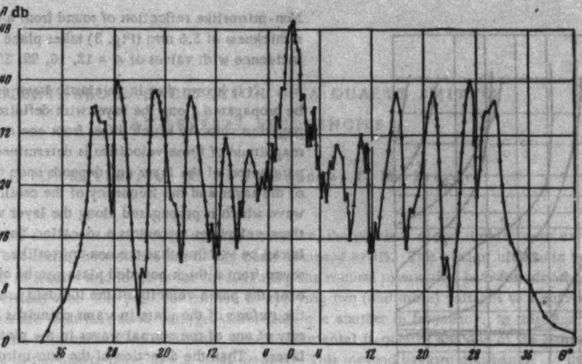

Fig. 2

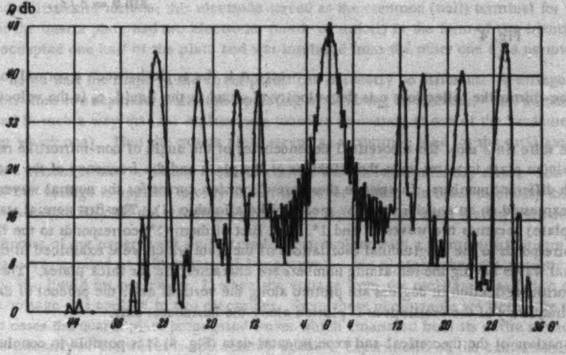

Fig. 3

The amplitude of the reflection (in db with respect to a certain standard level) is plotted along the vertical axis; the value of the angle of incidence in degrees is plotted along the horizontal axis. The circles show the measured amplitudes of the reflection.

Figure 1 shows the polar characteristic of a brass plate with a thickness of 7 mm. Non-mirrorlike reflection is observed in the region of angles of incidence which have values of θ = 14, 22, 26, 33, 39, 46°. The maximum of the polar characteristic in the region of the angle of incidence which has a value of θ = 0° corresponds to the reflection produced in the case of perpendicular incidence of the acoustic wave upon the plate. The polar characteristic of an aluminum plate with the same thickness is shown in Fig. 2. In that case non-mirrorlike reflection is observed in the region of angles of incidence which have values of θ = 6, 10, 15, 21, 27, 31°.

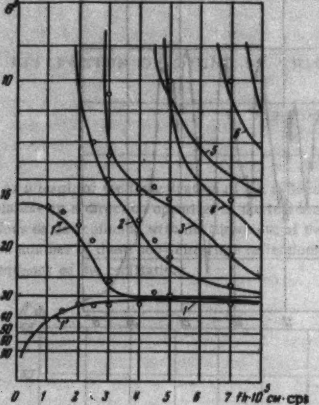

Fig. 4

Non-mirrorlike reflection of sound from a steel plate with a thickness of 5.5 mm (Fig. 3) takes place for angles of incidence with values of θ = 12, 16, 22, 30°.

It is known that in an elastic layer oscillations may be propagated along the layer with definite values of propagation velocity which differ from one another. The magnitude of these velocities is determined by the elastic parameters of the layer and depends upon the thickness of the layer and the frequency of the oscillations. Each wave which is propagated along the layer with one of these velocities represents a so-called "normal" wave. It can be verified that the non-mirrorlike reflection of sound from a thick bounded plate can be observed whenever the phase velocity of the incident sound wave along the surface of the plate in water coincides with the velocity of one of the normal waves in the plate (in the elastic layer). Then the direction of the non-mirrorlike reflection, as it is in the case of thin plates, will be determined by the relationship

$$\sin\theta = c / c_1, \tag{1}$$

where θ is the angle between a normal to the plate and the direction of the non-mirrorlike reflection, c is the velocity of sound in the liquid, c_1 is the velocity of the normal wave.

In Fig. 4 the solid lines show the theoretical dependencies of the angle of non-mirrorlike reflection of sound from a thick aluminum plate in water upon the thickness of the plate and the frequency of the oscillations for normal waves with different numbers. In essence these are dispersion curves for the normal waves in a thick aluminum plate, expressed on an angular scale by means of Relationship (1). The first normal wave for fh = $= 10^5 < 1$ (a thin plate) becomes two waves 1' and 1". The first of them (1') corresponds to the flexure wave, the second (1") corresponds to the longitudinal oscillations of the plate which were examined in the paper cited in [1]. The normal waves having the remaining numbers are characteristic for thick plates. The values of the angle of non-mirrorlike reflection in degrees are plotted along the vertical axis; the product of the thickness of the plate and the frequency of the oscillations is plotted along the horizontal axis.

From a comparison of the theoretical and experimental data (Fig. 4) it is possible to conclude that non-mirrorlike reflections of sound from a thick bounded plate in a liquid are actually caused by the waves which are propagated along the surface of the plate (by the normal waves).

LITERATURE CITED

[1] L. M. Liamshev, Reflection of Sound by Thin Plates and Shells in Liquids (Acad. Sci. USSR Press, Moscow, 1955).

Acoustics Institute, Academy of Sciences, USSR, Moscow

Received November 21, 1955

SIMULTANEOUS EXCITATION OF A QUARTZ EMITTER AT SEVERAL FREQUENCIES

G. D. Mikhailov, N. P. Tikhonova, I. M. Iadrova

As far as we can determine from available literature, the problem of the simultaneous excitation of a quartz emitter at several frequencies has hardly been discussed at all. This kind of ultrasonic wave emitter can be utilized both in liquids and in gases for investigating the mutual interaction between ultrasonic waves, for measuring dispersion, etc. The problem consists of applying two (and more) voltages to a quartz plate under conditions which are such that these voltages differ from one another in frequency. In this regard it is possible to make use of the harmonics of an oscillator. The fundamental frequency and one of the harmonics are simultaneously applied to the quartz plate in the usual manner. This method has two drawbacks: in the first place, excitation is possible only at multiple frequencies; in the second place, the phenomenon of mutual interaction between frequencies in the circuit itself is not eliminated (this interaction is due to the nonlinearity of the tube characteristic). As a result of a large number of experiments on the excitation of quartz at several frequencies we arrived at the following method. We took an ordinary round quartz plate. One side of this plate had a solid electrode applied to its entire surface; this electrode served as the common (null) terminal for two oscillators. The other side of the quartz plate had two electrodes (made of tinfoil) in the form of two identical sectors; each of these sectors occupied one half of the plate and was insulated from the other one by a narrow gap 1 mm wide.

It must be noted that the shape of the cover plates can evidently be different. A voltage was applied to each of the sectors from two separate oscillators operating at different frequencies. The thickness of the quartz plate was selected in such a way that the emitter was tuned to resonance at one of the fundamental frequencies (it did not matter which one). Thus the quartz plate served as a common load for the oscillators.

When such a system is used to excite a quartz emitter the question naturally arises: how does the quartz plate oscillate if the voltage is applied to only one of the cover plates? In order to clarify this question we photographed the acoustic field of the standing waves in the liquid by the usual shadow method.

For the purposes of our experiment we selected a quartz plate with a diameter of 20 mm and a thickness of 3 mm; the plate was excited at a frequency of 1 megacycle. We photographed the acoustic field of the standing waves in the liquid for two cases: 1) when the voltage from the oscillator was fed to only one electrode, and 2) when the voltage was applied to two electrodes. From these photographs we were able to draw the conclusion that in both cases the quartz plate propagated waves which emanated from its entire surface. However, in the first case the intensity of the waves is appreciably weaker. Experiments on the excitation of such an emitter at frequencies which were not multiples of the fundamental frequencies yielded positive results. It should be noted that in the literature a number of experiments on the local excitation of a quartz emitter are available. In relation to this a further problem naturally arises — that of investigating the dependence of the localization of the oscillations in a combined quartz emitter upon the frequency and viscosity of the medium.

Moscow Regional Pedagogical Institute

Received November 15, 1955

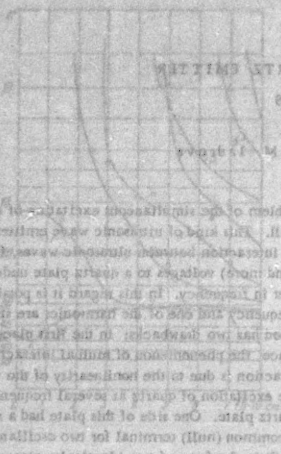

non-[illegible] reflection of sound from a steel plate with a thickness of 8.5 [illegible] (Fig. 3) takes place for angles of incidence with values of θ = 15, 35, 55, 80°.

[illegible] be propagated along the layer with definite values of [illegible] from one another. The magnitude of these velocities is determined by the elastic [illegible] the thickness of the layer [illegible] the frequency of the oscillations. Each wave which is propagated along the layer with one of [illegible]

In Fig. 4 [illegible] aluminum plate [illegible] ≫ 1 (a thin plate) becomes two waves 1' and 1''. The first of them (1') corresponds to the flexure wave; [illegible]

---

[1] L. M. Brekhovskikh, Reflection of Sound by Thin Plates and Shells in Liquids (Acad. Sci. USSR Press, Moscow, 1955).

Acoustics Institute, Academy of Sciences, USSR, Moscow Received November 21, 1955

SOVIET PHYSICS – ACOUSTICS VOL. 2, NO. 2 April-May-June, 1956

(Published by the American Institute of Physics December, 1956)

CONTENTS

	Page	Russian Page
Propagation of Waves in a Medium with Random Inhomogeneities of the Index of Refraction. (Survey). V. A. Krasil'nikov, A. M. Obukhov	103	107
The Mechanism of Cavitational Damage to Surface Films in an Acoustic Field. A. S. Bebchuk, L. O. Makarov, L. D. Rosenberg	111	113
Experimental Investigation of Relaxation Processes Which Arise When Ultrasonic Waves Pass Through Liquids. Iu. N. Bormosov, V. F. Nozdrev, V. D. Sobolev, A. M. Sultanov	118	118
Focusing of Acoustic Waves by Means of Inhomogeneous Media. L. M. Brekhovskikh	124	124
The Problem of Waveguide Propagation of Sound in Inhomogeneous Media. Iu. L. Gazarian	134	133
Some New Methods of Measuring Human Hearing and the Results Obtained by These Methods. G. V. Gershuni	139	137
A Modulation Method of Measuring Ultrasonic Dispersion. V. A. Zverev	144	142
The Scattering and Radiation of Waves by Statistically-Inhomogeneous and Statistically-Oscillating Surfaces. M. A. Isakovich	149	146
The Utilization of Layers That Eliminate the Formation of Transverse Waves When a Longitudinal Wave is Reflected from the Boundary of a Solid Body. M. A. Isakovich	154	150
Experimental Investigation of Ultrasonic Transition Layers. G. I. Kaminir, B. D. Tartakovskii	159	154
The Pulse Method of Fixed Distances; its Physical Basis and Practical Application. N. I Koshkin, V. F. Nozdrev, V. D. Sobolev, M. G. Shirkevich, V. F. Iakovlev	166	161
The Velocity of Sound in Liquids, Liquid Mixtures and Solutions. B. B. Kudriavtsev	172	167
The Transition to a Geometric Approximation in the Theory of Elasticity. M. L. Levin, S. M. Rytov	179	173
Scattering of Sound Waves by Sinusoidal and Sawtooth Surfaces. A. N. Leporskii	185	177
One Approximate Solution for the Problem of the Scattering of Acoustic Waves by an Uneven Surface. Iu. P. Lysanov	190	182
Non-Mirrorlike Reflection of Sound by a Thin Cylindrical Shell. L. M. Liamshev	198	188
Differential Method of Measuring the Absorption of Ultrasonic Waves in Liquids. I. G. Mikhailov, G. N. Feofanov	204	194
The Problem of Applying Ultrasonic Methods in the Investigation of Organic Substances in the Critical Region. V. F. Nozdrev	209	199
Certain Results of the Analysis of a Singer's Voice. S. N. Rzhevkin	215	205

(continued)

CONTENTS (continued)

	Page	Russian Page
Correlation Properties of a Wave in a Medium with Random Inhomogeneities. L. A. Chernov	221	211
The Problem of the Biological Effect of Ultrasonic Waves. I. E. El'piner	228	217

CHRONICLE

	Page	Russian Page
In Memory of Pierre Curie (1859-1906)	235	223
E. A. Sholpo (1891-1951) (On the Fifth Anniversary of His Death)	236	223

LETTERS TO THE EDITOR

	Page	Russian Page
Visualization of Ultrasonic Shear Waves in Transparent Solid Bodies. V. G. Aver'ianova, V. I. Makarov, S. N. Rzhevkin	237	224
A Nickel Ferrite Ultrasonic Emitter. I. P. Golliamina	239	225
Reflection of Sound by Thick Bounded Plates in a Liquid. L. P. Liamshev, S. N. Rudakov	242	228
Simultaneous Excitation of a Quartz Emitter at Several Frequencies. G. D. Mikhailov, N. P. Tikhonova, L. M. Iadrova	245	231

The expanded program of the American Institute of Physics comprises translation of four leading Soviet physics journals, as listed below. These translations, by competent, qualified scientists, will provide all research laboratories and libraries with accurate and up-to-date information of the results of research in the U.S.S.R.

Soviet Physics — Technical Physics

A translation of the "Journal of Technical Physics" of the Academy of Sciences of the U.S.S.R. The 1956 volume, which was originally announced as containing eighteen issues, is instead being issued monthly, in expanded issues. All issues of the original Russian journal for 1956 will be translated. Approximately 4,000 Russian pages. Annually, $90.00 domestic, $95.00 foreign.

Soviet Physics — Acoustics

A translation of the "Journal of Acoustics" of the Academy of Sciences of the U.S.S.R. Four issues per year, approximately 500 Russian pages. Annually, $20.00 domestic, $22.00 foreign. The 1955 issues of "Journal of Acoustics" U.S.S.R. will also be published. Will consist of two volumes, approximately 500 pages, and the subscription price will be $20.00 for the set.

Soviet Physics "Doklady"

A translation of the "Physics Section" of the Proceedings of the Academy of Sciences of the U.S.S.R. Six issues per year, approximately 900 Russian pages. Annually $25.00 domestic, $27.50 foreign.

Soviet Physics — JETP

A translation of the "Journal of Experimental and Theoretical Physics" of the Academy of Sciences of the U.S.S.R. Twelve issues per year, approximately 2,600 Russian pages. Annually $60.00 domestic, $64.00 foreign. Back issues of Volume 1 and 2 are available at a special price of $30.00 for both to subscribers to Volume 3.

Subscriptions should be addressed to the American Institute of Physics, 57 East 55th Street, New York 22, N.Y.